

VOLUME 50 2025

ISSUE 108

# Helictite



AUSTRALIAN  
SPELEOLOGICAL  
FEDERATION



**Published by Australian Speleological Federation**

ISSN: 2652-483X (Online)



# Helictite

## Journal of Australasian Speleological Research

ISSN: 2652-483X (Online)

*Helictite* was established in 1962 by its foundation editors, Edward A. Lane and Aola M. Richards. It is intended to be wide ranging in scope from the scientific study of caves and their contents, to the history of caves and cave areas and the technical aspects of cave study and exploration. The territory covered is Australasia – Australia, New Zealand, the near Pacific Islands, Papua New Guinea and surrounding areas, Indonesia, Borneo and South-East Asia.

In 1974 the Speleological Research Council agreed to support the Journal with financial assistance and in 1976 took over full responsibility for its production. From 1974 to 1997 the Journal was edited by Julia James assisted by other members of the Speleological Research Council Ltd. In 1998 Susan White and Ken Grimes took over as editors with Glenn Baddeley as Business Manager. Stefan Eberhard joined the editorial team in 2003.

In 2000 ownership was transferred to the Australian Speleological Federation Inc. (ASF) and the Journal is now administered by the Helictite Commission of the ASF.

Greg Middleton took over as Chief Editor in 2016. The accidental death of Ken Grimes in August 2016 led to further changes in editors, with Tim Moulds and Kevin Kiernan taking on the roles.

### Helictite Commission of ASF as at December 2025

#### Editors

Greg Middleton   Tim Moulds   Kevin Kiernan

#### Commission Members

Susan Q. White (Chair)   Glenn Baddeley   Grace Matts   Jill Rowling

The aim of the Helictite Commission of the Australian Speleological Federation is to publish the results of scientific studies in all fields of speleology in *Helictite – Journal of Australasian Speleological Research*.

This work is ASF Copyright. Apart from fair dealings for the purpose of private study, research, criticism or review permitted under the *Copyright Act*, no part may be reproduced without the written consent of the publishers and acknowledgement of the source.

Copyright of the original text and figures is retained by the authors, but the layout is copyright to the ASF.

### ***Helictite in Digital Format***

From 2017 *Helictite* has been published in digital format only. Papers are published online, and are freely available to all. There is no subscription fee – the ongoing costs of production and archiving are borne by the Australian Speleological Federation.

Submitted papers will still be reviewed and edited as before, but the layout may be varied to suit a digital format. Each paper will be published on line as it is ready as part of what is intended to be an annual volume. Intending authors should read the latest 'Information for Contributors' on the Helictite website.

#### *Helictite web site*

The Helictite web site is part of the parent ASF site. The URL is: <https://helictite.caves.org.au>

The web site is maintained by Business Manager, Glenn Baddeley. It provides contact details, information for contributors, contents, abstracts and complete PDF versions of all papers ever published in *Helictite* (i.e. since 1962).





## Contents

**Physical evidence for past cold-climate events at Wombeyan Caves, NSW: Broken speleothems and other relict features within Fig Tree Cave and Victoria Arch**

*Jill Rowling*

**1**

**Seri Thai System, a large cave in the quartz sandstones of North-east Thailand, geology, morphology and genesis**

*Liviu Valenas, Martin Ellis & Maliwan Valenas*

**27**

**Military impacts on some Australian karsts**

*Kevin Kiernan*

**45**

**Observations on the geology and geomorphology of a large doline in dolostone at Forest Hills, Tasmanian Wilderness World Heritage Area**

*Rolan Eberhard & Chris Sharples*

**75**

Cover: Forest Hills karst area, Tasmania: V-shaped canyon in dolostone at the point where the stream enters rockfall at the entrance to Forest Hills Cave, which is directly behind the figure in the image, Grant Dixon (Photo by Rolan Eberhard).

*Helictite*, Volume 50, 2025 consists of single issue.

*Helictite* is published by the Australian Speleological Federation Inc. Except for abstracting or review, the contents may not be reproduced without permission of the publishers.

Address for correspondence: [ozspeleo@gmail.com](mailto:ozspeleo@gmail.com)

This issue is published December 2025 (individual papers may have been published on-line earlier).







# Physical evidence for past cold-climate events at Wombeyan Caves, NSW: Broken speleothems and other relict features within Fig Tree Cave and Victoria Arch



**Jill Rowling**

2 Derribong Place, Thornleigh NSW 2120 Australia.

jillr@speleonics.com.au

Unless otherwise stated, all photographs and graphics are by the author.

## Abstract

A preliminary study of broken speleothems and speleogens in Fig Tree Cave, Wombeyan Caves, NSW, suggests that a combination of cave geometry, chimney effect and past climatic conditions caused ice build-up in the cave during past ice ages. As temperatures fluctuated around freeze and thaw, stresses from ice expansion broke large speleothems and fractured bedrock in flakes. This empirical approach is supported by physical calculations of stress on a measured stalactite and extrapolated estimates of cave temperatures during the last glacial maximum. Additional support for the argument is based on the appearance of possible cold-temperature speleothems and bedrock grooves.

## Introduction to the concept of permanent ice in karst caves

Limestone caves in Australia do not currently contain permanent ice, although seasonal ice may be present temporarily near entrances of caves in areas subject to snowfall. Some Australian caves, however, exhibit features such as naturally broken speleothems and bedrock, similar to those which occur in European caves containing permanent ice. The purpose of this preliminary study is to present observations and evaluate physical evidence supporting the idea that in the past, perennial bodies of ice existed within some Australian caves. The work also looks at unusual speleothem shapes, cave geometry and considers the effect of the past climate.

Kempe (2004) examined several famous large broken speleothems in the Postojna caves of Slovenia, and concluded that they had been broken by ice. He suggested that the ice came from more extensive regional glaciation during the Pleistocene than is generally accepted. A model was shown for one speleothem's breakage based on calculated ice expansion and contraction, and suggested a block-slide of ice was responsible for some other breakages, although the forces were not calculated.

Permanent ice is a feature of some of the world's limestone caves due to their cooler average annual temperature. This is caused by their geometry, higher latitude and in some cases higher altitude. Cave geometry is an important factor, allowing the

pooling of cold, dense air in winter and preventing cool air from draining out of the cave in summer. This chimney effect creates cold traps containing ice in some caves (Gabrovšek 2023). Prevailing winds can also alter air movement in caves (Kukuljan and others 2021). In Europe, for example, dolines can fill with snow in winter and thaw in spring. Rainwater then percolates through cracks in the limestone. When groundwater encounters a much colder cave environment such as a cold trap, it can freeze to form icicles and other ice deposits such as flowstone and columns (for example, Figure 1) and can slowly move downwards in channels, enlarging holes and plucking loose stones which can act as an abrasive. By late summer, when warmer air has penetrated part of the cave, some of these deposits thaw, flow further into the cave and can re-freeze (see Hill and Forti 1997, pp. 123-124, 127-130).



**Figure 1.** Ice in Demänovská Ice Cave, a limestone showcave in Slovakia, July 2013. (Photographed during the 16th ICS post-conference trip.)



## *Cold-climate Events at Wombeyan*

Ice showcaves of Slovakia have been instrumented and, for example, in Dobšinská Cave, solid ice flows slowly downwards like a small glacier at 2–4 cm per year (Zelinka 2008, p. 91).

Cryogenic Cave Carbonates (CCC) are common in limestone caves containing ice, with CCC precipitating as a grit on the surface of freezing limy cave water from the outgassing of CO<sub>2</sub>. The CCC is comprised of two different calcites, formed under different conditions. The main differences between the two are in morphology (fine versus coarse grain sizes) and stable isotope ratios, with the fine ones precipitating when a thin film of water freezes on existing ice in a cave, and the coarser ones precipitating as cave dripwater from thawing permafrost above the cave (Munroe and others 2021). The presence of these deposits is considered to be an important proxy for past cold temperatures in caves (Munroe and others 2021).

The force exerted by water expanding as it freezes to ice at atmospheric pressure is well known in physical chemistry. In limestone caves containing ice, broken stalagmites are sometimes found and it used to be thought that the breakage was from the flow of ice, or possibly earthquakes, but when stalagmites of various sizes and ice geometries were numerically modelled for ice deformation under gravity, a simple ice flow down a slope and past a stalagmite can only generate 0.05 MPa shear stress, which is considerably less than the 2 to 7 MPa shear stress needed to break stalagmites of the diameter seen in the field, and earthquake breakage leaves characteristic tectonic features in caves, not seen in the study site (Spötl and others 2023).

The same team noted that since the study site also had cryogenic cave carbonates, thermal expansion and contraction of ice was thought to cause the stalagmite breakages, so a different numeric model was run taking thermal expansion into account, using a stalagmite with a breaking strength of 4.3 MPa, various physical geometries and thermal ranges. This showed that the net force on a stalagmite embedded in ice undergoing thermal expansion near its freezing point is primarily upward; that is, a stalagmite embedded in expanding ice is subject to considerable stress from the differential thermal expansion characteristics of calcite and ice, sufficient to lift the stalagmite off its base with a very small displacement (Spötl and others 2023).

A speleothem type, called “cryogenic ridges”, is formed by calcite stalactites undergoing cold conditions in which dripwater freezes, forming pronounced ridges on their surfaces, with a fine channel along the ridge (Onac and others 2023), and isotopic analysis indicated the calcite near the ridges formed at much lower temperatures compared with the calcite forming the bulk of the speleothem.

In a detailed study of Kents Cavern, Devon, United Kingdom, Lundberg and McFarlane (2012) showed that calcite flowstone had been broken by episodes of frost heaving during Pleistocene glacial periods, even though the sites were periglacial and not subject to actual glaciation. Calculations showed that the breakage was caused by cold conditions over periods of time, enhanced by passage geometry, air movement and multiple entrances on different levels causing parts of the cave to exhibit extensive cooling. Wet sediment under flowstone heaved as it froze, causing the overlying flowstone to crack.

## **Geological and geomorphological setting of Wombeyan Caves**

Wombeyan Caves is located in the southern highlands of New South Wales at an altitude of about 600–650 m asl. The area (see map, Figure 2) is drained by Mares Forest Creek and Wombeyan Creek which are part of the Hawkesbury/Nepean catchment. The caves are developed in Silurian limestone which has been significantly marmorised (metamorphosed) to a creamy saccharoidal marble by Devonian granite intrusions and volcanoclastics (Thomas & Pogson 2012). Marble used to be quarried from the area. showcaves are located in the eastern part of the marble, around the steephead of Wombeyan Creek as it passes through Victoria Arch. Other caves are found throughout the area. The underground drainage is complex. Wombeyan Creek occasionally floods, re-arranging alluvium in flats upstream of Victoria Arch, resembling a small polje. Downstream of the Arch, Wombeyan Creek is often dry and runs in a small gorge south to Mares Forest Creek.

## **Wombeyan climate today**

The temperature regime for Wombeyan Caves is similar to that of Taralga. Wombeyan is a little lower in altitude, but lies in a frost hollow. Taralga Post Office, station 70080 (Bureau of Meteorology) lies at 845 m AMSL and the mean maximum and minimum temperatures are 26.2 and 0.7°C respectively, with July the coldest month.



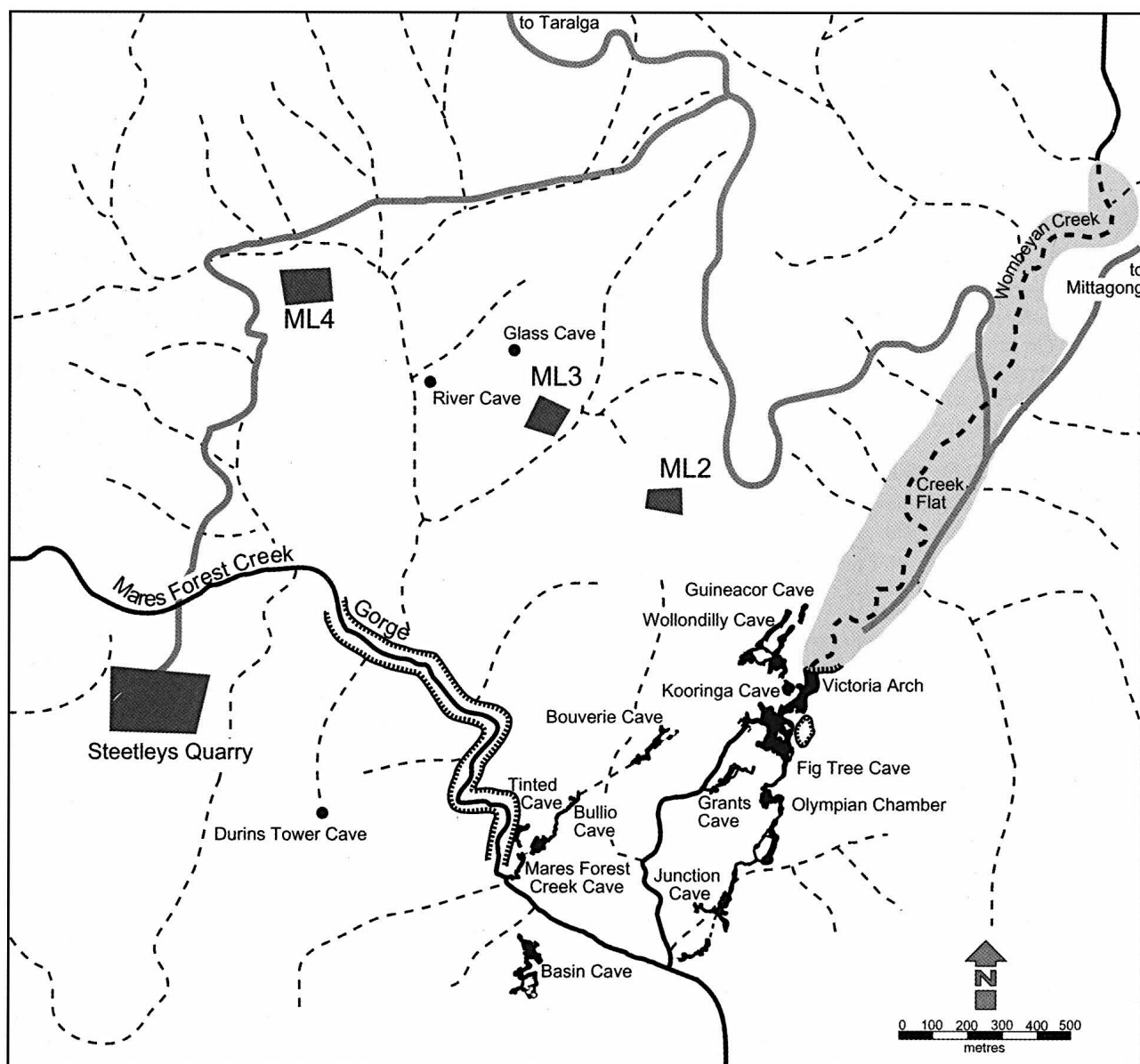


**Figure 2.** General map of the Wombeyan Caves area, reproduced from James and others (2004), p. 36.

The lowest recorded is  $-3^{\circ}\text{C}$  in 1982. Wombeyan Caves camping ground lies at 600 m AMSL, roughly the same for the lower part of Victoria Arch and Wombeyan Creek flowing through it. Anecdotally, cavers have reported temperatures as low as  $-7^{\circ}\text{C}$  outside the caves office. Although the cave temperatures are typically the average annual temperature, the temperature ranges within some caves can vary, as there are multi-entranced caves, heat domes and cold traps. The caves at Wombeyan respond to changes in the weather, based on their geometry, and some caves have airflow reversals which alter the humidity in the caves (Halbert & Michie 1982). Experiments at Bullio Cave, for example, showed a variation of around 5 degrees Celsius in temperatures across parts of the cave in winter, and slightly less variation in summer. There has not been much work done recording the

temperature variability in Fig Tree Cave, although the thermal variations are well known by both cave guides and cave surveyors.

### Previous work at Wombeyan Caves

Platey exfoliation of the marble occurs in a phreatic tube near the exit gate of the Fig Tree Cave, and a similar large flake in Creek Cave (James and others 2004, pp. 135-136) which is part of the Fig Tree system. The exfoliation is similar to that caused by water getting into cracks and freezing, but it was not thought that the cave could get cold enough, based on current average annual temperatures. Several ideas were put forward to explain the exfoliation but dismissed, e.g. salt wedging, gypsum crystals, tectonics, plants. It was noted that on the Nullarbor, salt wedging tends to obliterate the soft bedrock rather than causing platey

## *Cold-climate Events at Wombeyan*

exfoliation. Wombeyan marble is more competent, but no salt has been observed at Wombeyan. Further work on the topic was recommended (James and others 1982).

Hockey Gully at Wombeyan Caves contains periglacial deposits comprising angular rock fragments from fine gravel to cobble size in roughly downslope beds of various sizes and with various amounts of fine grained material between the fragments. This was dated to 19 ka using radiocarbon dating of wood (Jennings and others 1982, pp. 62-63).

Toppled and then re-grown speleothems were noted in Fig Tree, Wollondilly and Koorunga Caves, and it has been suggested that straw stalactites growing from the stub of the large fallen stalactite near the platform at the northern end of the Colonnades could be a few hundred years old, based on their length, but the cause of the original break was unknown (Sefton & Sefton 1982; James and others 2004). Condensation corrosion occurs at Wombeyan Caves when a thin film of water condenses onto a calcite surface due to moist air encountering a cooler surface, and CO<sub>2</sub> from the air dissolved in the water makes the water aggressive to calcite (James and others 2004, p. 42).

Gillieson and others (1985) examined a solifluction deposit in Basin Cave at Wombeyan Caves. The material, found in the cave's lower entrance, comprised angular gravel of elongated platy to blocky clasts of Wombeyan marble with charcoal layers. This was carbon-dated to 27.8 ka. They concluded that since the processes which caused this and other solifluction deposits in the area were no longer occurring, that more extreme winter climates occurred at Wombeyan during the last glacial.

McDonald & Drysdale (2004) measured temperatures and groundwater drips in Wollondilly and Koorunga caves at Wombeyan. Two naturally-broken stalagmites from the Mulwaree Extension were analysed using U/Th techniques, suggesting that one of the stalagmites grew from 133 ka to 83 ka, and the other began growing at 79 ka, although the Wombeyan speleothems are particularly poor in uranium.

Wombeyan marble is well-known from an architectural perspective (e.g. its use in the floor of the Mitchell Library, Sydney) for both its creamy colour and unusually large calcite grain size. Various workers have modelled and analysed

the strength of Wombeyan marble in a laboratory and found its strength varied depending on how it was confined and any imperfections in the piece. In low confinement, marble samples failed at 3.5 MPa, compared with 100 MPa in high confinement (Bahrani and others 2011). Other workers found unconfined samples failing below 35 MPa by spalling or shearing, with low-end failures at 0.1, 3.5, 10 and 14 MPa, but in high confinement, 70 and 100 MPa, it has ductile behaviour and microfractures can be associated with acoustic emission long before peak stress is reached (Hueckel 2016, pp. 11-12).

Low-altitude periglacial scree slopes occur in several sites around NSW, including the volcanoclastics at Hockey Gully, Wombeyan Caves at 650 m (Barrows and others 2021). During the mid-Pleistocene, winter temperatures could be on average some 8 degrees Celsius colder than at present and there was a lack of trees during this time, which increased erosion; rivers were larger, with high sediment loads. Techniques used with the Wombeyan site included radiocarbon (24 ka) and stratigraphic logs (Barrows and others 2021). In a study of relict periglacial block deposits of the New England area, it was suggested that mean annual temperatures during the last glacial cycle were on average more than 8 degrees Celsius colder than today (Slee and others 2023).

Members of Sydney University Speleological Society (SUSS) have surveyed and mapped Fig Tree Cave and Victoria Arch. The map (see Figure 3) has been drawn up by the author using "Therion" software, and a model prepared and viewed using "loch" software (see Figure 4). This paper arose during the author's project to describe the cave, as some speleological problems emerged regarding the past climate.

## **Study sites and methods**

The study sites for this project are Fig Tree Cave and Victoria Arch. These sites were chosen as they are relatively easy to access for repeat visits, they are large showcaves and contain features which are difficult to derive using conventional karst solution and deposition.

As this project is at a preliminary stage, the methods involved physical measurements using a Leica Disto A4, a steel tape and a Suunto Twin (for levels), and photographs using a Canon EOS digital camera with a hand-held LED lamp. No sampling was done for this stage of the project.



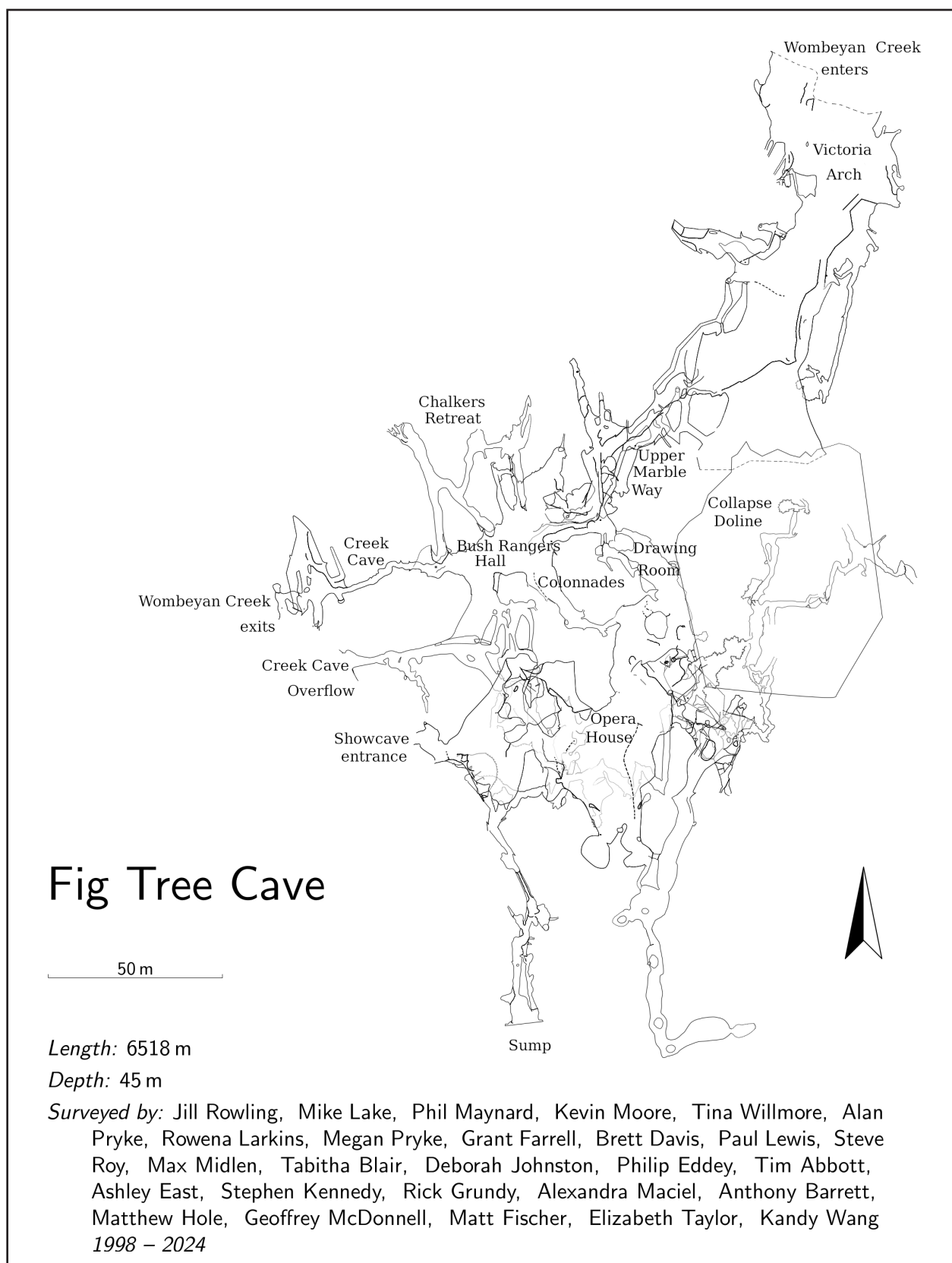


**Figure 3.** Plan of Fig Tree Cave (simplified). 50 m scalebar.

The author took the photographs and physical measurements, often assisted by members of SUSS. Disto measurements were to 4 decimal places but when aimed at irregular shaped speleothems were downgraded to  $\pm 1$  cm; tape measurements were

$\pm 5$  mm but similarly downgraded to  $\pm 1$  cm; inclinations are  $\pm 0.5$  degrees from horizontal.

Broken speleothems were viewed and noted, whether they were considered old breakages (typically embedded in flowstone) or whether the

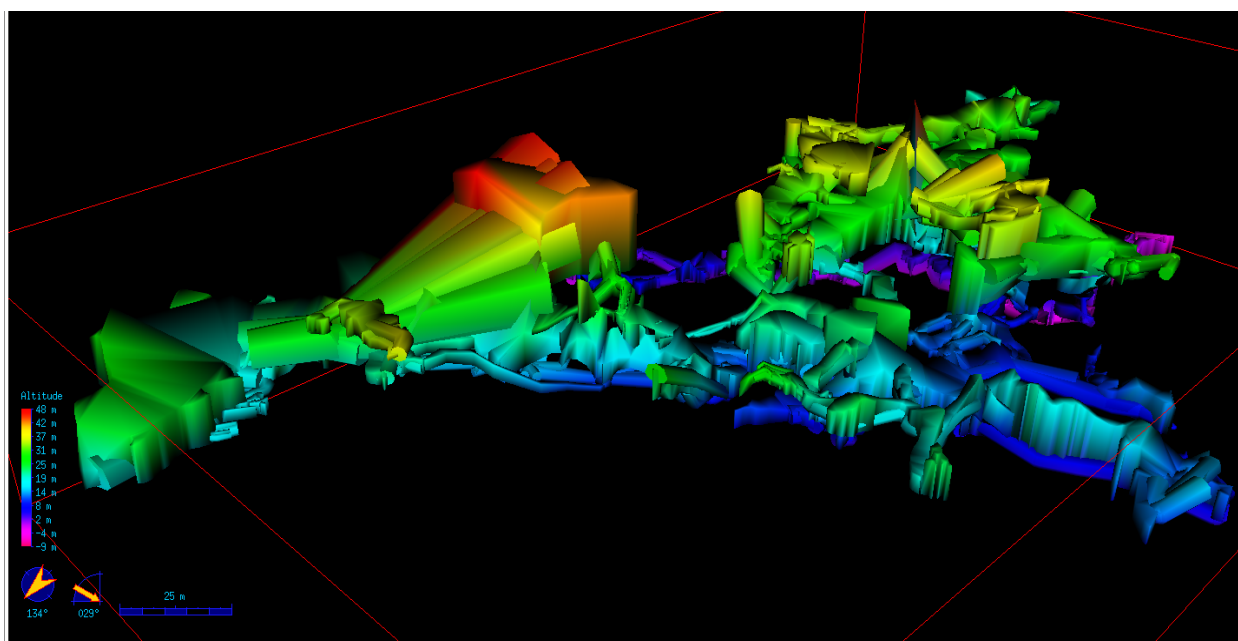


**Figure 4.** 3D model oblique view to the south-east of Fig Tree Cave and Victoria Arch. Scalebar is 25 m. Coloured by height. Speleothem breakages are mostly in the area shaded light blue-green, about 20 m above the level of the sumps (shaded purple).

breakage could have been anthropogenic. Wall notches of various sorts were viewed for scallops or other patterns such as striations. Sediments such as cobbles were checked for roundness. Also the general shape of a passage was considered for the type of erosion it had apparently experienced. In particular, cold-climate effects were considered in cases where a site had a combination of features in one area such as spoon-shaped wall hollows, broken speleothems or speleogens in a line, small ridges on speleothems with a fine line running along them, striations and grooves in the wall. Some speleothem settings, dimensions and geometry were measured, with particular attention given to the large broken stalactite at the platform near the junction of three passages: Upper Marble Way, Colonnades and Bush Rangers Hall. The methods of Spötl and others (2023) were considered as a general guide to modelling the likely forces produced by ice on a stalagmite. These concepts were extended to include other geometries and settings such as the theoretical forces required to break a large speleothem (canopy).

### Brief description and nomenclature of Fig Tree Cave and Victoria Arch

Referring to the map (Figure 3) and 3D model (Figure 4), Fig Tree Cave is a large, self-guided showcave, and was opened as a guided cave a little after 1897. It has at least 5 entrances and connections to two other caves (Lots O Numbers Cave and Junction Cave). Victoria Arch is considered part of the cave and has been noted since at least 1828.

It was likely well-known to the local Gundungurra Aboriginal people. Wombeyan Creek flows into the spacious northern entrance of Victoria Arch, down Marble Way and exits through Creek Cave at times of high flow. It also flows through a series of sumps, appearing in Junction Cave to the south. A large daylight hole in the south side of Victoria Arch, called the “collapse doline”, has a steep scree slope comprising cave sediments and marble bedrock. This is in contrast to the volcanoclastic and granite cobbles in the bed of Wombeyan Creek below the scree slope. The Fig Tree showcave comprises several large well-decorated chambers and a high cantilever pathway above the canyon of Marble Way to Victoria Arch. The showcave entrance is on the western side of the cave, and opens out to a large chamber with pits in its southern and northern end which connect to the lower sumps and Creek Cave Overflow respectively. The Opera House is a large chamber in the middle of the cave with a relatively flat ceiling and large boulders on the floor. The Drawing Room is a steeply sloping chamber off the northeast of the Opera House, connecting to several other areas and lies below the western wall of the collapse doline. The Colonnades is a rift passage between the Opera House and Bush Rangers Hall, which is a large chamber in the northern part of the cave through which Wombeyan Creek flows. The northern end of the Colonnades has a platform overlooking Bush Rangers Hall and illuminating both halves of a calcite canopy called the “large broken stalactite”. Chalkers Retreat, in the northwest part of the cave, is an abandoned passage at the same level as the Colonnades but on

the other side of Bush Rangers Hall. Creek Cave and Creek Cave Overflow are two streamway passages west of Bush Rangers Hall. Upper Marble Way is the north-east trending passage in the north part of cave and is a developed showcave track on a cantilever walkway above the underground part of Wombeyan Creek. Victoria Arch is the large daylight arch in the most north-eastern part of the cave.

Within Fig Tree Cave, sedimentary deposits range from conventional calcite speleothems to sediment fines with charcoal layers, bat guano deposits, red earth layers, rounded and angular gravels and other fluvial deposits including large cobbles similar to those seen outside in Wombeyan Creek. The cave has apparently experienced a range of climatic changes different from the present environment. Being a multi-entranced cave, it is common to find a range of temperatures across the cave, with the coolest parts usually being experienced around Marble Way, Creek Cave and Chalkers Retreat.

During the survey of Creek Cave, a near-vertical south-dipping fault was found by examining slickensides in the ceiling near the Creek Cave entrance. The general trend of Creek Cave follows the strike of this fault, roughly 80° from North, and it may correspond with the southern end of Victoria Arch, that is, the northern end of the collapse doline. Although bedding is mostly destroyed by marmorisation, apparent bedding in the cave dips about 45° to the north-west, striking roughly north-east as measured in Bush Rangers Hall, Drawing Room and Opera House.

## Cave Observations

Observations are listed in order of a speleological visit to the cave, starting in the upper Fig Tree showcave entrance, then the Opera House, the Drawing Room, Creek Cave, Chalkers Retreat, Upper Marble Way through to the exit in Victoria Arch. These observations concentrate on unusually broken speleothems and speleogens. Surface coatings are also noted such as apparent calcite “dribbles” (small sinuous forms resembling candle wax dribbles, discussed later) and possible cryogenic forms. Some of the cave has been modified as part of track development, so it is plausible that most of the toppling and breakage discussed here was from natural causes.

Near the top of the pit at the northern end of the Fig Tree Cave entrance chamber is a small stalagmite, apparently broken in half. In the middle of the Opera House, a long stalactite (possibly a cave shield) has broken off the ceiling and

lies almost intact on the rockpile 15.5 m below, near the large stalagmites in the main part of the Opera House, yet not exactly under its apparent detachment point on the ceiling. The enormous boulders forming the central rockpile have not come from the ceiling, which is relatively smooth apart from a ceiling canyon. Instead, they may have either come from the walls or the collapse of an intermediate level early in the cave’s development. Toppled and broken speleothems and speleogens lie on a slope in the northern end of the Opera House below the Drawing Room.

The Drawing Room contains a small forest of columns and many broken stalagmites (e.g. Figure 5), with many of the broken bits lying nearby or cemented into the flowstone. The substrate is a rockpile, well-cemented by flowstone in its northern end. As the lower part had been used in the early days as a basic showcave, we ignored all the loose broken speleothem tips which had apparently been “tidied” into lower areas west of the mini-track. Apparently bent columns (for example, Figure 6) with multiple areas of regrowth resemble calcified tree roots, although no organic material was seen. Bent speleothems and tree roots are discussed later. Fine lines on a flowstone shelf and nearby speleothems also resemble plant roots but again no organic matter was seen.



**Figure 5.** Columns, broken and flat-topped stalagmites, Drawing Room.

Apparently bent stalactites and stalagmites occur in the area. Surfaces of speleothems here commonly feature “dribbles”. Regrowth has occurred on some broken stalagmites and on numerous columns. Typical breakage varies, but seems to have mainly affected the smaller speleothems, although some larger ones have cracks. Cave welts are speleothems similar to cave shields, but have formed along a horizontal crack in a column, as per Hill and Forti (1997, p. 99). Nearly every column has a welt,



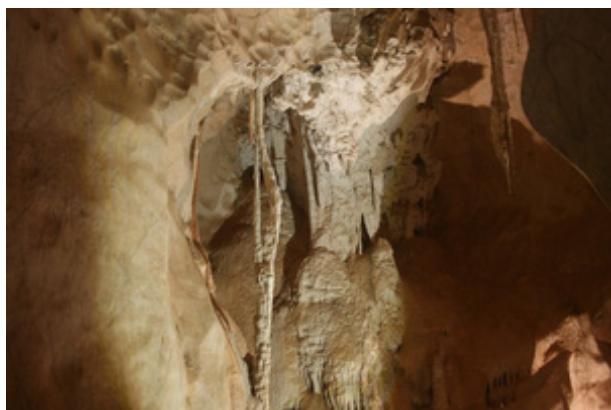


**Figure 6.** Apparently bent column, Drawing Room.

which was thought to be due to movement (Figure 7), discussed later. The columns have a variable diameter, assumed to correspond with varying drip rates, with the length ratio of stalactite: stalagmite typically 3:1. Regrowth of some broken stalactites and stalagmites was around 8 cm, indicating considerable age. On the ceiling in the middle part of the chamber, fairly high on the east side, we noted one broken cave shield and on the other, lower (west side), cave shields were intact. A glittering cave shield has a fringe of stalactites and columns below it. On the fringe, the small columns are perfect but stalactite tips have been broken suggesting the force that broke them was insufficient to break the small columns and could have been rotational. Some of these are cemented to the flowstone substrate below the shield, not far from where they originated. It was unclear as to how they were broken.

The northern end of the chamber features a scalloped ceiling channel with apparent flow from the east (high side). Scallops are more intense in the ceiling, whereas lower down they are much broader (around 1 m across). Just below the ceiling scallops are faint shallow horizontal grooves, 20 – 30 cm long x 10 cm high, which appear to have worn smooth earlier scallops.

A thinner part of a pendulous marble speleogen at the upper north-eastern corner of a side passage is broken off, suggestive of some force having been applied to the corner. The broken-off piece can be seen embedded in flowstone on the passage floor and has not moved far horizontally (Figures 8, 9). Below the flowstone lies a deposit of sub-rounded gravel and cobbles, indicating that at an earlier time, a stream flowed through this part of the cave. Oddly, the side passage has little scalloping, yet it connects to an area of the scalloped passage right through the scallops. Opposite this passage is a similarly broken section of bedrock (Figure 10).



**Figure 7.** Column with well and regrowth in the Drawing Room.



**Figure 8.** Part of broken speleogen embedded in flowstone, Drawing Room.



**Figure 9.** Area from where speleogen apparently fell, and scalloping, Drawing Room



**Figure 10.** Wedged bedrock, Drawing Room.

The northern part of the Drawing Room is adjacent to, and slightly above the Stalactite Cluster of Upper Marble Way, described later. A short drop



connects these two parts of the cave. Air flows freely between these chambers, and sometimes during a weather change, a fog will develop where cold air flows from Creek Cave / Marble Way through the Drawing Room and down to where it meets the warmer, more humid air of the Opera House.

When walking from the Opera House to the Colonnades through the narrow connecting passage, the most obvious difference is a change in atmospheric temperature. The Opera House is relatively warm and humid, whereas the Colonnades is often cold and draughty. Broken stalactites in the Colonnades could be from human activity although some are quite high up and could be due to other causes. Thickness of regrowth on some of the broken pieces suggests the breakage pre-dates showcave development. A group of three stalagmites near the north-eastern wall have “dribbles”; one has an apparent lean. Closer to the track are several stalagmites with flat tops which appear to have all broken at the same level (Figure 11).

**Figure 11.** Stalagmites broken at similar level, Colonnades.

The floor of Bush Rangers Hall is covered with cobbles and gravel deposited by Wombeyan Creek, but there are also some water-worn broken



speleothems. Some of these have clearly toppled by undermining of the gravel on which they developed, but others appear to have fallen from the ceiling. On the western wall (the left-hand side of the viewing platform) is a relatively horizontal angular cut in the bedrock, which lines up with a crack in a column (Figure 12).

Very high up in the ceiling are broken canopies (Figure 13). One of these was measured as having broken about 5.9 metres below the ceiling, about 10.5 m above the platform. The lower part of the

**Figure 12.** Crack in speleothem group, Colonnades; lines up with notch in wall of Bush Rangers Hall.

“large broken stalactite” is lit, showing its complex folds (Figures 14, 15). The dimensions of this speleothem are described below. The stub end of the remaining upper part has small active straws, 100 – 200 mm long (Figure 16). The actively depositing part of the canopy is its outer edge, and the straws are not very active. 4.1 m below the sheared end is a stalagmite boss in which a variety of broken speleothems are embedded – mainly shawl and stalactite tips. These broken pieces are





**Figure 13.** Broken canopies, Colonnades, Bush Rangers Hall.



**Figure 14.** "Large Broken Stalactite", upper area, upstream side from Upper Marble Way.



**Figure 15.** "Large Broken Stalactite", lower area, upstream side from Upper Marble Way.

assumed to originate from nearby broken-tipped speleothems, and a straw tip which is presumably from the sheared area above (Figure 17). The rest of the lower canopy near the wall appears quite firmly cemented, forming pillars, and only a couple of additional broken-tipped stalactites can be seen on the upstream side. Also upstream is a blade of bedrock with a damaged upper part.



**Figure 16.** Straw stalactites have regrown under the "Large Broken Stalactite", Bush Rangers Hall.



**Figure 17.** Broken speleothem tips embedded in stalagmite boss below the "Large Broken Stalactite", Bush Rangers Hall.

### Detailed measurements of the large broken stalactite

The bottom points have broken from the large detached part of the "broken stalactite". Its remaining tips face upstream and a collection of broken stalactite tips lie close to it in sediment near the drop to the creek, but it is unclear whether these were moved during showcave development or are in their natural position (Figure 18). They would add another 30 cm or so to the length which is 0.95 to 1.4 m long, depending on which broken tip is measured. Adding in the tips would mean the length of the detached part could be up to about 1.7 m - see Hb in Figure 19.

By surveying the "broken stalactite" from a nearby post, relative vertical positions were calculated for the top of the canopy and the base of the canopy using measured distance  $x$  sine (inclination). Thus the length of the upper remaining canopy,  $H_t$ , was calculated as 2.2 m. Adding in the length of the broken pieces,  $H_b$ , it is possible to estimate the original canopy height  $H$ :  $2.2 + 1.7 = 3.9$  m. So it has broken a little less than half-way along.





**Figure 18.** Detail, broken lower part of "Large Broken Stalactite", Bush Rangers Hall.

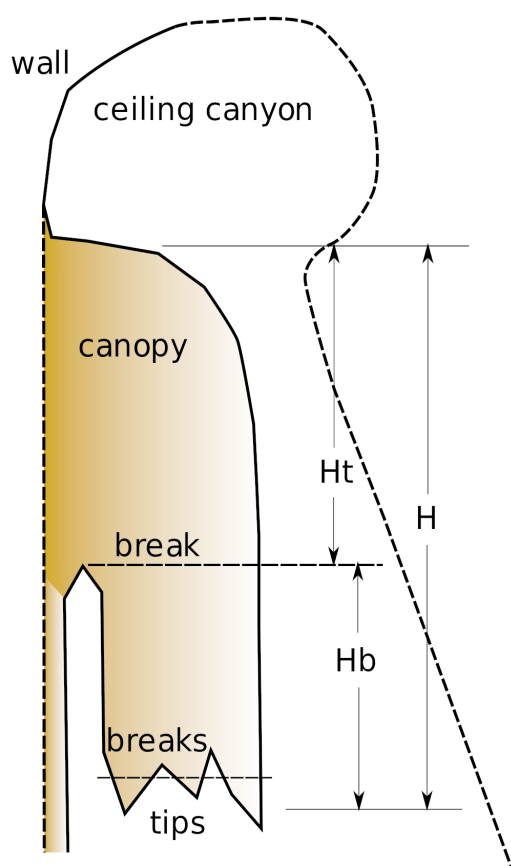


**Figure 19.** Sketch of the "Large Broken Stalactite" virtually reconstructed canopy near platform at Bush Rangers Hall with dimensions discussed; based on Figures 14 and 15.

The illuminated end of the detached part is roughly oval shaped (Figure 20) with oval diameters 1.8 x 1.1 m, and faces downstream. Ribbing is pronounced on one side. A photograph of the broken surface of the stalactite was used to estimate the percentage of calcite compared with gaps, by counting pixels in Gimp software and the face was estimated to be roughly 80 to 86% calcite by volume. Its calcite cross-sectional area,  $A$ , could be estimated as  $A = 0.8 \times \pi \times d1 \times d2$ , about 5 m<sup>2</sup>. These values will be used later (see Discussion).



**Figure 20.** Oval shaped break, "Large Broken Stalactite", Bush Rangers Hall.

Continuing with the cave observations, the embankment on which the platform is developed contains the remains of other broken and toppled speleothems, some of which appear corroded by bat guano, but are no longer in position (Figure 21). Bats no longer roost in this area in significant numbers.



**Figure 21.** Tilted stalagmites, Bush Rangers Hall.

At the junction of Creek Cave and Creek Cave Overflow a bedrock outcrop has grooves in the otherwise scalloped marble, and some of the scallops have been flaked off (Figure 22). This is in a similar area to a large flake described by James and others (1982). The distance from the site to the nearest entrance of Creek Cave Overflow is about 50 m. Nearby, a couple of cave shields have come off the ceiling and the remains of one is in the gravel nearby. This area floods at times. However, judging by the patina on the remaining scallops, and grooves cutting through the scallops, it would seem that the scallops, then grooves and flake formation were due to earlier processes, and removal of the flakes was a more recent process. This area can get quite cold depending on the direction of the wind blowing in from the entrances. There is a short length of broken bench in this area that is difficult to see when buried



**Figure 22.** Bedrock with grooves, scallops and flakes, Creek Cave.

with flood debris. It may have been undermined in past floods.

In the western end of Chalkers Retreat is a broken and apparently bent speleothem with oval cross-section. Broken pieces lie nearby but since the area was subject to many historical visits, it could have been broken by people (but not bent). Nearby, high on a wall is a slightly bent “broomstick” stalagmite. A groove (or wall notch) in the lower part of the northern wall lines up with other grooves along the wall, suggesting something abraded the wall at a particular height (Figure 23). Some of the broken-topped stalagmites in this area have regrowth, although it is unclear whether the breakage was from people or not. Speleothem “dribbles” on the walls are a feature and are best viewed with side lighting. At first glance, they resemble veins or candle wax dribbles, but closer inspection shows that they appear to have been formed in fine layers. They generally lack conventional microgours, unlike the usual flowstone or shawls seen at Wombeyan Caves.



**Figure 23.** Wall notch, Chalkers Retreat.

Where the floor changes or there is a shelf, one sees a type of concrete-like coarse-grained flowstone which also lacks conventional microgours and appears to be associated with the “dribbles” and

stalagmite breakage (Figure 24). Below a scalloped ceiling channel in the north-east area, grooves in the bedrock have apparently obliterated scallops in some areas but not others. One pendant appears almost cut through (Figure 25). We perceived a fairly large temperature difference between the humid eastern part and the cooler western part of Chalkers Retreat, which has a connection to the vertical Lots O Numbers Cave as well as the various other entrances of Fig Tree Cave.



**Figure 24.** Broken stalagmite stumps, concrete-like flowstone and dribbles, Chalkers Retreat.



**Figure 25.** Cut bedrock pendant, Chalkers Retreat.

Upper Marble Way (map, Figure 26) follows a ceiling canyon above the creek along a cantilever walkway. Broken stalagmites can be seen near the illuminated stalactite cluster near the junction of Upper Marble Way with the north-trending Belfry and the Drawing Room. Small flat-topped stalagmites lie below the illuminated stalactite cluster which also has broken tips and regrowth. Judging by apparent regrowth, the breakages appear to have occurred a long time ago. The surface texture of some of the speleothems appears unusual. Regrowth appears as “normal” calcite, covering an earlier growth of finer “dribbles” and crenulations. For convenience, we identified particular stalagmite sites with letters A, B, etc. On the opposite (south) side of the path, the showcave

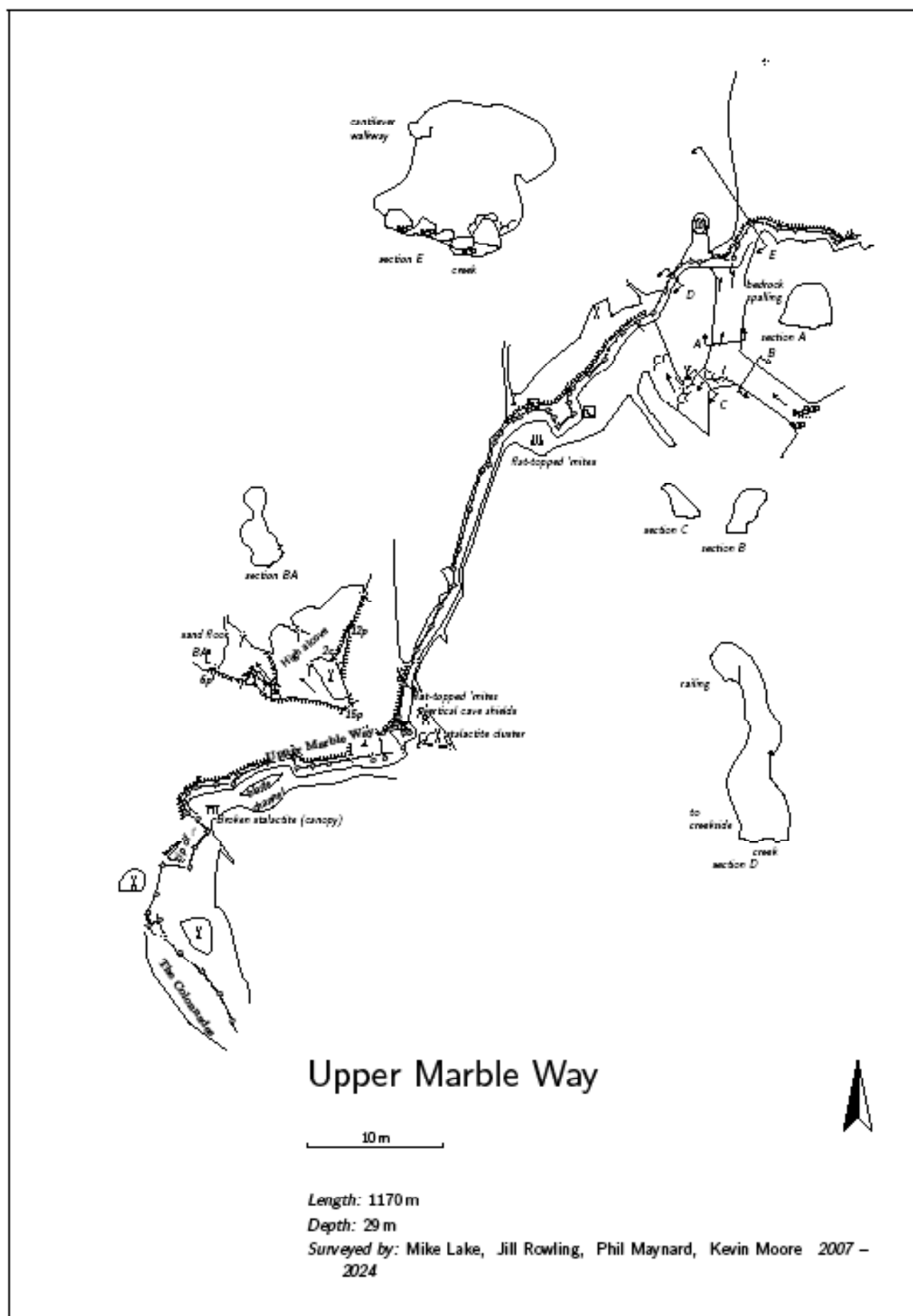


Figure 26. Plan of Upper Marble Way by the author. 10 m scalebar.



handrail has been installed over a broken stalagmite with regrowth. Another, site “B”, is on the SE side of the path at the bottom of the steps, and another one, site “E”, a little further to the northeast. Near E is a broken bedrock pendant and a deposit of flowstone resembling concrete. The area between B and E was potentially open to flood debris from the Belfry, although the creek is considerably lower down (about 10 m below). The positions of the tops of both stalagmites were surveyed, and the inclination was only 3° (the top of B is slightly lower – see Table 1). In the ceiling of this area is a sheared-off bedrock pendant, 4.4 m above a rocky surface which could be the missing piece. Above this again, the ceiling is scalloped but an area below that is devoid of scallops and instead has a smooth surface with broad horizontal grooves (Figure 27). The reddish material near the ceiling in the middle of the photo appears to be a flowstone, possibly the same material as occurs in the Drawing Room and apparently eroded by the same process that removed the scallops which are otherwise readily seen at this level.



**Figure 27.** Grooved ceiling canyon, Upper Marble Way.

A disc shape on the ceiling is most likely the site of a broken cave shield. Nearby are smaller intact shields, a sideways-flattened stalactite and a very thin, curved column with a surface texture of “dribbles”. Further NE along the track there is another group of broken speleothems (Figures 28, 29). Here, some of the broken bits are loose but others are naturally cemented near to where they came from. The force which broke them appears to have come from upstream, but was not enough to wash away the broken pieces. This group includes a broken stalactite cemented to the floor, and broken-topped stalagmites. One stalagmite still has the top nearby and is bottle-shaped from overgrowth. Some of the breaks show uneven parting (Figure 28). A partially toppled stalagmite has been covered with considerable flowstone (Figure 29) and has regrown



**Figure 28.** Broken stalagmite (detail), Upper Marble Way.



**Figure 29.** Broken stalagmites and dribbles, Upper Marble Way.

in place. Also, in this figure one can see vein-shaped “dribbles” and a conventional microgour flowstone coating some of the speleothems. One cemented stalactite (Figure 30) looks very similar to the cryogenic ridges described by Onac and others (2023).

Further northeast are more broken-topped stalagmites, “dribbles” and angular cuts in the bedrock. These cuts are deeper than exfoliation, and occur along parts of the southern wall of Upper Marble Way (Figure 31). They are typically about 10 – 20 cm high and 10 – 30 cm long, possibly 5 cm deep. Spoon-shaped grooves in otherwise normally eroded cave walls might have been caused by something rubbing across the wall. This is not the same as polishing (e.g. by rock wallabies or people) and is mostly found in inaccessible areas such as near the ceiling and can occur in the same area as angular bedrock cuts and apparent cryogenic ridges.

Closer to the exit gate, the platy exfoliation of the bedrock, noted by James and others (1982) was verified along the north-eastern wall of a short, steep tubular passage in bedrock, linking the upper Marble Way path to a daylight hole in the southwest



Site in Fig Tree Cave	From	To	Inclination	Notes
Colonnades	Flat-topped south stalagmite	Flat-topped northern stalagmites	0°	Three in a row close together, 14th September 2024. Figure 11.
Chalkers Retreat – cloister / vestry near section 12	Top of flat-topped south stalagmite	Top of flat-topped northern stalagmite	5°	Survey book p. 118, 22nd June, 2024. Includes regrowth.
Chalkers Retreat as above	Top of flat-topped south stalagmite	Top of flat-topped northern stalagmite	3° to 5°	Survey book p. 118, 22nd June, 2024. Excludes regrowth.
Upper Marble Way near the Stalactite Cluster	Flat-topped northern stalagmite E	Flat-topped stalagmite B, at bottom of steps SE of path	-3°	Survey book p. 109, March 23-24, 2024. About 5 m apart.

**Table 1.** Surveyed inclinations between flat-topped stalagmite groups, accurate to half a degree in inclination.



**Figure 30.** Broken speleothem with possible cryogenic ridges near light fitting, Upper Marble Way.

side of Victoria Arch. A darker colour on the walls near the plates is thought to be due to algae, as this area is in twilight, being dimly lit from its proximity to Victoria Arch. The plates themselves appear rather delicate, only about 1 cm thick and ranging from hand-sized to about a metre in length. They occur on the passage's eastern wall and are composed of marble (Figure 32, Figure 26 section B).

As one exits the Fig Tree showcave and walks eastwards past the gate, light from the south side doline of Victoria Arch highlights additional



**Figure 31.** Bedrock wedges and dribbles near hand rail, Upper Marble Way.



**Figure 32.** Platey exfoliation, Upper Marble Way.



## Cold-climate Events at Wombeyan

features. Elongated cut-off holes similar to phreatic tubes can be seen high in the south-western and north-eastern parts of Victoria Arch. Upper level tubes have an unusually elongated shape (inverted tear-drop) and their walls lack scallops (Figure 33).



**Figure 33.** Elongated holes, Victoria Arch.

Near the tube entrances, the volume of cave behind the tube does not appear to be great. Horizontal grooves occur in the bedrock. One is at around the same level as the aforementioned exfoliated bedrock and may be related to the passage with a similar feature. Another horizontal groove at the far north-eastern end of Victoria Arch appears to be roughly on the same level, although it curves upwards a little at its northern end and has a vertical slot partway along (Figure 34). At the northern end of the Arch, at a similar level to the platform built in 2024, is another notch with horizontal grooves (Figure 35). None of these high level Arch notches have scallops, although scallops are certainly plentiful in the lower passages of the Arch.



**Figure 34.** Grooves, northeast Victoria Arch.



**Figure 35.** Grooves, north Victoria Arch.

## Discussion

### Past climate and cave cold trap calculations

To estimate the current range of Wombeyan cave temperatures, a lapse rate of 6.5° Celsius per 1000 m was used based on the published mean temperatures for nearby Taralga (see Table 2). This data suggests a current mean minimum temperature at Wombeyan Caves of about 2.2°C which is not cold enough to significantly alter long-term speleothem development. However, where there is strong airflow, it is certainly possible for the air temperature in particularly draughty parts of Fig Tree Cave to get below zero temporarily. Ice expansion would break small water-filled speleothems such as straw stalactites in these areas. However, during the last glacial maximum (LGM) of the Pleistocene, winter temperatures could be on average some 8 Celsius degrees colder than at present (Barrows and others 2021). During that time, global sea levels were on average some 122 m lower than today, which would effectively put Wombeyan that much higher in altitude. The following methods used estimate the in-cave temperatures during the LGM:

- 1) Using the lapse rate, calculate the mean cave temperature ranges based on present ranges at the closest known weather station;
- 2) A simple subtraction of 8 Celsius degrees to estimate the expected range during Pleistocene glacial times.

On this basis, the mean annual temperature (underground rock temperature) in Fig Tree Cave would have been about 7°C during LGM, and the cold traps would be from -0.1° to -5.8° Celsius



(Table 2). Clearly the cave's geometry will dictate the actual temperatures possible.

Cave sumps, well away from diurnal temperature variations, would be expected to remain relatively constant at 7°C. Cold traps and chimneys then become significant in the caves. For example, if the valley's winter mean air temperature was -5.7°C during the LGM, then the chimney effect in a multi-entranced cave like Fig Tree Cave could result in cave cold traps remaining below freezing during the cooler months. This could have become significant if it was coupled with an increase in snow melt as suggested by Barrows and others (2021), as the mean annual temperature would have been positive. So, deep within most caves would have been ice-free; but in a cave's cold traps, pools of water could freeze over, incoming dripwater could form icicles (like the world's current ice showcaves for example Figure 1) and condensate from the sumps (discussed below) could freeze onto surfaces. The overall effect could be ice build-up in some areas which could take centuries to melt out, as presently occurs in Dobšinska Cave, Slovakia (Zelinka 2008). The effect of summer / winter temperature variations would melt ice surfaces near boundary areas, resulting in local expansions and

contractions of the ice and apply significant force to anything encased within it, as discussed below.

### Sources of moisture, warm and cold air

Referring to the cave model (Figure 3), most of the broken speleothems and speleogens are located at a level about 20 – 30 m above the current cave sump. As discussed by Halbert & Michie (1982) and modelled by Gabrovšek (2023), cave sumps are a source of relatively stable, warm humid air. During winter nights, dense cold air can descend shafts and displace warm humid air upwards from lower in a cave. At Wombeyan, this can result in areas of condensation at cold traps. If one extrapolates the modern temperatures back to Pleistocene glacial times, as in Table 2, it seems plausible that there could be ice build-up in areas where condensation would have occurred, assuming a similar cave geometry. Another source of moisture is groundwater dripping from stalactites, discussed later. The two sources of water (condensate vs. groundwater) would have different chemical composition, with condensate tending to be corrosive to speleothems (James and others 2004, p. 42), while groundwater would tend to precipitate speleothems.

Site	Taralga	Hockey Gully	Bullio Cave cold trap	Victoria Arch saddle	Camping Ground, and Wombeyan Ck in Fig Tree Cave
<i>Values for each site, where known</i>					
Present altitude, m AMSL (approximates are from topographic map)	845	650	620 m approx.	620 mm approx.	620 mm approx.
Tmax mean maximum temperature, °C	26.2		20		
Tmin mean minimum temperature, °C	0.7		7.9		
<i>Estimates below for present, derived from lapse rate of -6.5°C/1000 m, using Taralga values</i>					
Tmax mean maximum temperature, °C		27.47	27.66	27.66	27.79
Tmin mean minimum temperature, °C		1.97	2.16	2.16	2.29
Rock temperature, °C (average annual temperature of site)	13.45	14.72	14.91	14.91	15.04
<i>Temperature estimates below for the Last Glacial Maximum (LGM) – see text for explanation</i>					
LGMTmax (Tmax - 8), °C	18.2	19.47	12	19.66	19.79
LGMTmin (Tmin - 8), °C	-7.3	-6.03	-0.1	-5.84	-5.71
LGM rock temperature, °C (LGM average annual temperature of site)	5.45	6.72	5.95	6.91	7.04

**Table 2.** Present values for site elevation and mean temperatures compared with calculated temperature estimates for the same sites during the last glacial maximum. Site height estimates are based on the topographic map, +/- 10 metres for the approximate site heights.

## **Bedrock exfoliation, scallop removal and grooves in the rock**

Platey exfoliation, as seen near Upper Marble Way of Fig Tree Cave, and in Creek Cave, resembles an unloading effect as if the wall had been subject to pressure. The plates themselves are quite delicate and unlikely to survive much water or debris flow since their formation. Consider a marble tube in a cold trap during the last glacial maximum, ice filled, undergoing repetitive expansion and contraction as the temperature varies about the freezing point (as per Spötl and others 2023). The forces will be even all round, and as Hueckel (2016) indicated, most likely making noises as the Wombeyan marble is compressed towards its maximum strength, due to growth of cracks, fractures and plastic deformation. After the ice retreated, simple unloading will gradually form concentric rock flakes and plates. The same processes may have removed the scallops by local ice expansion, causing exfoliation, but many of the plates in Creek Cave have since been removed by floods. Only the colour of the patina shows us where the plates once were. Note this process has not occurred everywhere in the cave, but only where there are other apparent ice-influenced features.

Grooved rock surfaces as seen in Victoria Arch could be the result of ice very slowly flowing past, with entrapped rock debris creating grooves. That is, the ice itself did not abrade the bedrock, but rock debris spalled from the wall near the cave's entrances became entrapped in ice. Very slow movements of the ice and rock deposit would then erode the sides of the Arch. Another possibility is an ice-covered pool of water in the Arch, but in that case one expects the grooves to line up across the passage, which they do not. This aspect needs further investigation.

Angular cuts in the bedrock as seen in Victoria Arch, Creek Cave, the Drawing Room and Chalkers Retreat could be caused by a similar process but with a more directed force rather than an evenly-spread force. For example, the crack in the bedrock to the right of the fractured speleothem in Figure 12, where a thick block of ice may have formed on the top of a lake, undergoing temperature variations near the freezing point.

Spoon-shaped grooves in cave walls could be caused by a flow of ice gradually moving across that part of the wall. Embedded calcite grit

(cryogenic calcite) could assist the ice to erode and polish the wall.

## **Breakage of the “large broken stalactite” – a theoretical approach**

Speleothem breakage is commonly dismissed with a handwaving argument when no other information has come to light. In the case of the “large broken stalactite”, ideas have been suggested such as flood events, earthquakes or just being too heavy. Let us consider how the speleothem could have been damaged by examining the forces needed to break it, and compare that with forces expected from 1) being “too heavy”, 2) an earthquake, 3) a log propelled by a flood, 4) a mass-flow event and 5) by ice expansion.

Assumptions: We do not have exact values for the strength of Wombeyan stalactites and in any case they are likely to be variable in strength as they are all different shapes and have different growth histories, but as they are made of calcite they are unlikely to be greatly different from the European examples. We assume a calcite speleothem may break with about 1 to 5 MPa under tension (Spötl and others 2023). This is 1 MN to 5 MN / m<sup>2</sup>. The face of the detached piece was estimated earlier to be about 5 square metres of calcite, so the amount of force required to pull it apart would be 5 MN to 25 MN. If force is applied as a cantilever, the force required to break the speleothem is similar to that under tension, as it is unconfined. If the force is applied to the side of the speleothem, the area is the full length 3.9 m long by 1.8 m width. Ribbing tends to make this shape somewhat resilient to crack propagation, and the calcite crystals are usually arranged with their C axes pointing outwards. This should give the canopy similar structural properties to marble bedrock.

### ***Case 1: Could it break under its own weight?***

As an exercise, let us consider the mass of the stalactite and what force is needed to break it. Compare the mass of the broken part to the mass of the entire speleothem. Calcite density is 2.71 g/cm<sup>3</sup> or 2.71 tonnes per cubic metre. From the dimensions given earlier, the broken lower bit could be considered a cylinder with an oval cross-sectional area of  $\pi \times 1.18 \times 1.4$  m and length of 1.7 m, so its volume would be (multiply all above times 0.8 for fluting) 7.05 m<sup>3</sup> and its mass would be 19 tonnes.

The mass of the original (reconstructed) canopy, assuming similar oval cross section:

$0.8 \times 3.859 \times \pi \times 1.18 \times 1.4 \times 2.71$  tonnes = 43 tonnes.

The weight of the (now-broken) lower part when originally attached to the upper part would be usually (under static conditions)  $9.8 \text{ ms}^{-2} \times 19000 \text{ kg} = 186200 \text{ N}$  which is significantly less than that required to fracture the stalactite (5 MN). Thus, it is not plausible that it broke from being too large.

### ***Case 2: Could the damage be from an earthquake?***

A massive earthquake could break the stalactite but one would also expect there to be some considerable rock movement, damage along existing joints and cracked flowstone which is not found in that area. At least one known near-vertical fault can be seen striking roughly eastwards near the western entrance of Creek Cave. A bench has collapsed in Creek Cave Overflow, but it is localised and appears to have been undermined. Also, there are plenty of delicate speleothems in the cave which have not been damaged. Other large speleothems such as the fallen stalactite in the Opera House should have shattered, but it appears relatively intact, so something cushioned its fall. Generally, earthquakes are only felt strongly on the surface and are not felt deep underground. If there was ground movement, one expects it would topple large stalagmites, breaking them from their bases. Some have a strong lean but this could also be from other causes such as substrate movement. Most other breakages seen are part-way down the speleothem. If there was movement along the known fault, one would expect the “large broken stalactite” to be damaged near its attachment point, which is intact (Figure 14).

Using the values from Case 1, the lower 19 tonne portion of the stalactite would have to oscillate considerably to break off from the rest of the canopy. It is plausible that there was an earthquake. However, there would need to be a lot more damage to the cave for the earthquake concept to be more convincing.

### ***Case 3: Was it struck by a log in a flood?***

Consider a horizontal force applied to the lower end of the original canopy, forming a cantilever. If a log came down the creek during flood, could it break the drapery? Typical floods rush in the confined space below at around 2 m/s. When

floating logs interact with objects, they tend to move about in the channel. Consider the force  $F$  applied to the end of the stalactite by a log of mass  $m$  travelling at 2 m/s striking the stalactite during a flood. Let us assume that the stalactite can flex a little, and the floating log takes 0.1 seconds to come to a complete standstill. The deceleration  $a$  of the log is 2 m/s per 0.1 s, so  $a = 2 / 0.1 \text{ ms}^{-2} = 20 \text{ ms}^{-2}$ . Then the force applied, using  $F = ma = 1000 \text{ kg} \times 20 \text{ N} = 20 \text{ kN}$ . This is significantly less than the force needed to break the canopy, although it could break something smaller such as the tips. If we decrease the hypothetical stopping time, it is still hard to get close to the 5 MN needed to break the “large broken stalactite” within the confines of the canyon and the setting. The scenario is therefore implausible.

### ***Case 4: Was it damaged by a mass-flow event?***

Consider a hypothetical major flood event creating a mass-flow of mud, water and sediments rushing past the “large broken stalactite”. Most of the hypothetical slurry goes past without interacting, but the part impacting the stalactite applies a force from its deceleration over the impacted area. Such an event would have left material behind, yet there is nothing obvious at the site which would suggest such dense material flowed down this part of the canyon. The scenario is thus implausible.

### ***Case 5: Was it damaged by ice expansion?***

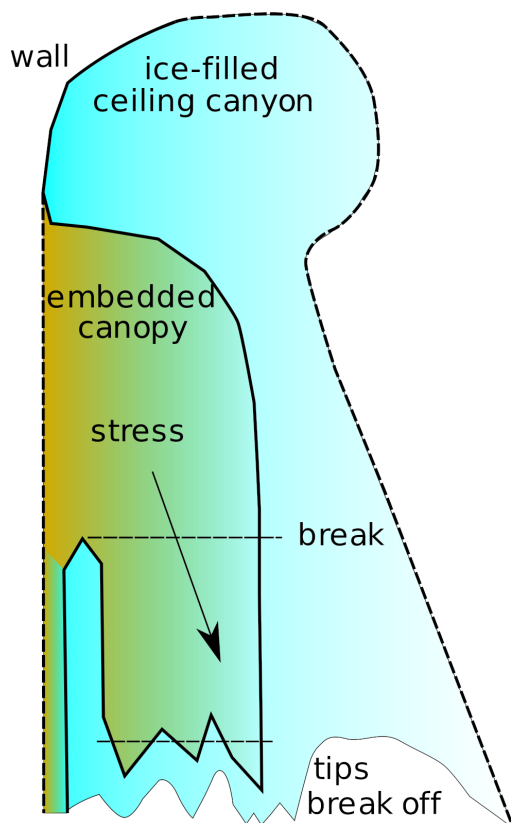
As noted earlier, a simple flow of ice will not crack the speleothem. But thermal expansion cycling around freeze / thaw temperatures in a confined space will easily reach the pressures described above if the speleothem is completely encased in ice.

Let us assume the site is a cold trap during the last glacial maximum. Refer to Table 2 for expected temperatures. In this situation, ground temperatures are still high enough for groundwater to be liquid, but the site air temperature is well below freezing, so water dripping onto the canopy will quickly freeze. Ice will build up over the original intact canopy, possibly filling all the space above and around the canopy as shown in Figure 36. Assume there is considerable thickness of ice buildup compared to the diameter of the speleothem, and the ice is in contact with the speleothem surface and the walls. Now allow the mean temperature to vary above around the ice freezing point which allows ice to expand and contract more than the calcite, due to their differing thermal coefficients of expansion.



This will stress the speleothem in directions in which the ice can move: downwards, sideways, both upstream and downstream. The forces applied are from stress proportional to the temperature and ice thickness, as well as the overall mass of the speleothem (discussed in the Case 1 scenario). Repeated thermal cycles will crack the speleothem and eventually break it.

**Figure 36.** Sketch showing how the "Large Broken Stalactite" may have been stressed by ice during an ice age.



Perhaps the lower stalactite tips broke first, being thinner and weaker. Once the larger piece was broken, it could slowly sink into ice and sediment, then all the ice eventually melted leaving just the sediment and the lower portion of the speleothem in its current position. So this scenario is plausible.

### Other broken speleothems and speleogens

Other broken canopies and stalactites (Figure 13) were seen in the ceiling a few metres to the west of the "large broken stalactite". The largest is broken 5.9 m down from the ceiling channel which is relatively flat-topped, and it is interesting to compare this with the "large broken stalactite" which has broken 5.8 m down from the ceiling channel. This is a similar level to the other areas

of Upper Marble Way with broken speleothems and speleogens. This type of clustered breakage was noted by Spötl and others (2023). The broken stalactite or shield in the Opera House has not shattered where it fell, but may have also come down onto a cushioning pile of ice. The toppled stalagmites in Bush Rangers Hall may have been assisted by ice expansion. The fracture seen in a calcite column in Bush Rangers Hall lines up with a wall notch nearby (Figure 12) and the various breakages in the Colonnades, suggesting a common cause such as a frozen pool of ice at the same level, together with ice build-up on speleothems.

Some of the broken stalagmites along Upper Marble Way are broken about half way along, and are not chamfered along the typical calcite cleavage as would be expected from a knock, but rather they are parted in steps as though pulled apart, with the steps most likely associated with a dusty layer where calcite deposition was not continuous, for example, Figure 28. Others have broken with a typical chamfer but have considerable regrowth suggesting the break happened long before the showcave was developed.

Fractured and broken speleogens may have been damaged by a mechanism similar to that of the stalactites. For example, the rock pendants damaged in the northern end of the Opera House, the Drawing Room, Chalkers Retreat and Upper Marble Way.

Although the main break of the "large broken stalactite" was likely to have occurred during the LGM, the straw regrowth of a "few hundred years" (James and others 2004) may be correct; perhaps the straw stalactites do regrow, only to be broken during the next cold period. A "few hundred years" could even be the "Little Ice Age" of the 16th – 19th centuries. A drop of only one degree Celsius could lower the Wombeyan average minimum temperature, and frosty winter nights may have been more frequent then. Straw stalactites growing in a cold trap would then be a temporary feature, and perhaps the loose straw seen on the stalagmite boss came down during a recent frosty night.

Throughout the cave, many broken-off pieces of stalagmite or stalactite are cemented to flowstone in dry areas. This does not indicate how the breakage occurred, but it does indicate that the breakage occurred long before the showcave was developed, and there was no great flood of water or debris through the area immediately post-breakage, otherwise the pieces would have been washed away.

## Bent speleothems

Bent columns, curved stalagmites and stalactites could be caused by growth around tree roots or by wind deflection, even rockpile movements. However if they occur in the same area as other potential ice-related features, then pressure from ice expansion could also apply. The geometry could be checked to be more certain, and each speleothem will be different. It is possible for marble to be bent under constant pressure if it is confined, as per Hueckel (2016). Another consideration regarding bent stalactites that resemble tree roots: if the speleothem was formed during mid-Pleistocene, when there was a lack of trees as per Barrows and others (2021), then it is less likely that tree roots caused these bends. More work is needed in this area.

## Cave welts in the Drawing Room

Welts are a feature of most columns in the Drawing Room (Figure 7). Hill and Forti (1997, p. 99) noted that they develop similarly to a cave shield, where a slowly opening crack guides carbonate solutions to the outside of the crack, allowing calcite to precipitate around the edges. In the case of the Drawing Room welts, the upper side has a deposit resembling concrete, and the lower side is more stalactitic. This suggests the material on the upper side may be deposited from material dribbling down to the welt, and the lower cascade of stalactites may be from excess material coming out of the welt's crack. The ceiling is bedrock, and the floor is a sediment of unknown depth. A common structural change has allowed welts to develop only on the columns, but not single-ended speleothems such as stalagmites. This could arise from heaving of the substrate, temporarily compressing the columns which will then slightly bend. Continued compression will crack the centre of the column where the bend is greatest, and a slow subsidence back will expose the cracks in the columns, allowing the welts to form. If instead, the substrate had subsided first, the columns would then be subject to tension. This would typically have eventually detached them from one of their end points such as the ceiling, and one would expect a set of helictites (for example) to develop at the top of the columns. This has not occurred, so it is more likely that the substrate heaved first. If the substrate had been wet, then froze sufficiently, this could temporarily cause heaving. The process may be similar to that described by Lundberg and McFarlane (2012) in Kents Cavern where periglacial conditions and

air flow in the cave led to lowered temperatures, substrate frost heaving and flowstone cracking.

## Cryogenic ridges

The ridged surface of some stalagmites in the Drawing Room, and at least one of the small, toppled speleothems in Upper Marble Way, look like cryogenic ridges. Further work could be done in this area, in particular stable isotopic analysis to clarify the temperatures of deposition, as there are similarities with tropical deposits such as moonmilk (B. Onac pers. comm. to the author, 29 and 30 October 2024).

The current temperature regime may support a small amount of cryogenic calcite formation during the coldest month (July). Some of the ridges could be associated with substrate cracking, so could result in small stegamites. The area can get quite cold at times and this aspect should be investigated.

Are the ridges caused by tree roots? This is more problematical to disprove, but we could not see the remains of tree roots. Usually if they had been present, there would be dark organic remnants and these areas seem quite devoid of such material. Tree roots do exist in the northwest of Chalkers Retreat, near its connection with Lots O Numbers Cave, above. Cryogenic ridges should be considered where speleothems are claimed to be from tree roots, but no actual organic material is found. If they are cryogenic ridges, they should have hairline gaps longitudinally down the ridges. If tree roots are suspected, one should be able to see actual tree roots in the area. Most tree roots do not descend deeply into bedrock; they follow the water lines. Also, tree roots tend to be larger towards the tree, whereas the fine gaps in cryogenic ridges are generally more irregular in width. Note also the previous comments about the lack of trees during the mid-Pleistocene, if the speleothem developed during that time.

## “Dribble” speleothems and concrete-like flowstone

At Wombeyan Caves, the surface texture of many active calcite speleothems is usually of the fine microgour style, and smooth textures are sometimes due to moonmilk. “Dribbles” of presumed fine grained calcite deposited on stalagmites or walls do not appear to have been described, at least not at Wombeyan. Since we have only found them in areas with other possible ice features, it is thought that they are related to colder depositional

temperatures. In the same areas we found coarse-grained concrete-like flowstone deposits which appeared to be related to the “dribble” features. Whether they are from fine or coarse CCC (Munroe and others 2021) is unknown. More work is needed to clarify what they are. What we know so far about them is that they occur in areas of the cave with other suspected cryogenic activity. They are on mostly vertical to near-vertical surfaces. They appear to be comprised of fine layers of calcite with a chalky appearance; their edges are slightly undercut and uneven; they generally have a sinuous shape. They may have a deposit of concrete-like flowstone at their lower end, and their upper end may be indistinctly developed on the bedrock. They may branch and re-join. Their surface may have a very fine microgour pattern, much finer than “normal” microgour flowstone.

### Large elongated holes in Victoria Arch

The elongated holes (inverted tear-drop shape) seen in Victoria Arch are usually described as abandoned phreatic tubes, which they may be. Normally, active phreatic tubes transition to vadose with a slot canyon or similar, and sometimes the other way around for vadose to phreatic, but the holes seen fairly high in Victoria Arch are either simply round, or have a ring of flaked bedrock near the outer edges, as though there was some pressure evenly distributed around the outer edges. Those with an inverted tear-drop shape could have been shaped by grit being moved along the lower part of the channel. Possibly during one of the past ice ages, there may have been a build-up of ice filling smaller phreatic tubes, wedging the outsides and enlarging them. In Slovakia, in 2013, the author saw ice in the lower slots of abandoned phreatic tubes in ice showcaves, and presumably expansion / contraction grinds grit along their lower edges, to be washed out in the thaw along with any CCC grit.

### Implications for Pleistocene fauna

Fossil vertebrates at Wombeyan Caves include *Burramys parvus*, now only known from alpine regions (Hope 1982). Undated bones of megafauna and other material extracted from a nearby active quarry suggest a Pleistocene age for them, possibly 13 ka – 17 ka based on the faunal assemblage. This suggests the area may have had an alpine vegetation at the time, which agrees with other studies such as Barrows and others (2021). As the cave ice thawed seasonally, karst springs would have been available to fauna at the time in an otherwise relatively dry

landscape. Further afield, the author has seen a large broken and re-cemented stalactite at Wellington Caves (also, incidentally, a Pleistocene megafauna site). Cave ice thaw typically lags surface snow melt as, for example, if compared with modern showcaves containing ice deposits. The opening times for modern “ice showcaves” in central Europe reflect this, where the showcaves are closed in autumn during their ice thaw. The period over which groundwater was available from snow and ice melting would be extended in areas where caves contained ice deposits compared with those which had no ice.

### Other cave areas with naturally broken speleothems

Large broken speleothems have been recorded by various photographers in Eastern Australian caves at Jenolan, Yarrangobilly, Mole Creek, Wellington, Cliefden and Abercrombie. There may be many more sites within south-eastern Australia.

In south-east Asia, people have reported large broken speleothems in caves in Vietnam and Malaysia. Many of these caves appear to be good initial candidates for consideration as Pleistocene cold caves given their large size, the possibility of chimney effect and their location near mountainous areas.

### Conclusions

It is suggested that Fig Tree Cave and Victoria Arch once had deposits of permanent ice, possibly during the Last Glacial Maximum of the Pleistocene, based on evidence for speleothem and speleogen damage by ice expansion and contraction as the temperature varied about the freezing point. Ice build-up could have been caused by cave geometry, promoting cold traps in specific areas of the caves, even though ice may not have been a permanent feature outside of the caves or even deep in the caves. Individual features such as speleothem breakage would not be conclusive evidence for past cold-climate processes, but a collection of many features all in the same localised area is more convincing. The presence of ice in the cave could also explain both the bedrock exfoliation and the “large broken stalactite” seen in the cave.

As other caves also have broken speleothems and features similar to those described here, it is suggested that the caves were particularly cold during winters of the last glacial period. At present,



ice does not build up in the caves to any significant amount, but during past glacial periods, ice did build up, mainly from the chimney effect. The presence of suspected cryogenic speleothems and types of damage caused to parts of the cave may help us to gauge the significance of cooling in the area at the time. This could be used as a palaeoclimate proxy for the region, complementing the periglacial scree slope measurements by Gillieson and others (1985), studies of relict periglacial block deposits by Slee and others (2023) and regional climatic studies by Barrows and others (2021).

Most caves are very complex, and numeric modelling of air flow can become complicated. It should be possible to estimate a cave's cold-trap Pleistocene temperatures by measuring its current cold-trap temperature ranges over a couple of years, then use the methods described here. If possible, there should be several points of temperature measurement as there can be differences with wind direction. Some assumptions may need to be made about the air flow with the past cave geometry compared with its current geometry (removal of sediments, or addition of gates and bridges, for example).

### Further work

Better analysis of apparent cryogenic cave carbonates would include stable isotope studies to help determine the temperature during formation, and Scanning Electron Microscopy could help to distinguish moonmilk from other calcites or aragonite. X-ray Diffraction could be used to determine mineral species present. Monitoring of current temperatures around various sites in the caves would give insight into how variable the temperatures can be at present, and then extended to calculating what they could have been during past colder periods. Stratigraphy may help constrain the dates of the deposits and hence which cold periods could have been involved. Further work is needed to determine what the apparent calcite "dribbles" and concrete-like flowstones are. Similar features from other caves in the Wombeyan area will be documented, especially the show caves such as Koorina Cave and Wollondilly Cave. The work will be extended to include Jenolan Caves and Yarrangobilly Caves as they are at higher altitudes than Wombeyan, and Abercrombie Caves which also have fractured stalagmites and sculpted bedrock forms. Large toppled and broken speleothems with upright regrowth have been

reported from other caves in eastern Australia and elsewhere, and it would be interesting to see if the techniques described here could indicate where other caves may have contained permanent ice deposits during previous colder times.

Further work could be done on modelling breakage for particular stalactite geometries, including the welts in the Drawing Room, and modelling airflow within the cave system as per Gabrovšek (2023), as well as obtaining more temperature data for particular caves. Further investigation is needed on the grooves and other patterns in the Arch.

### Acknowledgements

The author is grateful for the assistance of staff with the New South Wales National Parks and Wildlife Service for access to the showcaves; to members of the Sydney University Speleological Society who surveyed the caves; to Dr Mike Lake and Dr Phil Maynard for general assistance during this project, and to Prof Bogdan Onac for helpfully commenting on possible cryogenic ridges of Figure 30, and suggesting further work. The author is most grateful for the constructive criticism of reviewers, which has helped to improve the article.

### References

- BAHRANI, N., VALLEY, B., KAISER, P.K. & PIERCE, M. 2011 Evaluation of PFC2D grain-based model for simulation of confinement-dependent rock strength degradation and failure processes. *45th U.S. Rock Mechanics / Geomechanics Symposium, San Francisco, California, June 2011*. Paper Number: ARMA-11-156.
- BARROWS, T.T., MILLS, S.C., FITZSIMMONS, K., WASSON, R. & GALLOWAY, R. 2021 Low-altitude periglacial activity in southeastern Australia during the late Pleistocene. *Quaternary Research*, 107: 125-146. <https://doi.org/10.1017/qua.2021.72>
- GILLIESON, D., SPATE, A. & HEAD, J. 1985 Evidence for cold climate processes at Wombeyan Caves, Southern Tablelands, New South Wales. *Search*, 16(1-2): 46-47.
- GABROVŠEK, F. 2023 How do caves breathe: The airflow patterns in karst underground. *PLoS ONE*, 18(4): e0283767. <https://doi.org/10.1371/journal.pone.0283767>

## Cold-climate Events at Wombeyan

- HALBERT, E. & MICHIE, N. 1982 Climate above and below ground. [in] DYSON, H.J., ELLIS, R. & JAMES, J.M. (Eds), *Wombeyan Caves: Sydney Speleological Society Occasional Paper*, 8: 137-154.
- HILL, C. & FORTI, P. 1997 *Cave Minerals of the World*. Second Edition. National Speleological Society, Huntsville AL.
- HOPE, J. 1982 Fossil vertebrates from Wombeyan Caves. [in] DYSON, H.J., ELLIS, R. & JAMES, J.M. (Eds), *Wombeyan Caves: Sydney Speleological Society Occasional Paper*, 8: 155-164.
- HUECKEL, T. 2016 Instability phenomena in geomechanics - A review from a multi-physics point of view (pp. 11-12) [in] SULEM, J., STEFANOU, I., PAPAMICHOS, E. & VEVEAKIS, M. (Eds) *ALERT Doctoral School 2016 Modelling of instabilities and bifurcation in geomechanics*, pp. 3-28.
- JAMES, J.M., JENNINGS, J.N. & DYSON, H.J. 1982 Mineral decoration and weathering of the caves. [in] DYSON, H.J., ELLIS, R. & JAMES, J.M. (Eds), *Wombeyan Caves: Sydney Speleological Society Occasional Paper*, 8: 121-136.
- JAMES, J., BARNES, C., & WARILD, A. 2004 The magic of marble. [in] R. ELLIS (Ed.), *Caves and karst of Wombeyan: Sydney Speleological Society Occasional Paper*, 13: 75-84.
- JENNINGS, J.N., JAMES, J. & MONTGOMERY, N.R. 1982 The development of the landscape. [in] DYSON, H.J., ELLIS, R. & JAMES, J.M. (Eds), *Wombeyan Caves: Sydney Speleological Society Occasional Paper*, 8: 45-64.
- KEMPE, S. 2004 Natural speleothem damage in Postojnska Jama (Slovenia), caused by glacial cave ice? A first assessment. *Acta Carsologica*, 33(1): 265-289.
- KUKULJAN, L., GABROVŠEK F. & COVINGTON M.D. 2021 The relative importance of wind-driven and chimney effect cave ventilation: Observations in Postojna Cave (Slovenia). *International Journal of Speleology*, 50(3): 275-288. <https://doi.org/10.5038/1827-806X.50.3.2392>
- LUNDBERG, J. & MCFARLANE, D. 2012 Gryogenic fracturing of calcite flowstone in caves: theoretical considerations and field observations in Kents Cavern, Devon, UK. *International Journal of Speleology*, 41(2): 307-316. <http://dx.doi.org/10.5038/1827-806X.41.2.16>
- MCDONALD, J. & DRYSDALE, R. 2004 Palaeoclimate research in Wollondilly and Kooronga Caves. [in] R. ELLIS (Ed.), *Caves and karst of Wombeyan: Sydney Speleological Society Occasional Paper*, 13: 75-84.
- MUNROE, J., KIMBLE, K., SPÖTL, C., MARKS, G.S., MCGEE, D. & HERRON, D. 2021 Cryogenic cave carbonate and implications for thawing permafrost at Winter Wonderland Cave, Utah, USA. *Nature Scientific Reports*, 11 (6430). <https://doi.org/10.1038/s41598-021-85658-9>
- ONAC, B.P., CLEARY, D.M., DUMITRU, O.A., POLYAK, V.J., POVARĂ, I., WYNN, J.G. & ASMEROM, Y. 2023 Cryogenic ridges: a new speleothem type. *International Journal of Speleology*, 52(1): 1-8. <https://doi.org/10.5038/1827-806X.52.1.2416>
- SEFTON, A. & SEFTON, I. 1982 The show caves. [in] DYSON, H.J., ELLIS, R. & JAMES, J.M. (Eds), *Wombeyan Caves: Sydney Speleological Society Occasional Paper*, 8: 13-44.
- SLEE, A., BARROWS, T.T., SHULMEISTER, J., GONTZ, A., KIERNAN, K., HAWORTH, R., CLARK, D., FIFIELD, L.K. 2023 The age and paleoclimate implications of relict periglacial block deposits on the New England Tablelands, Australia. *Quaternary Research*, 111: 121-137. [doi:10.1017/qua.2022.32](https://doi.org/10.1017/qua.2022.32).
- SPÖTL, C., JAROSCH, A.H., SAXER, A., KOLTAL, G. & ZHANG, H. 2023 Thermoelasticity of ice explains widespread damage in dripstone caves during glacial periods. *Nature Scientific Reports*, 13 (7407). <https://www.nature.com/articles/s41598-023-34499-9.pdf>
- THOMAS, O. & POGSON, D. 2012 *Goulburn 1:250 000 Geological Sheet S1/55-12*, 2nd edition, explanatory notes. Geological Survey of New South Wales.
- ZELINKA, J. 2008 Cave microclimate [in] PAVEL, Bella (Ed.) *Caves of the World Heritage in Slovakia*, pp. 87-94. State Nature Conservancy

of the Slovak Republic, Slovak Caves Administration, Liptovský Mikuláš.





This page is intentionally blank

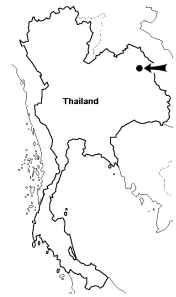
# Seri Thai System, a large cave in the quartz sandstones of North-east Thailand, geology, morphology and genesis

Liviu Valenas<sup>1,3</sup>, Martin Ellis<sup>2</sup> & Maliwan Valenas<sup>3</sup>

1 TU Bergakademie Freiberg, Institute of Geology, Chair of Hydrogeology and Hydrochemistry, Gustav-Zeuner-Str. 12, 09599 Freiberg, Germany. liviu.valenas@gmail.com

2 Shepton Mallet Caving Club, Somerset, BA4 5TT, UK. thailandcaves@gmail.com

3 Speleological Club "Z" Nuremberg, Germany. maliwan.valenas@gmail.com



## Abstract

North-east Thailand was considered relatively uninteresting from a karst and speleological point of view until a few years ago, as 90% of its area is quartz sandstone, which was wrongly considered to lack karst. In 2011, systematic research began in North-east Thailand, noting that the entire area contains large caves in these sandstones, as well as other karst phenomena such as karren, sinkholes, blind valleys, ponors and karst springs. Since 2023, the research has been supported by the Technical University of Freiberg, Germany.

One of the caves studied for the first time was the Seri Thai System. This is a highly labyrinthine underground complex, 1,124 m in total length, comprising three parallel branches, connected either by extremely narrow joints or low galleries and has 28 entrances. The System is a good example of a karst on sandstone, which may also be called "silicate karst". It is a dendritic labyrinth, active only during the monsoon season when it exhibits a complex hydrogeological organization, complete from sink and resurgence. The formation of this system is the result of a combination of factors, primarily the process of arenisation of quartz sandstones under monsoon climatic conditions, accentuated by corrosive processes due to tropical vegetation. The Seri Thai System is also a lithological contact cave, as it occurs between different layers of quartz sandstones and clay.

## Introduction

The Seri Thai System is located in Sakon Nakhon province in North-east Thailand (Figure 1), within the Phu Phan National Park, near the Seri Thai historical monument. The surrounding area is 90% forested with various tropical and subtropical trees (Figure 2). Because this area is strictly protected, the vegetation has remained intact. The most common tree species are *Dipterocarpus tuberculatis*, *Dipterocarpus obtusifolius*, *Shorea obtuse* and *Shorea siamensis*. However, *Dipterocarpaceae* predominate. In the area the predominant soils are ferarsoils, Acrisols and laterites (Figure 3).

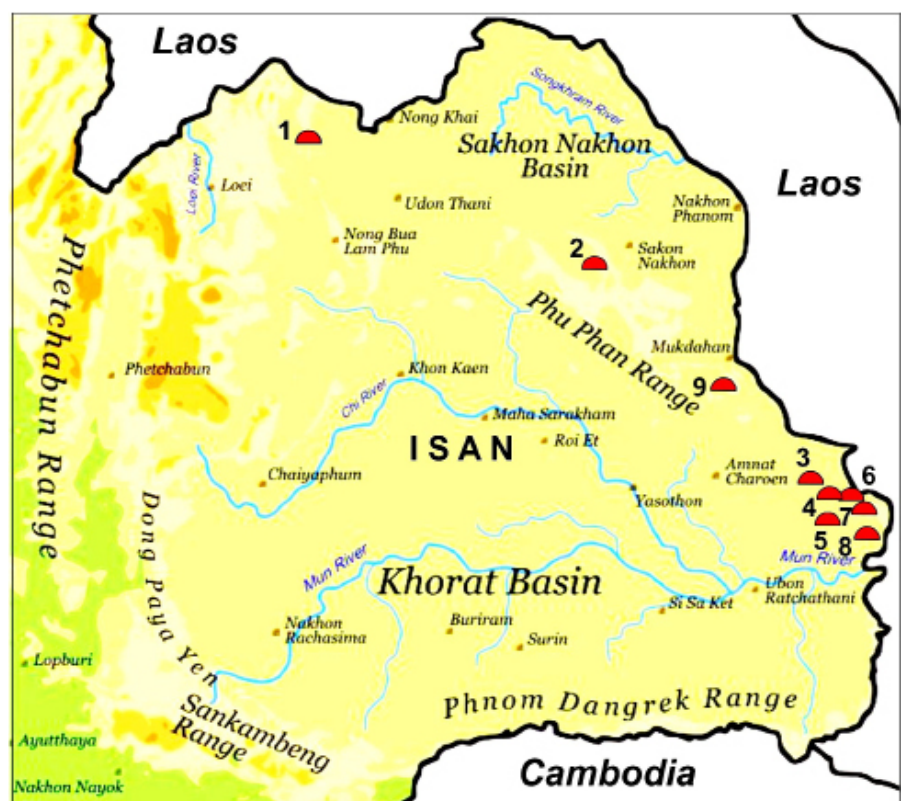


**Figure 1.** Map of North-east Thailand showing the main sandstone caves. 1 Tham Din Pieng, 2 Seri Thai System, 3 Tham Phu Pom No. 1, 4 Phu Phanom Di System, 5 Tham Nam Lot, 6 Tham Ghia, 7 Tham Meut, 8 Tham Patihan, 9 Tham Phusi Kew.





**Figure 2.** Forest in the immediate vicinity of the lower entrance to the Seri Thai System (entrance No. 20).



**Figure 3.** Typical landscape in the Seri Thai System area.

The upper (or “historical”) entrance is located at 17.099°N, 103.972°E at an altitude of 318 m asl.

North-east Thailand consists mainly of the Khorat Plateau, the altitude of which varies from 140 to 180 m asl with several mountain ranges, such as the Phu Phan Range, rising to more than 666 m asl (Pfeffer 2013). Geologically, the plateau and the mountain ranges are mainly composed of quartz sandstones and, in some places, volcanic rocks (Figure 4).

The quartz sandstones are currently known to contain 290 caves (Ellis 2017), three of which

exceed 1 km in length. The Seri Thai System is a dendritic labyrinth, active only during the monsoon. The system has a total length of 1,124 m (for comparison with other similar caves in the country, see Table 1) accessed through 28 entrances, 25 of them in the form of potholes (Figures 5, 6, 7 and 8). The cave was formed from the Middle Pleistocene, mainly by the process of arenisation of the quartz sandstones, but also by other processes (e.g. accelerated corrosion due to tropical vegetation and active tectonic processes). The System well illustrates a karst on quartz sandstone, sometimes called “silicate karst”.

**Sandstone Karst Research in North-East Thailand**

The first speleological explorations of the sandstone caves of North-east Thailand were carried out by French geologist and caver Claude Mouret. He had field trips to the region between 1992 and 1994, together with Louis Deharveng, Lien Mouret and Philippe Leclerc. The caves they explored and surveyed included Tham Patihan (Ubon Ratchathani province), Tham Cham Pha Tong (Sakon Nakhon province) and Tham Wat Sila At (Chaiyaphum province). None of these cave surveys have been published, but geological and geomorphological observations

have been published (Mouret 2004, 2017, Mouret & Mouret 1994). Australian caver John Dunkley had four trips around the north-eastern region looking for sandstone caves between 2011 and 2017. The caves researched on these trips included Tham Din Pieng (Nong Khai province) and Tham Nam Tok Saeng Chan (Ubon Ratchathani province) while other caves visited included the Seri Thai System and Tham Wat Sila At. Some observations from these visits were presented at conferences (Dunkley 2011, Dunkley & Bolger 2017) and published (Dunkley and others 2018).

No.	Cave Name, Province	Length (m)	Explored by	Date of exploration
1.	Tham Din Pieng, Nong Khai	2,747	Valenas/Speleological Club “Z”	2024-2025
2	Seri Thai System, Sakon Nakhon	1,124	Valenas/Speleological Club “Z”	2023-2025
3.	Tham Patihan, Ubon Ratchathani	1,029	Valenas/Speleological Club “Z”	2024-2025
4.	Tham Meut, Ubon Ratchathani	525	Valenas/Speleological Club “Z”	2020-2025
5.	Air Raid Shelter Cave No. 1, Phitsanulok	361	Dunkley, Ellis & Bolger. 2018	2011
6.	Tham Phu Pom No. 1, Amnat Charoen	284	Valenas/Speleological Club “Z”	2019-2020

**Table 1.** The longest sandstone caves in Thailand, 2025

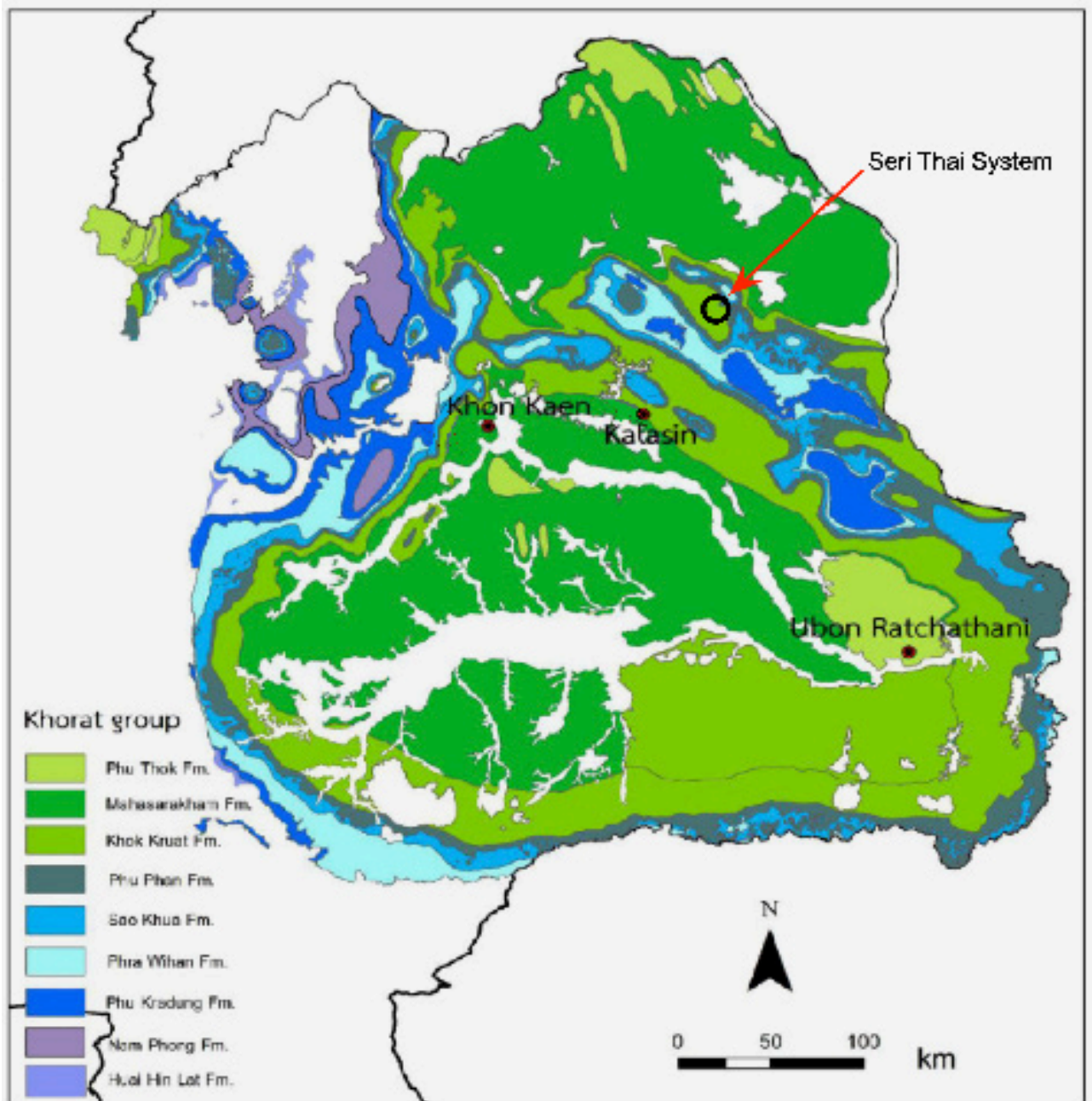


**Figure 4.** Geological map of Khorat Plateau, from Wongklo and others (2019).

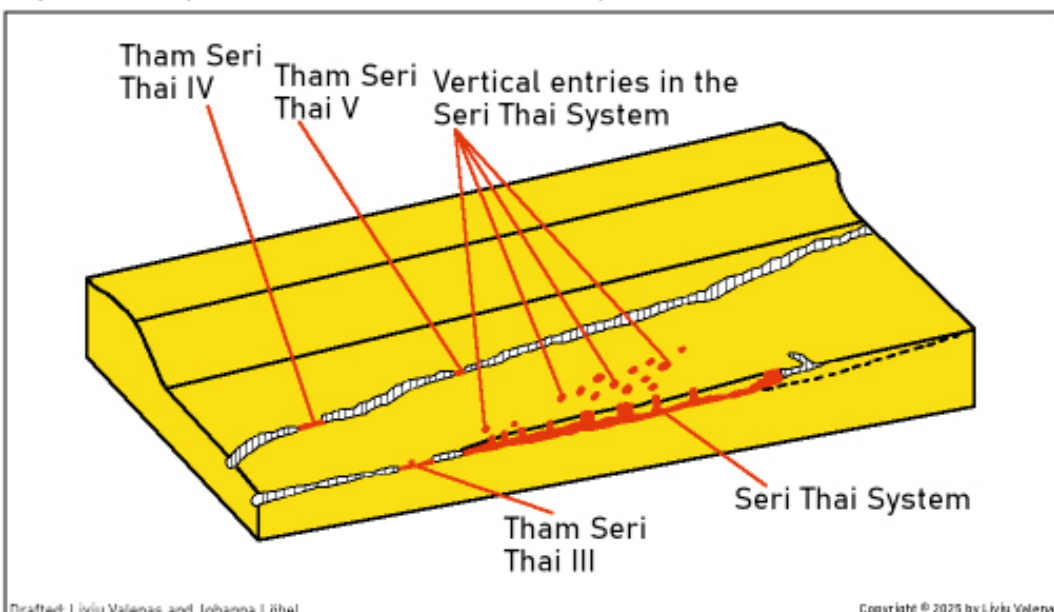


**Figure 5.** Block diagram of the relief in the vicinity of the Seri Thai System, showing the caves in the area:


Seri Thai System, 1,124 m long;  
Tham Seri Thai III, 55 m long;  
Tham Seri Thai IV, 32 m long;  
Tham Seri Thai V, 16 m long.





Total length: 1,124 m  
Depth: 22 m

<b>Survey:</b>	
2023-2025 Liviu Valenas	2024 Lim Yen Chen
2023-2024 Mallivan Valenas	2024 Ana Barilevici
2023 Suphakit Khamlioy	2025 Niamh Carman
2024 Timothy Callison Charlton	2025 Benjamin Robert
2024 Andrew David Filer	2025 Calvin Dorn
2024 Mindy Johnson Filer	2025 Rimma Jakovleva
2024 Dieuwert Grootaerd	2025 Mihai Wittenberger

Cartography: Liviu Valenas, 2025  
Speleological Club „Z”, 2025  
Map layout: Cristian Radu

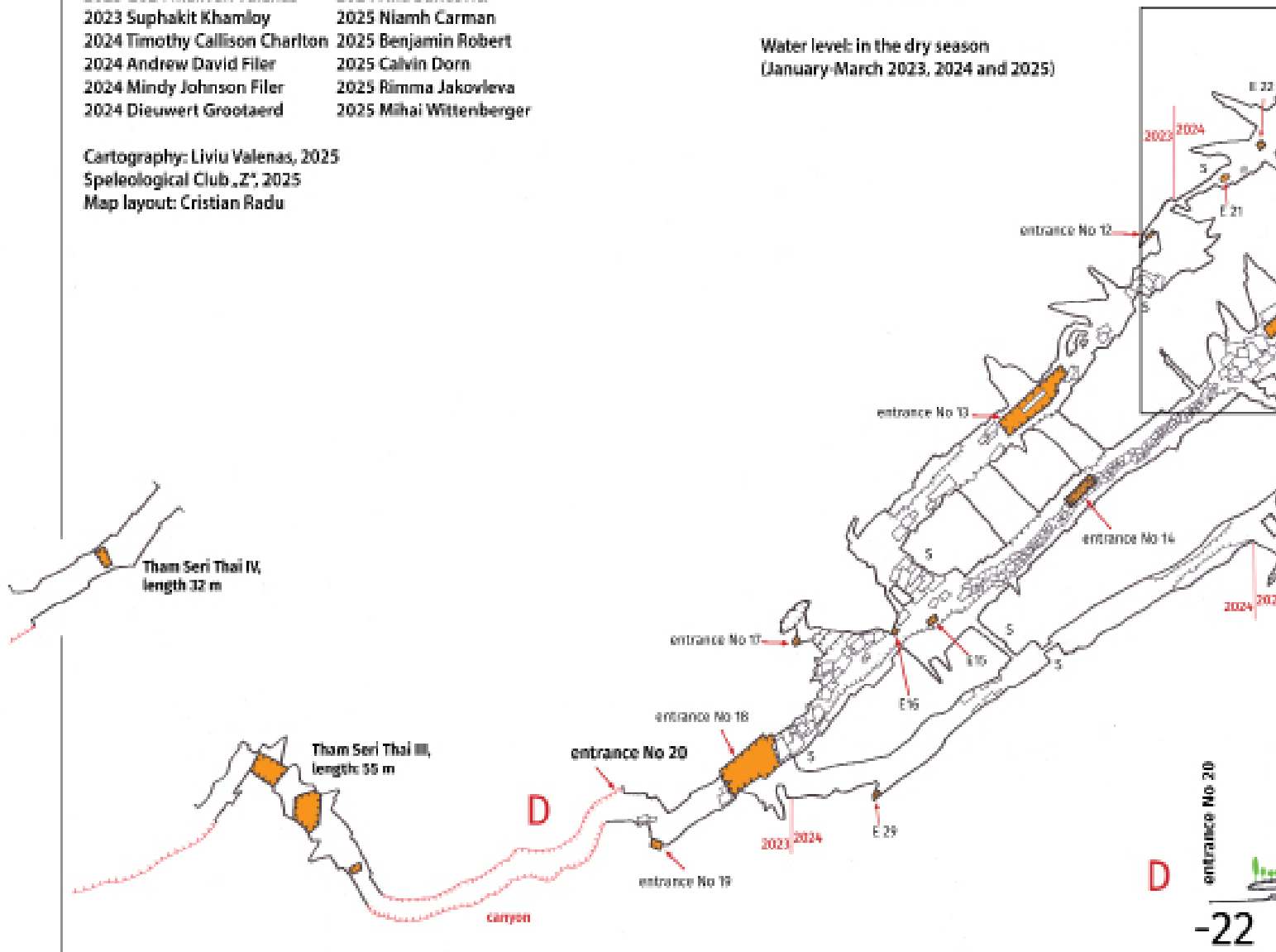
 Vertical entrances

 Surface relief (crevices, canyons, vertical walls)

 Explored but unmapped galleries

**I** = entrance  
**S** = squeeze

Water level: in the dry season  
(January-March 2023, 2024 and 2025)



Between 2016 and 2018 the cave research team of the Department of Mineral Resources (DMR) surveyed and investigated the geology of Tham Din Pieng (the results have not been published) and the long sandstone caves in Ubon Ratchathani province - Tham Patihan (Wilungkit and others 2021) and Tham Meut and Tham Ghia (Nakhiya 2020). In a review of the caves and karst in Thailand published by the DMR, Sattayarak (2021) summarised the

Since 2011 Liviu Valenas, together with members of the Speleological Club “Z” from Nuremberg, Germany, has been systematically exploring and surveying the most important caves

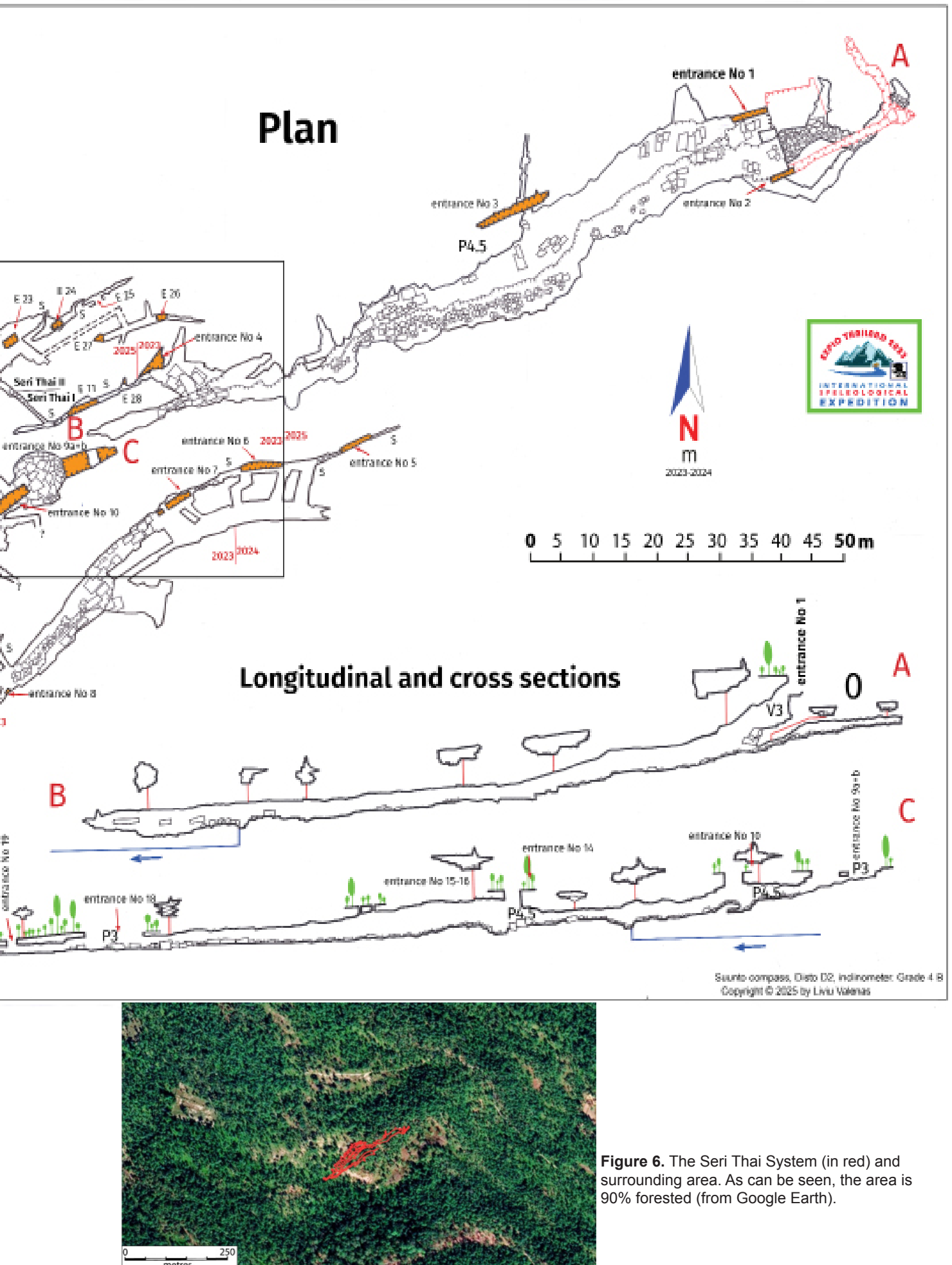


**Figure 6.** The Seri Thai System (in red) and surrounding area. As can be seen, the area is 90% forested (from Google Earth).



**Figure 8.** Entrance No. 27 of the Seri Thai System. The cave has a total of 28 entrances, the vast majority of which are vertical.

in the sandstones of North-east Thailand (Valenas 2019). This has resulted in the discovery or rediscovery of 95 caves, with detailed exploration and documentation. Prior to 2016 the longest known sandstone cave in North-east Thailand measured only 660 m in length, whereas currently three are known to exceed a kilometre in total length, one of which is approaching 3 km. Through these speleological explorations, the surface karst has been scientifically researched, with water samples from the sandstone karst in this area of Thailand being collected and analysed for the first time – at the Technical University of Freiberg, Germany. The results of these analyses have shown that the genesis of sandstone caves is much more complex and complicated than previously thought.

## Research and Exploration of the Seri Thai System

The upper cave (Tham Seri Thai I) has been known to the region's inhabitants for centuries. Between 1941 and 1945, the cave was used as a weapons and food depot by the Seri Thai ("Free Thai") organization during the Japanese occupation and between 1965 and 1983 it was used by the People's Liberation Army of Thailand, a guerrilla organization of the Communist Party of Thailand. It was not until 2011 that John Dunkley visited Tham Seri Thai I and estimated it to be (only) 150 m long (Dunkley and others 2018, Ellis 2017). In 2023 Liviu Valenas, Maliwan Valenas and Suphakit Khamloy conducted the first detailed speleological investigations of the cave, mapping 857 m of galleries (Valenas 2023a, 2023b, 2023c, 2024a, 2024b, 2024c). In that year, the Seri Thai System became the longest known sandstone cave in Thailand. In 2024 and 2025, Liviu Valenas

organized two international caving expeditions, resulting in the cave's known length reaching 1,124 m (Valenas 2025b, 2025c, 2025d).

## Methods

The Seri Thai System was surveyed with Suunto compass, Disto D2 and inclinometer. Cave entrances were positioned with a Garmin 62s GPS and later plotted on Google Earth. The underground photos were taken with a Nikon D 5200 camera, Tamron 18-155 mm lens, Metz 58 and Metz 62 flashes. The thin sections of sandstones were taken first with a reflected light microscope and secondly with double-polarized light. The pH value and temperature were determined at the sampling locations in

Tham Patihan using a HQ40D digital dual-channel multimeter from Hach Lange GmbH. The pH electrode (Hach Lange GmbH) was calibrated with pH buffer solutions with pH values of  $4.01 \pm 0.02$ ,  $7.00 \pm 0.02$  and  $10.01 \pm 0.02$  (25°C). The silica concentration was measured photometrically by DR890 colorimeter from Hach Lange GmbH, using the silicon molybdate method (measuring range: 1.0-100.0 mg/l SiO<sub>2</sub>). Chemical analyses and photomicrographs of the sections were performed in the laboratories of the Technical University of Freiberg, Germany.

## Lithology and Tectonics

The description of the Cretaceous formations of North-east Thailand by Meesook (2011) (Figure 4), indicates that the Seri Thai System is most likely located within the Khok Kruat Formation and this is confirmed by the stratigraphic column (Figure 9).

The Khok Kruat Formation is widely distributed in the outer parts of the Phu Phan mountain range (Veeravinantankul and others 2018). In general, the formation consists of brown to fine to medium-grained reddish-brown sandstone with some conglomerate layers, siltstone and reddish-brown claystone (Figures 10 and 11). Plant remains, bivalve fragments, and vertebrate fossils have been recorded in the formation (Meesook 2011). In the southern part of the Khorat Plateau the formation is widespread in Muang, Prathum Ratchawongsa and Phana districts of Amnat Charoen province; Trakanputphon, Kutkhaopum, and Si Muangmai districts of Ubon Ratchathani province, and parts of Patiu district of Yasothon province. The Khok Kruat Formation overlies the sandstones of the Phu Phan Formation (Meesook 2011).



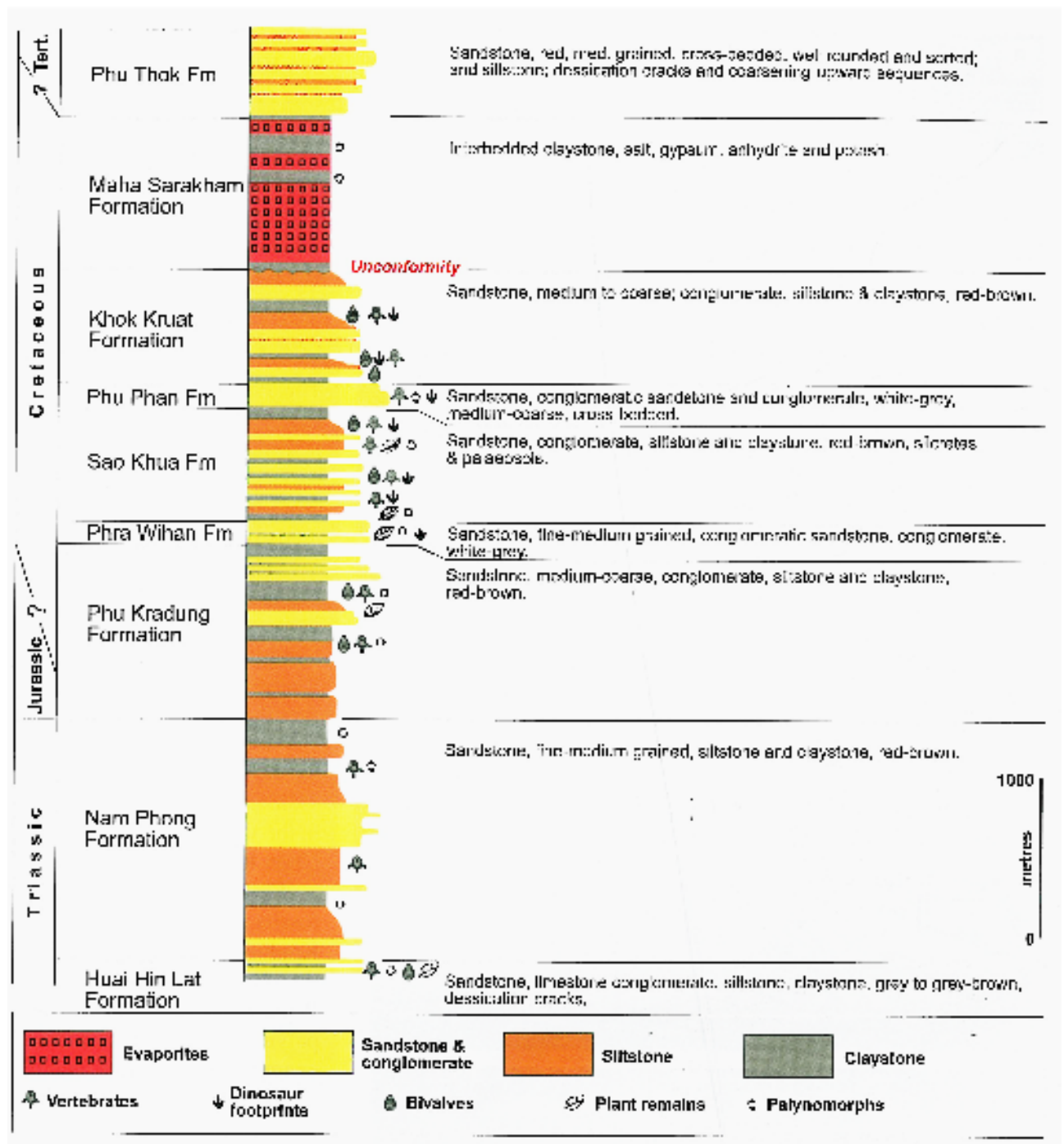
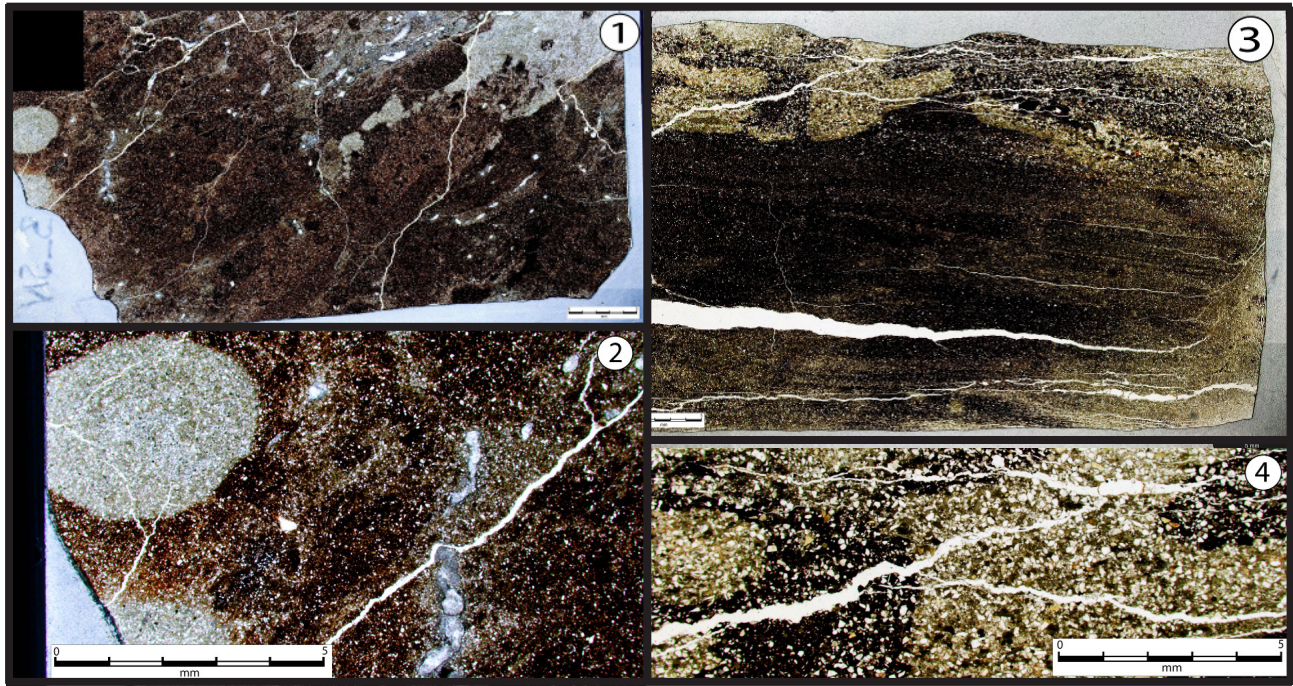


Figure 9. Mesozoic stratigraphic column for North-east Thailand, after Meesook (2011).

Plant remains, bivalve fragments, and vertebrate fossils have been recorded in the formation (Meesook 2011). Quartz sandstones are detrital sedimentary rocks in which the mineralogy is dominated by quartz (De Waele & Gutiérrez 2022), they should contain 95% quartz and <5% feldspars and lithics (Pettijohn and others 1987). Quartz is one of the most resistant minerals to chemical weathering. However, this resistance decreases significantly in tropical areas with high temperatures and heavy rainfall.

Although none of the authors cited above mention the presence of calcium carbonate in the cement that ensures the cohesion of the sandstones of the Khok Kruat Formation, this carbonate exists. Its presence is proven by chemical analyzes of the waters from the streams in the caves of this formation, and also by the speleothems (drapes, stalactites, rimstones, etc.) of calcium carbonate (Figure 12) that appear in the large caves in the Khok Kruat and Phu Pha formations. In the area of Tham Din Pieng, in the underground streams in the cave and in the main karst spring, the concentration





**Figure 10.** Photomicrographs of different layers of sandstones in the Seri Thai System. The sandstones contain varying percentages of feldspar, quartz, various rock fragments and calcite inclusions, cemented by syntaxial overgrowths. All quartz sandstone samples contain calcite veins. Photos by TU Bergakademie Freiberg.



**Figure 11.** Top, quartz sandstone layer with manganese mineralization; bottom, clay layer.





**Figure 12 (upper and lower).** Examples of calcium carbonate speleothems in the Seri Thai System.

of calcium carbonate exceeds even the waters of the limestone resurgences. When we refer to calcium carbonate, we are mainly talking about the cement that ensures the cohesion of sandstones and only secondarily about the calcite veins in quartz sandstones. The Seri Thai System is developed on a major fault, oriented north-east to south-west. At a distance of 10 to 15 m from this fault are two secondary, compressional faults, along which the parallel branches of the Seri Thai System are formed. Between these faults are several perpendicular joints on which the connecting galleries are developed. In other words, the Seri Thai System is formed on a “chessboard” tectonic system, that is, in a system of perpendicular faults. The cave system has been significantly affected by active tectonics. Many galleries are vertically cut by “micro-faults” with throws of between 5 and 10 cm. Gravitational distension cannot be taken into account because the sandstone package of the cave roof is very thin: from two to four metres. We believe that active tectonics is also directly responsible for the 25 vertical inlets (e.g. Figures 13 and 14) in the Seri Thai System.

As several seismic movements have occurred, staggered over time, under some vertical inlets the collapse cone is almost intact, while under others these collapses have been completely eliminated, by the process of arenisation and also by mechanical transport carrying out the debris by the underground stream during the rainy season. Similarly, only 70 km to the east, in Laos, the karst area near Thakhek has been and is affected by active tectonics. The caves here show sectioned columns and pillars, and massive cave collapses occur periodically (Valenas 2024d). The regional tectonics affect both areas.

### The Seri Thai System Description

A sinkhole descending a 3 m vertical drop leads to the “historical” entrance of Tham Seri Thai I, 4 m wide and 2.5 m high (Figure 15). After another 3 m vertical drop, the main gallery (Figure 16) is intercepted. To the north-east, it can be followed for 27 m. Downstream, to the southwest, the gallery is initially very wide (up to 11 m) and 3-4 m high. After 40 m, ascending a slope to the right, the second entrance is reached, in the form of a 5 m deep pit. The main gallery continues downhill, begins to narrow, and 120 m from Entrance No. 1 the gallery becomes impenetrable. Before the gallery ends, by climbing up a vertical slope, one encounters

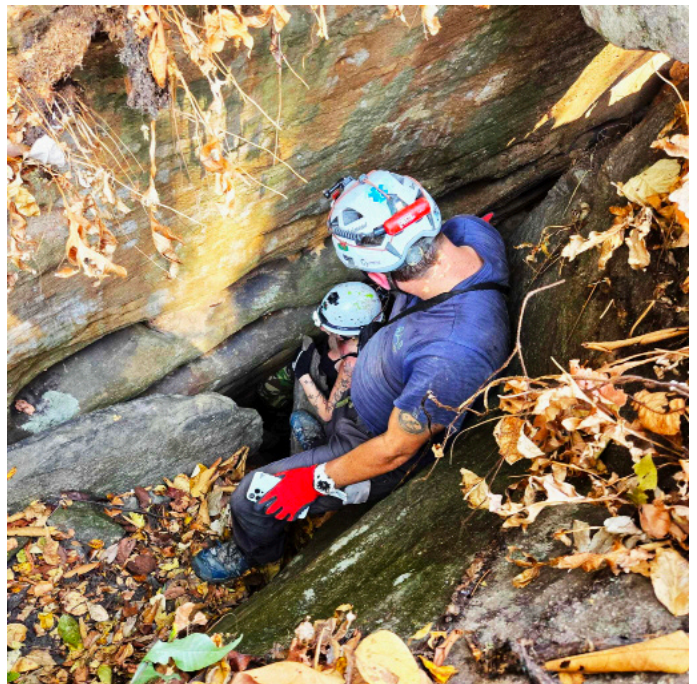


**Figure 13.** A vertical entrance to the Seri Thai System. Almost all of these are the result of active tectonics. (Photo by Calvin Dorn.)





**Figure 14.** Entrance to the Seri Thai System produced by collapse generated by active tectonics.

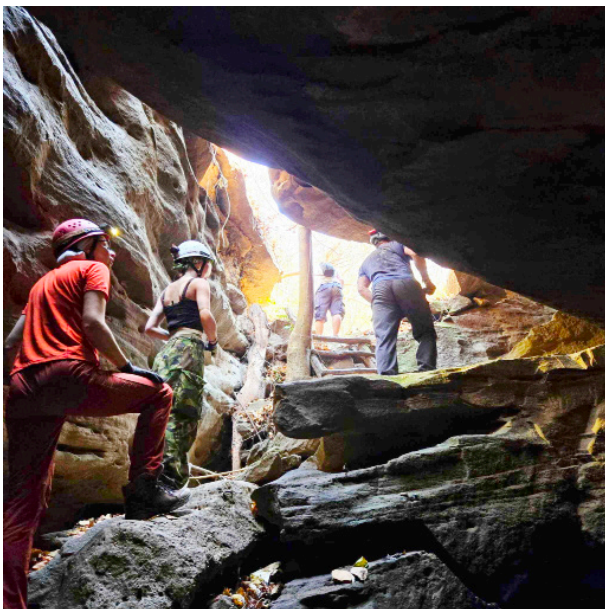


**Figure 15.** The "historical" entrance to Seri Thai I Cave. (Photo by Benjamin Robert.)

another exit through a 3 m pit (Figure 17). At the base of this vertical slope is the start of an extremely narrow gallery, shaped like an inverted T. The north-east branch provides the morphological connection with Tham Seri Thai II. In Tham Seri Thai II the main gallery begins just a few metres



**Figure 16.** The main galleries in the Seri Thai System are relatively wide and in many places wall flows of calcium carbonate occur.



**Figure 17.** Entrance No. 3 (P 3) to Seri Thai I Cave. (Photo by Andrew David Filer.)

from the end of Tham Seri Thai I, through a 3 m pit (Figure 18). It runs straight in the same general direction, southwest. It is generally a gallery 5 to 10 m wide and up to 4 m high. Along its entire length it has seven vertical entrances, shaped like potholes and up to 5 m deep. These are windows into the main gallery (Figure 19). After 149 m it opens to the surface with a horizontal entrance which, during the monsoon, has the character of a high-flow resurgence. From the traces left by a large flood on the walls of the main gallery of the Seri Thai System, we estimate that in the monsoon season the maximum flow of the main stream at the exit of the cave is 500 l/sec, exceptionally reaching about 1000 l/sec.

From the middle section of this gallery, through three relatively wide galleries, each no more than 1 m high, the connection is made with the northern branch of Tham Seri Thai II Cave. To the north-east, another parallel branch begins, 141 m long,





**Figure 18.** Entrance No. 9 (P 3) to the Seri Thai II Cave. (Photo by Maliwan Valenas.)



**Figure 19.** Vertical entrance in Seri Thai II Cave.

which includes several entrances, seven of which are potholes, up to 4.5 m deep. To the south lies the southern branch of the system, with a main gallery 147 m long. It begins with three letterbox-shaped potholes (that is, rectangular in shape, 5-10 m long, but with a very small width, between 20 and 100 cm), up to 6 m deep. The gallery then includes wide sections, but also three difficult squeezes. At its end, a bedding plane only 25 cm high provides a direct connection with the middle main gallery of Tham Seri Thai II Cave. The system has a total length of 1,124 m, a vertical range of 22 m and the distance between extreme points is 257 m, giving a branching coefficient of 4.4.

### Climatic Data

Climate has played and plays an extremely important role in the formation and functioning of this cave. The Seri Thai System is located at a latitude of 17° north, so it is in the tropical zone. However, the dramatic climate changes in recent decades have resulted in North-east Thailand starting to have a slightly subtropical climate. The characteristic of a climate strongly influenced by monsoon cycles remains. Global climate change has also manifested itself in the areas with water pits in North-east Thailand. The relatively dry months, December to April, have become extremely dry, with practically no rain at all in these months. Global climate change, characterized in the northeast of Thailand by 4 to 5 extremely dry months, transforms the plateaus into something similar to African savannas during these months. On the other hand, in the monsoon season, starting at the end of May, there are extremely heavy rains which have been the driving factor in the formation of the Seri Thai System. The average annual precipitation in the past was never high in North-east Thailand: 1399 mm in Khon Kaen province and 1515 mm in Surin province (Pfeffer 2013). In comparison, in Eastern Thailand, in Chanthaburi province, the average annual precipitation was 3235 mm, and in Southern Thailand, 2466 mm in Phuket province (Pfeffer 2013). With respect to average annual temperatures, we have data only for the neighbouring provinces: Khon Kaen (166 m altitude), average annual temperature 26.8°C and Udon Thani (178 m altitude), average annual temperature 26.7°C. These average data are only for the period 2003-2013 (Pfeffer 2013). Currently, with global climate change, temperatures are higher; in the hot and dry season they frequently exceed 40°C.

## Geomorphology and System Genesis

The Seri Thai System is complex, with a complicated genesis. Three major faults and their intersections with bedding planes initiated the dissolution process of the quartz sandstones. This process of arenisation (Martini 1979, Doerr 2000, Wray & Sauro 2017) is accelerated in a tropical monsoon climate. The first to use the term “arenisation” (Figure 20) was Martini (1979), based on his study of karst in sandstones in the Eastern Transvaal of South Africa. The term subsequently gained international circulation. It is a concept that attempts to explain the dissolution of rocks considered insoluble. The concept aims to “reconcile” two quite contradictory concepts, related to the occurrence of well-developed karst in rocks characterized by very low solubility and slow dissolution kinetics. Slow dissolution along crystal and grain boundaries reduces the coherence of the rock and increases its porosity. After that, the loose particles and crystals are eroded and transported by surface and subsurface flowing water. So, it is a mechanical erosive process. According to the concept developed by Martini (1979), dissolution is not responsible for the removal of a significant rock mass, but plays a critical preparatory role (De Waele & Gutiérrez 2022).

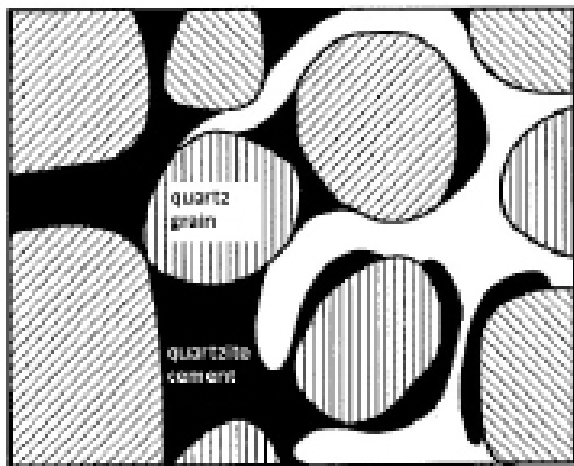


**Figure 20.** The arenisation process (after Doerr 2000).

The extremely humid and hot climate is the main driver of cave formation in the quartz sandstones of North-east Thailand, including the Seri Thai System. However, factors other than arenisation come into play. First, biocorrosion produced by organic acids released by tree roots (Figure 21). Initially, we assessed that biocorrosion caused by bats played a minor role (Valenas 2023b). However, after observing a radical change in



**Figure 21.** Massive root that runs horizontally through a sector of the main gallery in the Seri Thai System.

the pH of the Tham Patihan (Ubon Ratchathani province) underground stream, caused exclusively by bat droppings and urine in 2025, this view was discarded. Over a length of only 110 m the pH of the underground stream in Tham Patihan changes from 6.9 to 3.6, exclusively because of bats. Biocorrosion makes the groundwater even more acidic, which accelerates the dissolution of quartz sandstone cement.

At this point we must make some clarifications. Almost all authors see a direct relationship between the dissolution of silica (quartz) and high and extremely high temperatures and alkaline pHs (De Waele & Gutiérrez 2022, Wray & Sauro 2017), (Figure 22). But it is about silica, not quartz sandstones as a whole. With the exception of the water samples collected by us in 2023-2025 in Tham Din Pieng Cave, where the pH was alkaline, the rest of the dozens of water samples from quartz sandstones in North-east Thailand have a lowered pH; i.e. the waters are acidic or extremely acidic. Under these conditions why are quartz sandstones dissolved? The explanation lies in the nature of the cement that ensures the cohesion of these sandstones. Both the quartz sandstones of



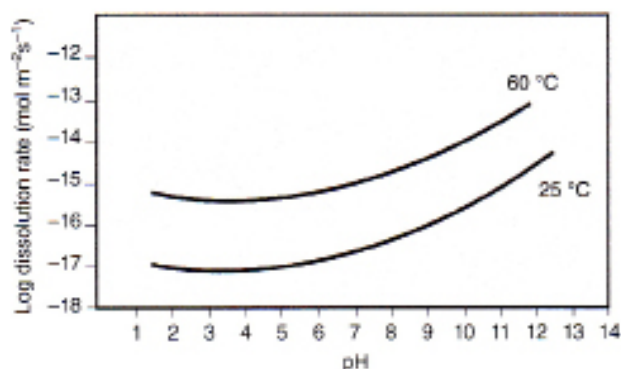


**Figure 22.** Dependence of quartz dissolution rate on the pH at 25°C and 60°C. (Source: De Waele & Gutiérrez 2022, adapted from Wray & Sauro 2017).

the Khok Kruat Formation and those of the Phu Phan Formation contain a significant percentage of calcium carbonate in their cement, and waters with an acidic pH act predominantly on this cement. Not only is the dramatic change in pH noteworthy, but also a substantial change in chemical composition. At the appearance of the underground stream in Tham Patihan, the calcium concentration was only 1.14 mg/l and that of calcium carbonate only 20 mg/l, after 110 m downstream the calcium concentration reached 74.4 mg/l and that of calcium carbonate, 175 mg/l (Table 2). The only explanation is the extremely acidic nature of the underground water, directly influenced by the large colony of bats in this gallery of Tham Patihan. It is certain that the same phenomenon occurs in the Seri Thai System during the rainy monsoon season.

Intensive research over two years (2023-2025) of the Seri Thai System has allowed, for the first time, the development of a theoretical model (Figure 23) for the formation of caves in quartzite sandstones in North-eastern Thailand. There are 6 factors that contributed to the formation of this large cave: (1) the arenisation process, (2) active tectonics, (3) mechanical erosion processes, (4) dissolution of calcium carbonate, (5) biocorrosion produced by

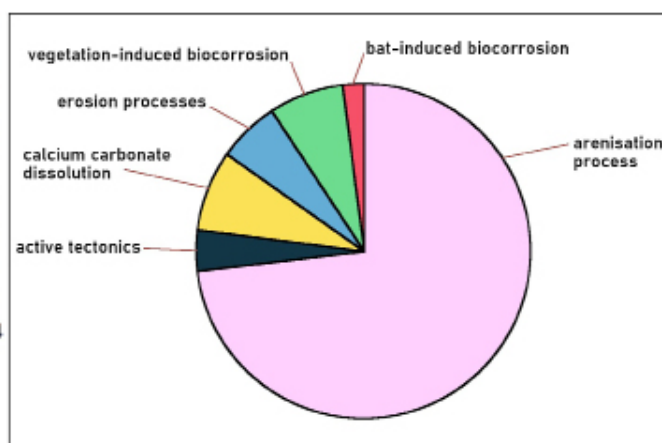


**Figure 23.** Theoretical model showing the six factors that created the Seri Thai System.

vegetation, through organic acids released by plant and tree roots and (6) biocorrosion induced by bats.

The arenisation process remains the main factor in the formation of this cave. Active tectonics produced most of the cave ceiling collapses, which led to the appearance of 26 entrances in the form of potholes. Active tectonics also acted massively due to the fact that the sandstone roof in the entire Seri Thai System is only 2-4 m thick. Erosion has been fully manifested in the deepening of galleries (Figures 24 and 25) in the vadose flow system, during the rainy season. Chemical analyses of karst waters from other caves in sandstones in North-east Thailand have shown a significant percentage of calcium carbonate. The explanation lies in the fact that the siliceous cement that fixed the quartz grains also contains calcium carbonate. There is no pure cement, composed only of silicates, in the sandstones of North-East Thailand. In addition, the sandstones also contain veins of calcite, which in the Seri Thai System are visible to the naked eye. Finally, the biocorrosion produced by bat colonies (and the Seri Thai System contains a relatively large colony) plays a not inconsiderable role in the dramatic change in the pH of the groundwater

Name	T (°C)	pH	Cl (mg/l)	NO <sub>3</sub> (mg/l)	SO <sub>4</sub> (mg/l)	Na (mg/l)	NO <sub>2</sub> (mg/l)	K (mg/l)	Mg (mg/l)	Ca (mg/l)	CaCO <sub>3</sub> (mg/l)	SiO <sub>2</sub> (mg/l)
Tham Patihan The Upstream Underground Course	24.5	6.9	1.40	3.61	1.4	0.99	0.16	0.77	0.26	1.14	20.0	7.2
Tham Patihan Downstream Underground Course	26.2	3.6	4.30	< 0.1	0.55	0.64	< 0.1	3.03	7.29	74.40	175.0	4.1

**Table 2.** Physicochemical values of the underground stream in Tham Patihan Cave show the massive influence of biocorrosion produced by a large colony of bats.



**Figure 24.** The main gallery in the Seri Thai System, remodeled by erosion in the vadose flow regime.



**Figure 25.** Another part of the main gallery in the Seri Thai System, also remodeled by erosion in the vadose flow regime.

in this cave during the monsoon season. Through the excrement and urine that reach the flowing waters of the cave, these become extremely acidic. Unfortunately, we lack chemical analyses of the waters directly from the Seri Thai System, because during all periods of our research in this cave (January - April), it was completely dry. Of course, these six factors acted on an adequate stratigraphic and tectonic framework (contacts between different layers of sandstone, between sandstones and clays and favourable tectonics: major faults and a network of joints).

We do not yet know whether this model can be applied to all quartz sandstone caves in tropical and subtropical regions. It may remain, at least for the time being, a valid model only for the quartz sandstone caves of North-east Thailand.

Returning to the structural factors, an important role in the formation of the Seri Thai System is played by the alternation of sandstones and claystones (Figures 26 and 27). Thus, the cave can also be considered to be a lithological contact cave.



**Figure 26.** Alternating sandstone and clay layers in the Seri Thai System.



**Figure 27.** The Seri Thai System can also be considered a lithological contact cave, not only between sandstones and clays, but also between different sandstone layers.



The Seri Thai System initially formed in an epiphreatic regime, starting in the Middle Pleistocene, and was then remodelled into a vadose system with the erosion levels fully demonstrating this. At the present stage of karst research in North-east Thailand, the age of the caves can only be established in correlation with the river and stream terraces in the studied areas. The Seri Thai System can be extrapolated as terrace 1 of the hydrographic network in the area and this terrace cannot be older than the Middle Pleistocene.

### Are the Seri Thai Landforms True Karst?

The findings of recent research involving the Seri Thai System have raised questions in some quarters as to whether these landforms can properly be classified as “karst”. Until recent times there were those who would consider only caves and surface relief on highly soluble rocks (such as carbonates, magnesites and halites) to represent karst. Similar landforms on much less soluble rocks (such as sandstones and quartzites) were termed by some, effectively following Knebel (1908 - cited by Halliday 2004) as “pseudokarst”. There has been considerable controversy around the use of this term but Eberhard and Sharples (2013) rejected it. They showed that it

- (a) [is] poor classification practice in principle;
- (b) unnecessarily duplicates mainstream approaches to landform classification; and
- (c) is a karst-centric terminology for non-karstic phenomena.

In 2010 Pfeffer concluded: *Siliceous rocks can form a true karst under conditions of intensive climate (precipitation and high temperatures)*. Wray & Sauro (2017) observed: *... limestone and similar highly soluble rocks were long believed the sole host for large karst drainage systems ... Quartzose caves and dolines are similar in size, though, to the vast majority of smaller limestone caves and dolines, and are thus significant, and often very impressive, sandstone karst features*. More recently, Brazilian researchers (Pereira and others 2022) confirmed that *Karstification in quartzitic sandstones is a reality demonstrated worldwide by the exploration and research of caves in sandstones*. At an international symposium in Karlow, Poland (May 2023), there was a heated discussion about whether the term “pseudokarst” had any scientific basis and most participants disputed the validity of the term. Bearing these studies in mind, it is

clear that the landforms developed on quartz sandstones in North-east Thailand, documented by Valenas (2023a, 2023b, 2024a, 2024b), should be considered a true karst.

### Conclusions

The Seri Thai System is an extremely complex underground network and is so far unique in Thailand among the sandstone caves. It is unique due to the arrangement of the galleries in a dendritic system. Large or relatively large caves in the sandstones of north-east Thailand (Table 1) are very different from each other. Tham Nam Lod (Valenas 2016, 2023a) is a tectonic cave, because the primary role in forming this cavity was a major rectilinear fault. Of course, this cave was also later remodeled through the processes of arenisation and subsequent erosion. Tham Meut and Tham Ghia (Valenas 2023a) are tunnel caves with a single, large, relatively straight gallery, developed on bedding faces. Tham Patiha is also unique among the sandstones of Thailand because it has two levels, the lower level being permanently active. Tham Phou Pom (Valenas 2023a) is a maze cave with narrow galleries developed along both bedding planes and tectonic joints. The maze caves of Tham Din Pieng (Valenas 2025a) and Tham Phusi Keu (Valenas 2025c, 2025d), developed in sandstone with carbonate cement, are unlike any others. The former, with a length of 2,737 m, is also the longest sandstone cave in all of South-east Asia. This brief list alone demonstrates the complexity of the subject. The Seri Thai System is formed on three parallel faults and on bedding discontinuities. It is also a lithological contact cave, between different layers of sandstone and claystone. Its formation is a direct consequence of the tropical monsoon climate, characterized in north-east Thailand by high rainfall and temperatures. The Seri Thai System is part of a true karst, albeit one developed on sandstone – hence it may be termed a silicate karst (Valenas 2023a), mainly due to the arenisation process of quartz sandstones, or a sandstone karst (Mouret & Mouret 1994).

### Acknowledgements

First of all, we would like to thank Professor Dr. Traugott Scheytt of the Technical University of Freiberg for his support of the scientific research on the Seri Thai System. Special thanks to Professor Dr. Thorsten Nagel and Sebastian Schram for the microphotographs of thin sections of rock samples collected from the Seri Thai System. We also thank

## Seri Thai System

Dr. Christine Viehweger, Stephanie Gimmmler and Dr. Anika Rogoll of the Technical University of Freiberg for the chemical analyses performed. Thanks also to Cristian Radu and Johanna Löbel for the computer graphics. Our gratitude goes to all the participants in the three international “Explo Thailand” expeditions in 2023, 2024 and 2025, who explored this challenging underground system with great professionalism. And finally, thank you to the Phu Phan National Park administration who allowed us to conduct this research in the Seri Thai System.

Photographs, unless otherwise attributed, are by Liviu Valenas.

## References

- DE WAELE, J. & GUTIÉRREZ, F. 2022 *Karst Hydrogeology, Geomorphology and Caves*. Wiley, Blackwell. 888 pp.
- DOERR, S. H. 2000 Morphology and genesis of some unusual weathering features developed in quartzitic sandstone, North-Central Thailand. *Swansea Geographer*, 35: 1-8.
- DUNKLEY, J.R. 2011 Tham Din Phieng, Thailand: An unusual maze cave in sandstone. *Proc. 28th Biennial Conference of the Australian Speleological Federation, Chillagoe, Qld*.
- DUNKLEY, J. R. & BOLGER, T. 2017 An unusual maze cave in sandstone, NE Thailand. *Proc. 17th International Congress of Speleology, Sydney*, Vol. 2: 153.
- DUNKLEY, J. R., ELLIS, M. & BOLGER, T. 2018 Unusual caves and karst-like features in sandstone and conglomerate in Thailand. *Helictite*, 43: 5-31.
- EBERHARD, R. & SHARPLES, C. 2013 Appropriate terminology for karst-like phenomena: the problem with “pseudokarst”. *International Journal of Speleology*, 42 (2): 109-113.
- ELLIS, M. 2017 *The caves of Thailand, Volume 1, Eastern Thailand*. Privately published, Shepton Mallet, UK. 311 pp.
- HALLIDAY, W.R. 2004. Pseudokarst [in] GUNN, J. (ed.) *Encyclopedia of Caves and Karst Science*. Fitzroy Dearborn, New York & London. pp.1291-1301.
- KNEBEL, W. VON. 1906 *Höhlenkunde-mitberücksichtigung der karstphänomene*. Braunschweig, F. Vieweg und sohn. 222 pp.
- MARTINI, J.E.J. 1979 Karst in black reef quartzite near Kaapsehoop, eastern Transvaal. *Annals of the South African Geological Survey*, 13: 115-128.
- MEESOOK, A. 2011 Cretaceous [in] RIDD, M.E., BARBER, A.J. & CROW, M.J. (eds.) *The Geology of Thailand*. Geological Society, London. pp.169-184.
- MOURET, C. 2004 La spéléogénèse des grès: quelques principes fondamentaux. *Actes de 14ème Rencontre d'Octobre, Florac, Spéleo-club de Paris*. pp. 55-56.
- MOURET, C. 2017 Some fundamental features of speleogenesis in sandstone. *Proc. 17th International Congress of Speleology, Sydney*. Vol. 2: 174-179.
- MOURET, C. & MOURET, L. 1994 Prospection des karsts gréseux du nord-est de la Thaïlande (Isan). *Spelunca*, 55: 6-9.
- NAKHIYA, T. 2020 Geological and speleological surveys in Pha Cham Samphan Bok Geopark. *Academic Report Sor. Thor. Khor. 3* 3/2563, Department of Mineral Resources, Bangkok. 79 pp.
- PEREIRA, M.C., VASCONCELOS, A.M., RODET, J., BIAZINI MENDES, J., CATARUCCI, A.F.M., SOUZA (DE), M.E.S., OLIVEIRA RODRIGUES (DE), P.C., COELHO, V.V. & ARAUJO, R.S. 2022 Overview of cave studies in quartzites, itabirites and granitoids in Southern Brazil. *Proc. 18th International Congress of Speleology, Savoie Mont Blanc*. Vol. III: 259-262.
- PETTIJOHN, F. J., POTTER, P. E. & SIEVER, R. 1987. *Sand and Sandstones*. Springer-Verlag, New York.
- PFEFFER, K.-H. 2010 Karst, Entstehung-Phänomene-Nutzung, *Studienbücher der Geographie*. Borntraeger Sciences Publishers, Stuttgart. 338 pp.
- PFEFFER, K.-H. 2013 *Thailandsvielfältige Landschaften – Geologie und Relief, Klima, Vegetation und Nutzung*. Gebrüder Borntraeger, Stuttgart. 194 pp.



- SATTAYARAK, N. 2021 Caves in sandstone [in] *Caves and Karst of Thailand*, Department of Mineral Resources, Bangkok. pp. 108-119.
- SIRIPORNPIBUL, C. 2021 Origin of sandstone caves and legends [in] *Caves and Karst of Thailand*, Department of Mineral Resources, Bangkok. pp. 176-187.
- VALENAS, L. 2016 *Explorari speologicae in gresile cuartitice din provincia Ubon Ratchathani – Thailanda*. Neodacii.com, Strasbourg.
- VALENAS, L. 2019 Speleological exploration in Thailand 2009-2019. *13th Eurospeleo Forum, Sofia, Bulgarian Federation of Speleology*. pp. 40-41.
- VALENAS, L. 2023a Geomorphology and hydrogeology of genuine karst in the quartzitic sandstones of northeast Thailand. *14th International Symposium on Pseudokarst, Karlow*. pp. 66-70.
- VALENAS, L. 2023b Silikatkarst in den quarzitischen Sandsteinen Nordost-Thailands. *Mitteilungen des Verbandes der deutschen Höhlen- und Karstforscher e.V.*, 69(3): 76-83.
- VALENAS, L. 2023c Explo Thailand 2023. *NSS News*, 81(12): 8-10.
- VALENAS, L. 2024a Geomorphology and hydrogeology of siliceous karst in the sandstones of northeast Thailand. *International Union of Speleology Pseudokarst Commission Newsletter*, 31: 30-41.
- VALENAS, L. 2024b Karst geomorphology on sandstones in the area of Ban Dong Tong (Nong Khai), Thailand. *Helictite*, 49: 19-26.
- VALENAS, L. 2024c Explo Thailand 2023. *Thailand Rundschau*, 37(1): 4-6.
- VALENAS, L. 2024d Geomorphology and hydrogeology of Tham Kammattan – a tectonically- modified epiphreatic cave from Central Laos. *Helictite*, 49: 1-10.
- VALENAS, L. 2025a Geomorfologie and Hydrogeologie der Tham Din Pieng, der längsten Sandsteihöhle Thailands. *Mitteilungen des Verbandes der deutschen Höhlen- und Karstforscher e.V.*, 71 (2): 49-55.
- VALENAS, L. 2025b Thaïlande : le Système Seri Thai - Une exploration particulièrement difficile. *Spéléo Magazine*, 132: 32-34.
- VALENAS, L. 2025c Internationale Höhlenforschung – Expedition EXPLO THAILAND 2025. *ACAMONTA*, 32: 147-148.
- VALENAS, L. 2025d Internationale Höhlenforschung – EXPLO THAILAND 2025. *Thailand-Rundschau*, 3/2025: 105-106.
- VEERAVINANTANKUL, L. A., KANJANAPAYONT, P., SANGSOMPONG, A., HASEBE, N. & CHARASURI, P. 2018 Structure of Phu Phan Range in the Khorat Plateau: its apatite fission track ages and geological syntheses. *Bulletin of Earth Sciences of Thailand*, 9(1): 8-16.
- WILUNGKIT, Y., JAIMUN, P., SIRIPATTARAPUREENON, R., HINSAENG, P., CHANPAENGNGERN, J. & DUANGWAEWRUEN, J. 2021 Exploration and research study of the Tham Patihan system, Ubon Ratchathani Province. *Academic Report Kor. Thor.* 3/2564 Geology Division, Department of Mineral Resources, Bangkok. 102 pp.
- WONGKLO, K., BUFFETAUT, E., KHAMHA, S. & LAUPRASERT, K. 2019 Spinosaurid theropod teeth from the Red Beds of the Khok Kruat Formation (Early Cretaceous) in Northeastern Thailand. *Tropical Natural History*, 19(1): 8-20.
- WRAY, R.A.L. 1997 Quartzite dissolution: karst or pseudokarst? *Cave and Karst Science*, 24(2): 81-86.
- WRAY, R.A.L. & SAURO, F. 2017 An updated global review of solutional weathering processes and forms in quartz sandstones and quartzites. *Earth Science Reviews*, 171: 520-557.



This page is intentionally blank



# Military impacts on some Australian karsts

**Kevin Kiernan**

15 Summerleas Road, Fern Tree, Tasmania 7054. [kevink15ft@gmail.com](mailto:kevink15ft@gmail.com)

---

## Abstract

Karst terrane provides a wide range of important environmental values but is both particularly susceptible to environmental harm and also prominent among those environments where environmentally damaging military activities have occurred globally. Although two Australian karst sites were briefly subject to bombing attacks during World War 2, the most significant known environmental harm caused to Australia's karst by military activity has occurred during the Cold War and in peacetime. This paper reviews persisting legacy issues arising from weapons testing during the 1950s-1960s in two Australian karst areas. It also examines the damage that has resulted from the siting in karst areas of two other military facilities that remain very active today. Further research is desirable into environmental impacts of the operations described in this paper and also into wider aspects of military impacts on Australia's karst environments including offsite effects such as disruption of natural karst process systems related to emissions into the atmosphere and impacts generated by the wider defence industry that supplies and services both the Australian military and weapons export markets.

---

## Introduction

Karst terrane provides a wide range of natural and cultural environmental values and can deliver important ecosystem services, but it is also particularly susceptible to environmental damage caused by human activities. This includes physical harm to landscapes and landforms; disruption of natural geo-ecological processes through disturbance of vegetation, soils and critical hydrological pathways; despoilation of soils through physical disturbance and contamination by water-borne and air-borne chemicals; contamination and other damage to surface and underground waters; and resulting harm to biota and other values that are dependent upon these attributes. Given the values and sensitivity of karst, it is therefore of particular concern that karst has also proven consistently prominent among those environments where military conflict has played out (Halliday 1976, Nunez Jimenez 1987, Day and Kueny 2004, Kiernan 2012, 2013). This is exemplified by current conflicts in the Middle East where karst groundwater beneath the West Bank is a critically important but threatened resource (Rofe and Rafety 1965, Mimi and Assi 2009, Jebreen and others 2018), the asymmetric abstraction of which has itself long been a source of conflict between Israel and Palestine (Walsh and others 2024, Zetoun and others 2009, Mansour and others 2012). Similarly, areas mapped as having been burnt during current

conflict in Lebanon (Walsh and others 2024) almost entirely coincide with karst terrane. However, while major environmental harm has typically resulted from conflicts in karst, the environmental impacts of actual conflict are only part of the story because significant environmental impacts that derive from preparations for war, such as weapons manufacture, weapons testing, and military training activities, must also be taken into account (Kiernan 2021a). Australia's karst areas have not been immune from such military impacts. Recognising and understanding the damage caused by military activities in Australia, and its implications, is a necessary precursor to stemming further harm to Australia's karst estate from this source. This paper reviews some of these Australian sites and synthesises some of the key issues, based on accessible literature and supplemented by some fine-tuning based on more recent reconnaissance-level field observations by the author at some of the key sites addressed.

Desirable as it may be, it would be unrealistic to expect the environment to be front of mind in the immediacy of actual conflict, especially when decisions need to be made rapidly and an opposing force unconcerned about its environmental impact may effectively be setting the stage and the agenda. The less pressured pre-conflict and so-called "post conflict" times seem more permissive of environmental concerns being given greater

regard. Indeed, many militaries now employ environmental specialists to guide more sensitive use of training areas or to safeguard against pollution, although there are limits as to what can be achieved if military or political directives are prioritised over all other concerns. However, specific provision is commonly included within national environmental protection legislation for exemptions where military activities are involved (Cottrell 2025). For example, Article 2(1) of the European Parliament and Council's *Regulation (EC) No 1907/2006*, which seeks to control the use of certain chemicals, provides for exemptions "where necessary in the interests of defence" (European Union 2006). In the USA, where military expenditure exceeds the GDP of all but 24 countries worldwide, most major environmental legislation, such as the *Endangered Species Act* and *Migratory Bird Act*, allows for exemptions for military activities (Smith 2019). Similarly in Australia, Section 158 (5) of the *Environment Protection and Biodiversity Conservation Act 1999* provides for the Minister to grant exemptions for military purposes. Nevertheless, Australia's 2016 *Defence White Paper* (Australian Government 2016) affirmed at section 4.71 that "Effective environmental management is an important part of successfully managing and ensuring the long-term sustainability of the Defence estate. The Government expects Defence to take its environmental stewardship responsibilities seriously, and to comply with relevant environmental legislation and regulations, including the protection of biodiversity on Defence bases". Australia is in the fortunate position of having a Department of Defence that is today relatively responsive to environmental concerns, but this also needs to be balanced against achieving its foundational defence and capability functions (Defence 2020).

While battlefield actions by an opposing force are largely beyond the control of any military, nation states do have the capacity to limit environmental harm by careful selection of sites where they choose to locate facilities that may attract attack or where weapons testing or other military preparations are undertaken. Both the 1954 *Hague Convention for the Protection of Cultural Property in the event of Armed Conflict*, and new United Nations International Law Committee (ILC) draft principles designed to improve environmental protection during armed conflict, limit protection to sites that do not contain a military objective. Hence, if states wish to reduce potential harm to

their special places, such as karst areas, then the onus is on them not to establish military facilities there. Two Australian karst sites came under attack during World War II due to the presence of bases there. Weapon testing has occurred at two further karst sites in earlier times when awareness of environmental concerns was much less developed than now. Some legacy issues in relation to these sites are considered in this paper. In addition, major military installations presently operate in two other karst locations, both of which have impacted upon karst groundwater resources and also make those sites legitimate targets for military attack should conflict occur. Some new military facilities are also being established on or proximal to Australian karst sites. The potential for environmental damage that may be caused by accidents involving materials in use at military establishments also warrants consideration.

The scope of post-conflict environmental assessments compiled by UN agencies is typically limited to contaminants or harm to biota (eg. UNEP/UNCHS 1999, UNEP 2004, 2007), but the geo-environment is now also beginning to receive some regard, including by some influential non-governmental organisations such as the UK-based Conflict and Environment Observatory (CEOBS) that aims to enhance the recognition of war's environmental harm, the documentation and understanding of that harm, and the development of improved international protocols (Kiernan 2021b, Watson and Shekhunova 2025). Karst figures significantly in a recent CEOBS report concerning the impacts on geodiversity of the current war in Ukraine (Watson and Shekhunova 2025). However, a similar approach to assessment of non-conflict phase military activities is also warranted. Such lessons as may be learned of past impacts on karst might usefully inform efforts to reduce the damage that might otherwise be caused to karst areas in the future. To this end, this paper examines the Australian experience.

## Legacy sites

### 1. Montebello islands

The Montebello archipelago lies just off the Pilbara coastline of north-western Australia, about 120 km from the industrial port city of Dampier. It comprises about 170 small limestone and sand islands with a combined land area of about 22 km<sup>2</sup>. The two largest islands are Hermite (1022 ha) and Trimouille (522 ha). Its military history includes



having been the site of the first atomic bomb testing conducted in Australia, from which a significant legacy of environmental harm persists.

### *The karst connection*

Modern coral reefs are commonly formed on older coastal (carbonate) ridges, and the submerged palaeoshorelines off NW WA are among the longest known anywhere. The Montebello Islands rest upon the same carbonate platform as underlies the larger Barrow Island, 20 km further south. However, while the low and undulating Barrow Island is almost entirely middle Miocene limestone (Trealla Limestone) similar to that in the Cape Range, 150 km further south-westwards, this unit does not crop out above sea level on the Montebellos, where only Quaternary calcarenites similar to those that fringe much of Barrow are exposed (Hocking and others 1987, Lebrek and others 2023).

While the presence of carbonates has been recorded in mapping by the Geological Survey of Western Australia, prior to this paper no previous recognition of karst being present in the Montebello islands is apparent in the mainstream Australian karst literature (eg. Matthews 1985, Jennings 1987, Finlayson and Hamilton-Smith 2003, Webb and others 2023). However, semi-circular bays that are almost disconnected from the sea, particularly evident along the contorted shoreline of Hermite Island, bear a striking similarity to the shoreline configurations of drowned towerkarsts elsewhere and are most probably drowned karstic depressions (Figure 1). Sea level was much lower than now during the Glacial Climatic Stages of the late Cainozoic when considerable volumes of water were locked in ice sheets and glaciers. At these times the Montebello islands, together with the larger Barrow Island (234 km<sup>2</sup>), now a low (65 m) undulating continental island, would together have

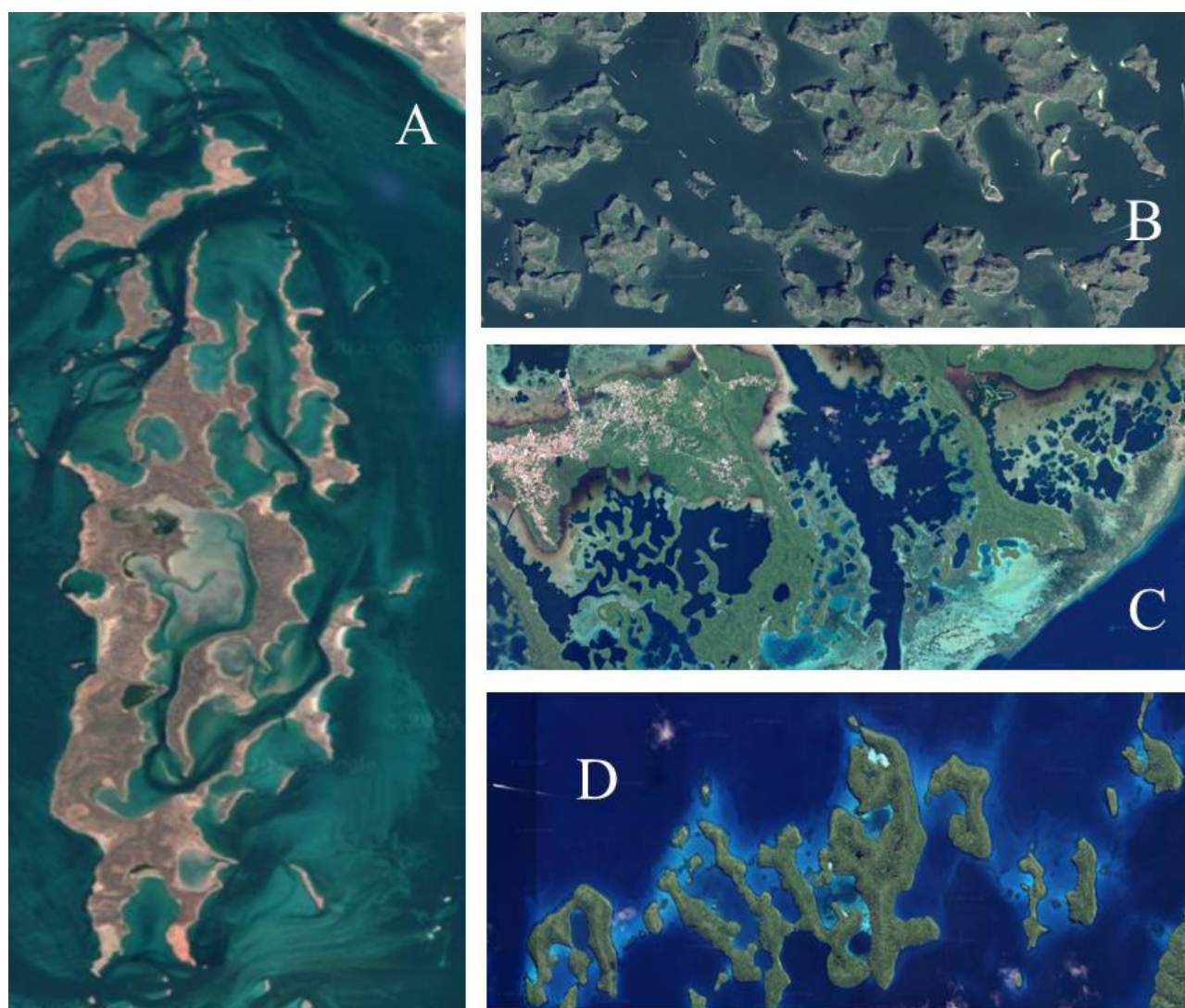


**Figure 1.** Convoluted shoreline of (A) Hermite Island, Montebello archipelago compared to drowned towerkarst shorelines in (B) Halong Bay, Vietnam, and (C & D) two sites in Palau. Images acquired from Google Earth.

formed a low range of hills rising from a coastal plain. The resultant lower base level of vadose erosion would have allowed vigorous karstification. Notwithstanding the submerged blue holes of the Great Barrier Reef, the Montebello karst may represent Australia's only example of this sort of karst landscape that is above sea level today – even if it is only just above sea level.

Adding to the significance of this karst are several caves that have been investigated for their archaeological contents but without their wider karst system context having been recognised or addressed. The oldest known occupation deposits, in Noala Cave on Campbell Island, have been dated to  $27,220 \pm 640$  BP (Before Present) (Veth and others 2007). Hence, this occupation occurred during the most recent episode of lower glacial-stage sea level. Potentially adding to the picture, the Montebellos lie less than 150 km from the extraordinarily rich archaeological sites of Murujuga/Dampier Peninsula on mainland Australia that were accorded World Heritage status in mid-2025. For most of Australia's human history its land mass was much more extensive than at present, up to 25% of the continental area then becoming inundated by the postglacial sea level rise responsible for today's shoreline. During the Last Glacial maximum the coastline would have lain about 160 km further offshore from Murujuga than is presently the case. Research into the drowned archaeology of this Murujuga "Sea Country" is in its infancy, but preparatory work involving satellite-derived bathymetric and multi-beam echo sounder datasets undertaken between the predominantly granitic islands of the Dampier Archipelago has revealed notch and visor slope profiles eroded into now-submerged carbonate rocks, that are typical of those that form along rocky limestone coasts, and numerous drowned closed depressions. When these data were revealed to the local Ngarda-Ngarli indigenous people, senior elders immediately recognised one pair of depressions as forming part of their Kangaroo song-line, oral tradition having preserved memory of this now hidden topography through many millennia (Kearney and others 2023). Stone tools were subsequently found associated with a submerged freshwater spring in one of these underwater enclosed depressions (Benjamin and others 2023). These findings highlight an inconsistency between the living cultural connection and actual cultural landscape versus the artificial cadastral boundary of what is now the Murujuga World Heritage site, which

appears to have been drawn such as to encompass only the islands above present sea level and which consequently incorporates only that portion of the sea country that fortuitously occupies the interstices between them. The earliest cultural deposits in the Montebello caves contain remains of mainly terrestrial fauna, but with a marine component to the diet of the cave-dwellers later becoming more evident up to the time when rising sea levels saw separation of the Montebellos from the mainland and then from Barrow Island about 7000 years ago (Veth 1993, Veth and others 2007). While there is no reason to assume continuous karst between Murujuga and the Montebellos, it seems reasonable to consider a contiguous cultural landscape likely existed, and that undersea karstic archaeological sites likely also exist around the Montebello islands.

### *Military activities*

Unwilling to conduct atomic bomb testing at home, Britain settled on Australia, where it had been testing rockets at Woomera since 1947. A request to use the Montebello islands was made within one year of Robert Menzies becoming Australian Prime Minister, and he unilaterally agreed to the request over the course of a single weekend (Tynan 2022, Grace 2023). Around the time of the first Montebello test there was concern in Britain about the possibility of a bomb being smuggled to a target in a ship, hence it was resolved that the first test, known as Operation Hurricane, should also facilitate assessment of the potential effects of this by deploying the 25 kt bomb 2.7 m below waterline in the hold of *HMS Plym* in October 1952. Operation Mosaic in 1956 involved above-ground tests designed to obtain knowledge to assist in moving beyond a fission bomb towards a fusion device, by using fusion to supplement fission. The initial experimental Mosaic G1 on northernmost Trimouille Island yielded a 15 kt blast with a minimal fusion contribution. Mosaic G2 was detonated on a 33 m-high tower on Alpha Island. It was reported as having been 60 kt but revealed in 1984 to have actually been 98 kt, about six times the size of the bomb dropped on Hiroshima and very much larger than had been agreed upon in an undertaking given to PM Menzies by British PM Eden that no future test would exceed twice the yield of the Hurricane blast. It has more recently emerged that Britain began work towards an H bomb in the mid-1940s and that this work continued in tandem with its atomic bomb testing, despite repeated assurances that it would not test thermonuclear materials in Australia. In



his 1961 memoir former British Prime Minister Anthony Eden acknowledged that his government decided in 1954 to make a hydrogen bomb (Eden 1961). By late 1955 the British were working on placement of a trigger bomb inside a common outer case with radiation-transmitting material between them. This detonation was boosted by using a light element (uranium) rather than the lead tamper used previously, effectively a stepping stone towards a thermonuclear device (Arnold 1987, Arnold and Pyne 2001, E. Tynan pers. comm.).

### *Environmental impacts and legacies*

The environmental damage inflicted on this karst by weapons testing included both physical damage and chemical contamination of soils and water. The water beneath *HMS Plym* was about 12 m deep and the 25 kt. bomb left a sea-bed crater about 6 m deep and 300 m diameter that remains discernible. The extent to which fractures may have been created in the bedrock below the detonation site, into which radionuclides may have been able to gain access deeper into the karst, remains unknown. However, it is important to note that there is no reason to expect that the sort of serious physical geological damage that was reportedly caused by French nuclear testing in the Pacific atolls of Muroroa and Fangataufa between 1966 and 1996 might also have occurred at Montebello because the two situations are in no way comparable. The damage in the Pacific was related to 137 underground tests within cavities excavated into volcanic rocks beneath these Pacific atolls, twelve of them causing formation of a chimney into the carbonates through collapse of the underground nuclear explosion cavities, potentially releasing tritium, strontium and caesium into the karst groundwater. An additional four tests released tritium into the karst despite expectations that volcanic cover rocks would contain contaminants. It was an accidental blast at only 400 m depth that reportedly caused the 2 kilometre-long and 40 cm wide crack that appeared on the atoll. Of the 41 atmospheric nuclear tests conducted by France only the first three involved detonation on barges similar to Operation Hurricane (Chiappini and others. 1999), but there seems to be no accessible data concerning their impacts on the deeper substrate that might offer any insight into possible effects of the blasts in the Montebellos. The remainder of the French atmospheric tests are also not comparable because they often involved much larger bombs than that detonated during Operation Hurricane and they were mostly detonated while suspended above ground-level beneath balloons.

Nevertheless, coral was obliterated by the Hurricane detonation. Whether any subsea karstic archaeological sites around the Montebellos may have been impacted remains unknown. Contemporary reports also indicate that detonation caused a massive wave to sweep across the islands. However, the significance of the environmental damage this wave caused needs to be considered in context with Bureau of Meteorology records of natural tsunamis along this part of the Australian coast, most recently reaching 6 m above sea level in 1977 locally, and extending 300 m inland in 1994. Another in 2006 locally reached 200 m inland, causing extensive erosion and vegetation damage and sweeping away coastal campsites on the mainland. The geological record hints at tsunamis up to 20 m high in the more distant past (Scheffers and others 2008, Playford 2014). Hence the Operation Hurricane wave damage appears likely within the bounds of natural events, and while it may have up-ended the natural rehabilitation of any preceding tsunami damage its physical effects are likely to have been surpassed by those of natural tsunami waves since the tests were concluded. However, radioactive materials left on and around the Montebello Islands are likely to have been distributed more widely into the marine environment by subsequent natural waves.

The tests also caused widespread distribution of airborne contaminants across the Montebellos and possibly even more distant karsts. Despite a fallout cloud from Operation Hurricane blowing across north-western WA, the safety committee reported to the Australian government that the required conditions were “fully met” (Walker 2014). Fallout from Operation Mosaic again spread across the mainland coast, the first public alert coming not from government but from a prospector in the Pilbara area who contacted a newspaper regarding his Geiger counter having gone off the scale. Fallout levels exceeded safe limits in places like Derby, Port Hedland and Broome (Tynan 2016). The government moved swiftly to silence the news, Supply Minister Beale much later revealing that the issue nearly led to his dismissal from his portfolio (Beale 1977). Excessive iodine-131 levels (<sup>131</sup>I) in sheep and cattle grazing on grass subject to fallout were detected as far afield as Rockhampton (Cross 2001), but the putative safety committee was unresponsive. A 1985 Royal Commission found that the safety committee’s positive report about the Mosaic tests was “grossly misleading and irresponsible” (McClelland and others 1985).

Considerable aeolian redistribution and mixing of radioactive material is also likely since the tests occurred. The Montebello area is highly exposed to extreme weather events, the strongest non-tornadic wind gust ever recorded on Earth (408 kph) having swept adjacent Barrow Island in April 1996.

Instantaneous devastation of the natural biota proximal to the detonations would seem inevitable. Many dead turtles were reported the year following the Hurricane detonation. Other potential impacts on the natural biota remain open to conjecture but, by analogy with demonstrated detriment caused to human health, longer-term harm would also appear likely. A disproportionately high rate of cancers have been reported among servicemen involved in the Montebello tests. Notwithstanding government reluctance to admit potentially costly legal liability, the probability that these cancers were caused by exposure during the bomb tests has effectively been acknowledged by the Australian government through its provision of some compensatory medical measures (Weber and Piesse 2017, Kagi 2018). In early 2024 formal proceedings were launched against the UK Ministry of Defence by surviving UK veterans alleging negligence in its duty of care to both the veterans and to their families before, during and after the tests that began at the Montebellos. It might reasonably be assumed from these health issues suffered by these people, who were present there only briefly, that the longer-term resident natural biota of the archipelago was also adversely affected. As part of a small archipelago elsewhere renowned for their coral reefs and marine life, the test sites are now managed by the WA Parks & Wildlife Service, which advises that no more than one hour should be spent ashore, that relics should not be handled, and that soil should not be disturbed.

No significant clean-up of the site was ever undertaken, nor any study of its radiation levels. Infrastructure from the tests remains, together with large fragments of *HMS Plym* located many hundreds of metres from the blast site. A report from the Australian Radiation Laboratories published in 1979 found that radiation in soils on Alpha and Trimouille islands remained above safe levels for continuous occupancy. Traces of cobalt 60 ( $^{60}\text{Co}$ ) were detected in marine organisms and traces of several radionuclides were detected in vegetation around the ground zeros (Cooper and Hartley 1979). Residual plutonium (Pu) was reported in 2013 (Child and Hotchkis 2013). While activity

levels of the fission and neutron activation products have decreased markedly, Pu levels remain elevated in soils, sediment and biota, with uptake of radioactive isotopes demonstrated in several terrestrial and marine animal species (Johansen and others 2019). Recent studies have found radioactivity concentrations to the northwest that presumably reflect the original fallout plumes. The highest remaining concentrations of strontium-90 ( $^{90}\text{Sr}$ ), caesium 137 ( $^{137}\text{Cs}$ ),  $^{238}\text{Pu}$ ,  $^{239}\text{Pu}$  and  $^{240}\text{Pu}$  in surface sediments were found in the northern part of the archipelago. However, a location 26 km south that was originally selected as an environmental control site revealed higher concentrations of  $^{90}\text{Sr}$  (121 Bq/kg),  $^{137}\text{Cs}$  (1.6 Bq/kg),  $^{238}\text{Pu}$  (80 Bq/kg),  $^{239}$  &  $^{240}\text{Pu}$  (402 Bq/kg) and Americium  $^{241}\text{Am}$  (28 Bq/kg) in comparison to other locations in the archipelago. A core from the base of the Hurricane crater formed beneath *HMS Plym* retained  $^{137}\text{Cs}$  and  $^{241}\text{Am}$  concentrations three times higher than in adjacent surface sediments (Williams-Hoffman and others 2022). Radioactivity levels may have been sufficiently high as to prove lethal to sea turtles for a decade after the tests were conducted, and the present population may carry some of the genomic legacy. Tests conducted in 2019 still found elevated radiation levels in sea turtle skin, bones, egg-shells, embryos and hatchlings, and in some of their diet items. The sands in which turtle eggs are deposited to develop and hatch retain elevated radioactivity levels throughout the depth range to which prospective turtle parents excavate for this purpose (Johansen and others 2020).

## 2. Maralinga

The Maralinga area lies in the Great Victoria Desert and was the site of British nuclear testing from 1955 to 1963. The detonations took place on the Tietkens Plains karst, which is located 175 km NNE from the head of the Great Australian Bight and 850 km NW of Adelaide. The Tietkens Plains karst is topographically very similar to the more celebrated Nullarbor karst to its south, from which it is separated by a range of hills named the Ooldea Range. The following comments are based upon accessible literature, the author's personal observations on Tietkens Plains in late 2022 and on various previous field trips to the Nullarbor.

### *The karst connection*

The Tietkens Plains karst is formed within the 10-20 m-thick Garford Formation dolomite which was deposited during the Miocene. The dolomite



is commonly obscured by aeolian sands from the Great Victoria Desert, upon which a calcrete layer up to 1 m thick has developed. Surface karst landforms include various dongas, rudimentary karren such as rain pits and solution pans etched into subaerially-exposed outcrops. Notwithstanding the presence of many solution cavities observed in one quarry exposure, surface openings have been largely in-filled by aeolian desert sands and other sediment including palaeokarst infills. Present-day permeability of the dolomite is also likely inhibited by some conspicuous case hardening and recrystallization. Negligible evidence for any significant present-day solutional weathering of the dolomite at Tietkens Plains was detected, consistent with its current aridity. Hence, it appears to be essentially a palaeokarst with a long and varied history.

However, as early as the late 1950s, evidence from 18 water bores between Watson on the northern edge of the Nullarbor Plain and Maralinga, and exposure in the historic Tietkens well (Figure 2) suggested that older limestone also existed deeper beneath Tietkens Plains. Given this, and also their topographic similarity and proximity, some



**Figure 2.** Garfield Dolomite beds exposed in Tietkens Well No 1.

clarification of the relationship between the karst at Maralinga and the Nullarbor karst is warranted.

At least two blowholes are known in the limestone on the southern side of the Ooldea Range but none to its north. In contrast to the dolomite karst at Tietkens Plains, the Nullarbor karst south of the Ooldea Range is formed in limestones of the Eucla Group which represents the largest onshore extent of Cenozoic marine sediments anywhere in the world (Clarke and others 2003). At its base is the 300 m-thick mid-Late Eocene (400-350 Ma) Wilson Bluff limestone, the top of which is a calcrete layer formed after the sea withdrew in the early Oligocene. This is overlain by the Abrakurrie Limestone which was subsequently deposited over only the central part of the Nullarbor, after which the sea again withdrew. The sea then returned to deposit the thin Nullarbor Limestone over most of the plain before it withdrew during the Late Miocene-Early Oligocene. The carbonate units were later uplifted and tilted 100-200 m down towards east (Hou and others 2008).

As at Tietkens Plains, karstification of the Eucla Group carbonates of the adjacent Nullarbor also has a long history. The few humanly-negotiable Nullarbor caves that reach the water table probably originated during the seasonally-wet Oligocene. A distinct band of smaller caves and shallow blowholes 25-30 km wide formed in the Abrakurrie and Nullarbor limestones ~75 km from the present coast, probably as flank margin caves on the mid-Miocene shoreline. Considerable speleothem deposition occurred during the Early-Mid Pliocene (5-3.5 Ma) before the peak of the present arid phase was reached about 1 Ma ago (Webb and James 2023). Discharge from some palaeochannels that originate from the north and west progressively sinks underground. While relatively few large caves can be descended to the water table, the vast majority of the known Nullarbor caves are much smaller and can be negotiated only to shallow depth. However, this relative paucity of large caves is likely due to the high primary porosity of the limestone, and it in no way demands any lack of aquifer continuity. Nor does it necessarily demand complete aquifer discontinuity between the Maralinga area and the Nullarbor should the limestone locally extend further north than its surface exposure suggests.

Much older strata predate the Eucla Basin sediments in this general area, including the world's only known Early Cambrian non-marine

oil generated in situ from playa lake source rocks within the Observatory Hill formation, including near the Emu Field test site north of Maralinga (Hibburt 1990). Beneath Maralinga, basal diorite is overlain by about 300 m of shales and sands, interpreted by Ludbrook (1958) as Marinoan (i.e. within the Precambrian) in age, that are in turn overlain by a thin series of grits likely to be either Permian glaciofluvial sediments or Mesozoic sediments containing reworked glacial material. Thin paralic Eocene silts and limestones rest upon these (Ludbrook 1958). Gravels and sands at depth within the Pidinga Formation fine upwards progressively to carbonaceous marginal marine and non-marine sediments. Conformably overlying and intercalated with the Pidinga Formation is the Middle Eocene Paling Formation, a carbonaceous limestone comprising ~75% carbonate. It is laterally equivalent to the Wilson Bluff Limestone although not in proven stratigraphic continuity with it (Hou and others 2023).

The Ooldea Range that separates the Nullarbor from Tietkins Plain is not a bedrock ridge but rather a massive ancient coastal sand dune complex 650 km long and located up to 300 km inland from the present coast. It formed at the end of the Eocene, following maximum marine transgression of the Eucla Basin. Together with the nearby Barton and Paling ranges, the Ooldea Range was formed from hinterland sands and may have originated as barrier islands that later amalgamated into dunes parallel to the coast as shoreline progradation continued. Their remarkable preservation for about 35 Ma likely reflects aridity, vegetation cover, the permeability of the sands, subsequent sea level history and basin hydrodynamics (Benbow and others 1982, Benbow 1990, Fairclough and others 2007). The Garford Formation sediments were deposited into a lagoon that was trapped behind coastal dunes produced by longshore drift around the coast of a massive marine embayment similar in form and scale to the present-day Gulf of Mexico in which the limestones of the Nullarbor accumulated (Morris and Benbow 1986, Hou and others 2003, 2008, Holden 2021).

While wholesale continuity of the Eucla Basin north of the Ooldea Range has largely been disproven (Ludbrook 1958) the precise inland extremity of the limestones of the Nullarbor at a local level is less certain, but it would have been influenced by the original topography upon which the Eucla Group sediments were deposited. The Maralinga area appears to overlie a now-deeply buried valley that was active during the Cainozoic

but was likely initiated considerably earlier. Glacial deposits at depth beneath this part of Australia date from the Permo-Carboniferous (Crowell and Frakes 2007, Mory and others 2008, Hou and others 2008, Fielding and others 2023) when glacial and glaciofluvial processes likely eroded multiple and varied re-entrants into the non-carbonate bedrock substrate into which subsequent sediments would have been deposited, including the Cainozoic sequences that are now targeted by mineral exploration ventures. Any such re-entrants that were unfilled or only partially filled when deposition of the Wilson Bluff limestone occurred would have allowed later localised marine intrusion and deposition of this limestone or facies variants thereof not only beneath Maralinga but perhaps also elsewhere. If the clays between the Garford dolomite and Wilson Bluff limestone equivalents are not continuous, this might theoretically permit linkages between the Tietkens Plains and Nullarbor aquifers anywhere such re-entrants existed.

### ***Military activities***

There is no evidence in the accessible literature of karst concerns having been considered prior to the atomic bomb testing program. Many thousands of kilometres of tracks were established across the most remote parts of Australia to facilitate this testing, and the Maralinga area was the epicentre of this landscape modification. In addition to establishment of an elaborate network of local roads, other infrastructure established included quarries, a massive airstrip, the Maralinga township on the Ooldea Range and the outlying Roadside Village on the karst itself. Vegetation removal and earthworks were also conducted around the test sites on Tietkens Plains. Between 1955 and 1963 seven atomic bombs were detonated at different sites at Maralinga, four ranging from 1-15 kt yield during Operation Buffalo from September-October 1956, and three ranging from 1-26 kt during Operation Antler from September-October of 1957. Hundreds of so-called minor trials were also conducted at three sites, under the code names Rats, Tims, Kittens and Vixen. These tests reportedly again focused on neutron activation to trigger fission (McClelland and others 1985). Only relatively recently has it become evident that the trigger/initiation trials at Emu and Maralinga involved field testing of components for thermonuclear bombs tested during Operation Grapple on islands in the Pacific. A perception of urgency at Maralinga is suggested by the fact that when the first Operation Grapple bomb was detonated in May 1957 it established Britain as



a nuclear state, just in time to pre-empt planned international negotiations towards establishment of a treaty to stem the spread of nuclear weapons that would otherwise have prevented Britain from joining the thermonuclear club (Arnold and Smith 2006, Rabbitt Roff 2022). The greatest radioactive contamination at Maralinga resulted from the 12 Vixen B tests conducted at the Taranaki site. These involved detonation of bombs in such a way as to avoid a full nuclear detonation, but they nonetheless caused 22 kg of plutonium to be flung nearly a kilometre skywards from the heavy metal structure on which the bombs were placed (Tynan 2016).

### *Environmental impact and legacies*

The most visually conspicuous environmental impacts of the testing program included development of the Watson and Roadside quarries and

gravel pits (Figure 3), and vegetation clearing and excavation for construction of the roads, airstrip, housing and other infrastructure, and of the test sites themselves (Figure 4). This frequently involved incision through the upper calcrete and sometimes into the older carbonate units beneath. The detonation of a 27 kt bomb 300 m above a large donga at the Taranaki site stripped the vegetation and evidence of tree damage is still evident beyond



**Figure 3.** Large limestone quarry site at Watson (top) and some of the rubbish dumped into it (bottom).



**Figure 4.** Area prepared for proposed test at Tufi site showing anchors for tethering of a balloon-suspended atomic bomb. This particular site was not ultimately used and hence reflects the landscape damage caused merely by site preparation, unmasked by subsequent explosive impacts.

the donga rim. A broad area around the Breakaway site ground zero similarly remains devoid of trees (Figure 5), factors likely to have been contributed to the lack of regrowth including soil removal by the blast, the production of trinitite by vitrification of the remaining regolith surface caused by the blast (Figure 6), and probably volatilisation of soil nutrients. Similar vitrification occurred elsewhere. At Marcoo a 1.5 kt bomb was detonated at ground level, producing a crater 50 m in diameter and penetrating 12 m deep towards the karst aquifer.

The karst was also seriously contaminated. The “minor trials” at Taranaki involved dispersal of 22 kg of plutonium, 47 kg of uranium and 18 kg of beryllium. At Wewak about 0.6 kg of Pu, 47 kg of uranium and 4 kg of beryllium were dispersed, while at Naya the corresponding figures are 1.2 kg (0.5 kg of which was collected and returned to the UK), 469 kg and 2.4 kg. Further east at Kuli over 7000 kg of natural and depleted uranium and 75 kg of beryllium was dispersed between 1956–63 (James and Williams 1989), while 28 kg of uranium was dispersed around Dobo. Many other contaminants such as asbestos were also left scattered over a wide area after the British left, together with numerous contaminated vehicles and a great deal of contaminated plant and equipment. British attempts to “dilute” the contamination prior to their departure included ploughing of the ground surface to break up the trinitite (Figure 7).





**Figure 5.** Extent of blast-pruned vegetation surrounding Breakaway site ground zero, as at 2023.



**Figure 6.** Trinitite produced through vitrification of the soil surface by the atomic bomb detonated at the Breakaway site.



**Figure 7.** Soil surface subject to ploughing by the British prior to their departure, to “dilute” radioactive contamination by breaking up the trinitite, which greatly complicated subsequent environmental remediation attempts.

In the late 1970s concern was expressed by Australian Defence Minister Jim Killen that the plutonium might be retrieved by communists and should be better secured (Toohey 1978). Britain secretly removed a small quantity in February 1979 but insisted that Australia pay for that exercise. In 1984 the Hawke government established a Royal Commission to determine the condition of the sites and their suitability for return to their traditional owners. In its report released in 1985 (McClelland and others. 1985), the Commission recommended major clean-up of the contaminated sites. The Australian Radiation Protection and Nuclear Safety Agency (ARPANSA) advised the Royal Commission that an estimated 25,000-50,000 contaminated fragments likely remained around Taranaki (Tynan 2016). In 1993 it emerged that the US Roller Coaster program in Nevada in 1963 had involved a series of non-nuclear detonations of Pu-bearing weapons similar to Britain’s so-called “minor trials” in Australia, and when the results were declassified it enabled re-estimation of the degree of contamination in Australia. It had been under-estimated by a factor of about 10 and this must have been known to the British who never conveyed this information to Australia (Anderson 1993). During the clean-up, undertaken from 1995 to 2000, contaminated surface soils were stripped from extensive areas and buried in pits. A trench 15 m deep, 205 m long and 140 m wide was excavated at the most heavily contaminated site, Taranaki, filled to within 3 m of the top with debris, and then covered with 6 m of uncontaminated soil (Figure 8). An estimated 3.3 kg of Pu was contained in the 220,000m<sup>3</sup> of soil scraped up and deposited into the trench. The crater at Marcoo was filled with contaminated debris.

Some information concerning the geology and hydrogeology of the Maralinga area was available prior to the latest clean-up (Morris and Benbow 1986) and a brief examination of the Tietkens Plains karst was also undertaken (James and Williams 1986). However, a report compiled by the Maralinga Rehabilitation Technical Advisory Committee (MARTEC) upon completion of the clean-up program makes virtually no mention of this information having been effectively brought to bear during design of the project, and no reassessment of impacts on the karst caused by either the tests or the clean-up exercise appears to have been undertaken over





**Figure 8.** Debris capping over shallowly buried contaminated materials at the Taranaki site.

the subsequent quarter century. The Hansard record of responses to questioning of one expert witness during Australian Senate's Supplementary Estimates hearing on 3 May 2000 (Commonwealth of Australia 2000) is less than reassuring:

*Senator ALLISON—...At page 8 of the attachment, Mr Davy says: The burial pits contain the contaminated materials at levels well below the base of the limestone ... How accurate is that statement, Mr Harris?... It states: The burial pits contain the contaminated materials at levels well below the base of the limestone ...*

*Mr Harris—We believe that is accurate.*

*Senator ALLISON—You believe that is accurate. Isn't it the case that the debris is only two or three metres below the top of the limestone, not at the base of it?*

*Dr Perkins—The limestone is the rock at the top of a thick sequence of flat-lying sediments. I think Mr Davy was referring to the upper crust of limestone. Beneath that there is a very solid sequence of limestone, sandstone and mudstone. It is a very stable bedrock environment.*

*Senator ALLISON—Indeed, but how could you say that it is well below the base of the limestone when it is just under the top?*

*Dr Perkins—I think what Mr Davy was referring to was the very top part of the limestone sequence.*

*Senator ALLISON—No. He says 'well below the base of the limestone'. It is quite clear.*

*Dr Perkins—Yes. He is saying 'the base of the limestone'. It is a thin sequence, say, of a metre or so. The base of the limestone is the cap, but there is a thick sequence of sediments underneath.*

*Senator ALLISON—A different kind of limestone?*

*Dr Perkins—Yes, that is right. There are limestones and limestones, but it is a layer of solid, stable rock.*

Notwithstanding that the development of subsurface karstic plumbing requires the action of water and Maralinga is presently an arid/sub arid environment where sand blown across the bedrock plains from the Great Victoria Desert further north further insulates the bedrock in some ways, it does still rain sometimes. Subsidence of some burial pits may reflect either compaction and settling, or the opening up of karstic voids due to material being flushed away from the excavation base. Hence, one cannot be entirely sanguine about the risks of contaminant dispersal through karstic conduits, nor perhaps potential local connectivity between conduits formed in the Garford dolomite and Wilsons Bluff limestone.

Dumping of contaminants into the Marcoo crater and excavation of the ditch at Taranaki brought contaminants closer to any unsealed palaeokarstic conduits in the dolomite or underlying limestone. It is also worth noting in the context of Marcoo that there is compelling evidence from battlefields elsewhere in the world for the detonation of even merely conventional bombs having triggered the formation of sinkholes due to bomb craters forming a focus into which runoff subsequently occurs, through the detonation having created new fractures in the bedrock that are susceptible to solutional enlargement, or by a combination of the two (Celi 1991, Kiernan 2013).

The potential for redistribution of contaminants across the karst by strong winds might also usefully be considered. Questioned in a senate hearing in May 2000, the head of the Coal and Minerals Industries Division within the Department of Industry, Science and Resources was dismissive, conceding only "that it may be that some grams of soil blew away" (Commonwealth of Australia 2000). But in arid Australia strong winds and dust clouds are common, and at Taranaki more than just "some grams" so impeded visibility that the clean-up work had to cease on 15 occasions, and once caused complete evacuation of the area (Parkinson 2007). Some of the dust blew back onto cleared areas. Dust was better suppressed at other sites later. On the windy Nullarbor proper there are low parallel ridges that are

believed to be the etched footprints of previously extensive desert dune systems, since blown away (Webb and James 2023). The subdued surface topography on the Nullarbor proper may favour relatively rapid transmission rather than long-term deposition of material entrained by the wind. Sinkholes and caves typically provide more effective aeolian sediment sinks. While the Ooldea Range partly impedes the spread onto the Nullarbor karst of sand blown from the Great Victoria Desert, the same may not be true for finer particles transported higher in the airstream. Analyses of a few samples from within some of the typically dusty Nullarbor caves might be informative.

When subject to physical and chemical weathering, Pu particles can be mobilised in solute or particle form, dispersed by water and taken up by plants and animals (Ikeda and others 2016). Research published in 2021 revealed that “hot” particles persisting at Maralinga, most likely formed by cooling and condensation of poly-metallic melts within the detonation plumes, occur as micro-nano particles. Some are inherently friable and most are susceptible to weathering, which in the arid desert environment at Maralinga is likely to be primarily mechanical, breaching their hard outer shell and facilitating the subsequent redistribution of the radioactive materials by water or as dust. When taken up by plants or soil biota that are eaten by animals it will accumulate (Cook and others 2021).

The aquifers beneath Maralinga may not all be palaeokarstic because Maralinga is not entirely dry. Short intense rain-showers can covert dry dongas into short-lived lakes, subsequent drying of which probably involves a combination of infiltration into the karst, and evaporation such as has been fundamental to calcrete formation. Moderately well incised drainage channels have been cut by runoff on at least the southern flanks of the Ooldea Range (Figure 9), and substantial water-bodies form at its foot on occasions. While hugely diminished since Pliocene times, the precipitation of dripstone speleothems has not entirely ceased beneath the Nullarbor and nor are karst processes likely to be entirely defunct beneath Maralinga. In addition, it has previously been suggested that some of the Nullarbor karstic features were not formed by meteoric water that descended from the ground surface but instead by water that rose up from beneath (Lowry 1967). The reported breaching of at least one blowhole during construction of a road



**Figure 9.** Drainage channel condition indicative of significant present-day rainwater runoff from the southern side of the Ooldea Range.

where no naturally open holes now exist (James and Williams 1988) emphasises the likelihood of continuing water movement through subsurface karst. Numerous subsurface solution cavities are evident in limestone exposed by quarrying on the northernmost Nullarbor at Watson and further east at Rawlinna, areas subject to similar long-term aridity as Tietkins Plains. Many are entirely filled with palaeokarstic sediments or younger red desert sands but others are only partially filled, and open solution cavities and fractures occur beneath and laterally adjacent to some of these infills (Figure 10). Blockage of subsurface conduits in the Maralinga area may well be similarly incomplete and some of the blockages that exist might yet be flushed out again in future, either due to the occasional intense rains or perhaps even in response to climate change.

Given the subsurface solution features and interstratal and fracture permeability evident in the limestone quarries, it is apposite that the material buried at Maralinga is varied and was not sealed. Some interactions recorded in Hansard from the Australian Senate’s Supplementary Estimates hearing on 3 May 2000 seem potentially apposite:

*Senator ALLISON—This option of concrete encasement is something that was floated in the options in the TAG report, was it not? Why has it suddenly become impractical?*

*Mr Harris—Yes, it was one option. But again we are looking to the outcome, and the process that we went through and the way we designed the burial trench has been approved by ARPANSA...the burial trench also has a couple of layers of plastic*



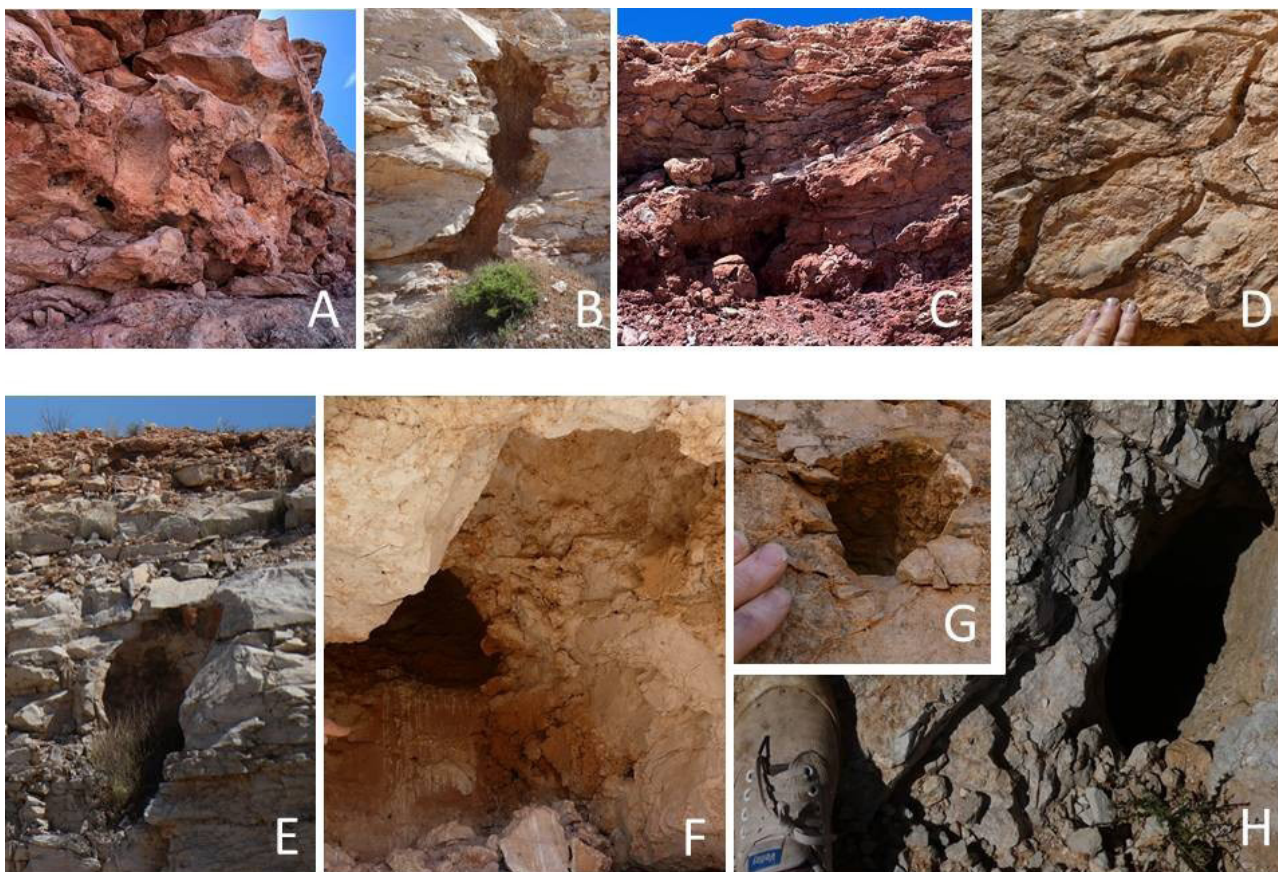


**Figure 10.** Quarry exposures of subsurface palaeokarstic and desert sand fills in solution cavities (A. Watson, B. Rawlinna); generally fractured condition of the limestone (C. Watson); open solution half tubes (D. Watson); and other open voids (EFGH. Rawlinna)

*to clearly identify for people who are wanting to intrude in that trench that they ought to pay attention to what they are doing. That is in addition to the signs that are placed around the trench and to concrete plinths that we are putting at the location.*

*Senator ALLISON—Just as a matter of interest, what is the life of the plastic?*

*Mr Harris—I can only tell you that we got some heavy duty plastic, and I think it is a few thousand years.*

*Senator ALLISON —A bit of plastic lasts a few thousand years? Fascinating.*

*Dr Perkins —We have a more durable marker horizon, a layer of vitrified block material that will last for a considerable time in a geologic sense.*

*[later:]*

*Senator ALLISON—If we can talk about the codes, you said in your press release, Minister, that the project had been conducted in a manner consistent with both international guidelines and domestic codes of practice. In your release on 17 April you said:*

*“Whilst the government was under no obligation to refer to the NHMRC Code of Practice for the near-surface disposal of radioactive waste in Australia (1992) as the Code was not specifically designed for a situation like Maralinga where there already was contamination, in the interests of enhancing safety, the Government elected to observe the Code”.*

*[then later again:]*

*Senator ALLISON—... The code says in clause 2.3.3(a):*

*Radioactive waste shall not contain corrosive materials, waste containing ... alkalis shall be treated to neutralise them.*

*As I understand it, 60 tonnes of soda ash, which is both a corrosive and an alkaline substance, from Ceduna was dumped in the burial pit. Was that material neutralised?*

*[then later:]*

*Senator ALLISON—I will read that clause to you again. It says that radioactive waste shall not contain corrosive materials, and waste containing*



## Military Impacts on Australian Karsts

alkalis shall be treated to neutralise them. Doesn't that suggest that you do not put those two substances together?

Mr Harris—What could be observed is that the limestone environment at Maralinga is an alkaline environment which has a natural neutralising effect on the soda ash.

Senator ALLISON—In 60-tonne quantities? How would it do that?

Mr Harris—There is a lot of limestone out there.

Senator ALLISON—How does it get to 60 tonnes of soda ash? Did you mix it with limestone as you put it in? That is my question. Did you neutralise it?

Mr Harris—It is fully surrounded by this sort of limestone material that the burial trench has been filled in with.

Senator ALLISON—Being surrounded by it does not mean it is necessarily neutralised, does it?

Mr Harris—I would have to refer to experts on how chemical reactions take place in an arid environment.

Just as a globally distributed layer of iridium produced by asteroid impact has been adopted as a marker for the end of the Cretaceous, so too does globally distributed radioactive fallout from bomb testing offer a potential marker bed for commencement of the Anthropocene, in which case Maralinga would be a contender for being the type site for Australia (Holden 2021, Burrows and others 2023). Regional aerial radiometric survey packages available from the South Australian Resources Information Gateway (South Australian Resources Information Gateway 2024) show various concentration points across this part of South Australia (Figure 11). Interpretation is complicated by the fact that there are naturally high levels of uranium in the Gawler Craton and in sediments derived therefrom (Hou and others 2023). However, elevated levels at the actual Maralinga test sites can reasonably be attributed to the testing there. Apparent concentrations further east conceivably involve natural occurrences rather than downwind fallout, but there is also a marked concentration 120-130 kilometres upwind of the test sites at the 20 km-wide Carle Thulka (Lake Maurice) and in a smaller lake basin 8 km to its north, both being located within a low point within Tietkins Plain.

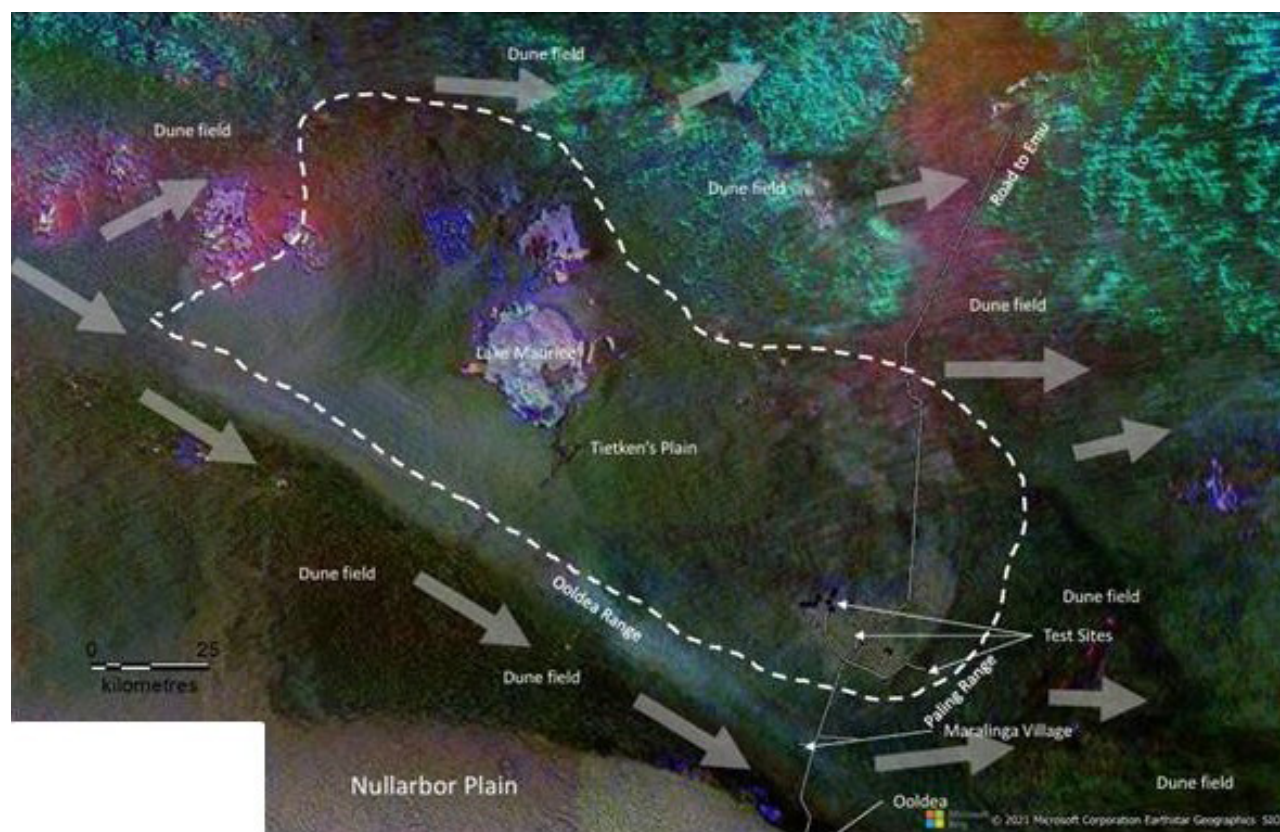


**Figure 11.** Portion of 2017 Gawler Craton Radiometric Survey (PRSA), showing radiation evident in Maralinga area (blue = uranium; green = thorium; red = potassium) and predominant wind directions (broad arrows), from Holden 2021. Most concentrations are natural occurrences but the concentrations around the bomb testing sites and Carle Thulka (Lake Maurice) are noteworthy.



Although a natural explanation for this cannot be discounted, carriage of radionuclides by waters from the test sites is also a possibility. Given that no linking surface plume extends between the test sites and the Carle Thulka area, the possibility exists that the isolated concentration in the latter area is due to evaporation from a point at which deeper karstic groundwater emerges (Holden 2021).

As in the Montebellos, no baseline data is available against which the impacts of bomb testing on cave biota might be assessed, but once again, documented impacts on human health suggest harm is likely. Prior to establishment of Maralinga, tests were also conducted 150 km further north at Emu Field. The Totem 1 test on 14 October 1953 occurred under windy conditions and produced a mushroom cloud that rose to only half the predicted height. While some Aborigines frequenting the test site had been forcibly removed to a refugee camp at Yalata further south, where some of their descendants still reside, others living to the northeast of Maralinga reported a mysterious “black mist” slowly rolling across the area and coating all in a greasy film. At least 45 people from the Yankunytjatjara people reportedly suffered from vomiting, peeling skin, bloody diarrhoea and headaches, and more than half died shortly afterwards. Similar effects reportedly struck people of the Kupa Piti Kunga Tjuta (McClelland and others 1985). The mist appears to have been similar to the “Black Rain” reported after the Hiroshima bombing, when ash from fires effectively seeded the clouds thereby triggering rain that carried high level radioactivity to the ground, this sticky dark radioactive water staining skin, clothing and buildings, contaminating drinking water, causing acute radiation symptoms, and leaving a similar greasy dark film (Yamaguchi 2021). The Emu black mist may have included cobalt-60 ( $^{60}\text{Co}$ ) from the bombs mixed with  $^{59}\text{Co}$  from the metal firing towers. However, anecdotal reports recorded years afterwards were insufficient for modern science because no baseline demographic or Aboriginal health data were available, hence harm to humans could not be scientifically proven to the much later Royal Commission into the Australian tests (McClelland and others 1985). Adverse effects on human health further downwind from Maralinga also appear to have resulted from later testing there, more than half of the plots in the Woomera cemetery dating from the 1950s and 1960s being still-born and newly born babies and toddlers – 23 still-born and 46 other children who died around that period.

An expectation of human health impacts is also implicit in the covert acquisition of human bones to be tested for  $^{90}\text{Sr}$ , involving over 22,000 deceased Australian people, mostly infants, and almost entirely without the knowledge of their families, that was not revealed for 21 years (ARPANSA 2001). It seems hardly likely that natural biota, including cave biota, was not similarly vulnerable to direct and lingering harm from the bomb testing.

Many Australians probably assumed that all was revealed by the Royal Commission in the 1980s, but although it was successful in bringing much information into the public domain concerning past events and remaining contaminants, it also reported having been hindered and frustrated by continuing British secrecy that denied it access to important information (McClelland and others 1985). Lawyers acting on behalf of nuclear veterans seeking compensation for harm caused to themselves or their descendants caused by their exposure have since unearthed over 250,000 pages of documents to which the Royal Commission was not given access (Walker 2014, Billington 2025). Files obtained under FOI in 2011 revealed that the main burial pit had already required significant remediation work. Of 85 pits surveyed in 2010, 19 had suffered erosion or subsidence, eight required “major work” and four contained exposed asbestos (Darling 2011). Under such circumstances, it does not seem unreasonable to revisit assurances regarding conditions at Maralinga today.

## Active Sites

### 1. North West Cape

North West Cape, a peninsula 120 km long and ~35 km wide parallel to the coastline, is one of the westernmost extremities of the Australian continent. Its spine is formed by the highly karstic Cape Range which rises to a little over 300 m altitude. The largest settlement is the town of Exmouth, located about 1100 km north of Perth and ~2000 km SW of Darwin. The Cape Range, the adjacent Ningaloo Marine Park that forms part of Australia’s longest fringing coral reef, and some surrounding coastal areas, are a UNESCO World Heritage site. North West Cape has also been an area of military activity since at least World War II. The following comments are based upon accessible literature, the author’s field observations in 1986 and 2022, and some basic first principles of karst geomorphology and hydrogeology.

### *The karst connection*

The Cape Range karst is formed in an anticlinal ridge of Late Oligocene-mid Miocene marine limestone. The basal unit is the marly 280 m-thick Mandu Formation which crops out only in deeply incised gorges. The overlying Tulki Limestone, ~100 m thick, is widespread. The latter is in turn overlain by the 200 m-thick Trealla Limestone. These units underwent uplift in the late Miocene (Collins and others 2006) and four prominent coastal terraces of Plio-Pleistocene age reflect slower but ongoing uplift. Aeolian calcarenite has formed over parts of the terraces and lower range. While an arid environment, it is subject to significant rainfall events, typically during cyclones. The hydrogeology of the Cape Range and Ningaloo Reef are likely integrated. Cave exploration accelerated in the 1980-90s, partly due to the threat posed by a proposed major limestone quarrying and export enterprise. Several hundred caves are now known, the larger ones occurring mostly on higher parts of the range. Smaller caves at lower altitudes appear to be of flank margin origin and formed during marine high-stands (Hamilton-Smith and others 1998, White and others 2023).

The groundwater system is of Ghyben-Herzberg type, comprising a lens of fresh water floating upon denser more saline waters (Hamilton-Smith and others 1998). In theory, the differential density between fresh and saline water means that any shrinkage of the fresh groundwater lens results in a disproportionately great rise in the level of the more saline water. In reality, the fresh and saline waters are capable of some mixing. The situation beneath Cape Range involves free-draining waters higher on the range, a freshwater lens that floats upon and grades into more brackish water and a wedge of sea water at the base. Allen (1993) suggests that the water table is only ~10 m above sea level even beneath the central part of the range.

The Cape Range karst contains an extraordinarily diverse fauna that contains elements that predate the dinosaurs. The anchialine zone (where fresh and saline waters meet) contains an ancient Tethyan Sea community with a least one genus and three species not known elsewhere in the southern hemisphere (Humphreys 1983). Cape Range is a world hotspot for subterranean biodiversity including stygofauna (Humphreys 2000, 2004, 2008), and it also hosts sites of cultural heritage importance, including archaeological sites up to ~34,000 years old (Morse 1993). In the mid-1990s it was proposed that the

area should be nominated for World Heritage status (Hamilton-Smith and others 1996) but resistance to this proposition was not overcome until it was eventually listed as a World Heritage Area (WHA) in June 2011.

### *Military activity*

North West Cape is the closest base location on the Australian mainland to the South China Sea and other locations in southeast Asia that are relevant to Australia's defence. It is also close to northern Australia's principal mineral, oil and gas resources, and has the most direct all weather land supply lines from Perth and the eastern states. During World War II army contingents were posted to the area, an airfield constructed and a US submarine base established. The Exmouth Gulf area was subject to Japanese air attacks on 21 and 22 May 1942. A further raid on 16 September 1942 was the southernmost Japanese bombing during World War 2. There are two military properties enclosed within the WHA boundaries, namely the Learmonth Air Weapons Range towards the southern end of the Cape Range, used for live fire training exercises and weapons testing, and a naval communications station, principally at the tip of the Cape. The latter was established in 1967 as US Naval Communication Station North West Cape, then renamed in 1968 as Naval Communication Station Harold E. Holt. It is a joint USA/Australia facility and is probably the most powerful transmission station in the southern hemisphere. The highest of its 13 towers (387.4 m) was for many years the tallest human-made structure in the southern hemisphere (Figure 12). This base provides crucial very low frequency transmission to US, Australian and allied ships and submarines in the western Pacific and eastern Indian oceans. In addition, part of the United States Space Surveillance Network commenced operations in October 2022. Given the military importance of these facilities there is probably a high risk of this karst area coming under attack should actual conflict arise.

### *Environmental consequences*

Adverse environmental impacts upon the karst in the Air Weapons Range area are inevitable given the nature of the activities conducted there. Detonation of explosive devices close to or on the ground surface are likely to cause rock shattering and disturbance of ground surface contours and hence rainwater infiltration patterns into the karst. Nitrogen and phosphorous compounds are released





**Figure 12.** Tower array at Naval Communication Station Harold E. Holt, North West Cape.

from explosives at relatively minor levels (Diaz and others 2012). Non-retrieval of unexploded ordnance (UXO) implies the possibility of other chemical agents being slowly released. Heavy metals such as zinc, copper, cadmium and lead are known contaminants of firing ranges (Barker and others 2021). Once again, it is difficult to estimate likely impacts on biota other than by analogy with human health impacts. As one extreme example, Bobonis and others (2020) have demonstrated a decrease in congenital anomalies within proximal human populations following the cessation of bombing practices in Puerto Rico.

Establishment of the town of Exmouth to support the NW Cape tracking base in 1967 resulted in considerable ground surface disturbance associated with construction of roads, houses and services for the very large number of US personnel stationed there during the Cold War years. This population influx resulted in massively increased groundwater abstraction compared to that from the few bores previously established by sparse agricultural enterprises. Water demand was further exacerbated by provision of recreational facilities that included establishment of an 18-hole golf course, bowling greens and playing grounds in this arid environment (Spate and others 1998). Although recycled water was used to establish attractive green areas, as the town developed in subsequent years, and tourism began to flourish, the “Green Oasis Syndrome” also arose, whereby efforts were made by businesses and residents to establish and maintain lush garden plant species that would not otherwise survive. The limited fresh groundwater beneath the Cape Range karst is now drawn upon at the main Exmouth borefield, by borefields established by the RAN and RAAF, and by pastoral, commercial and private parties. The local Water Corporation is cognisant and responsive to the difficulties posed by the karst, but there are also private bores in Exmouth and on Defence Lands.

In addition to the pressure on karst groundwater and its ecosystems that have been created by the water demands generated by military activities, and tourism development, the question of water quality also arises. The risk of increasing salinity due to excessive abstraction from the fresh groundwater lens is far from the only concern. As in several other parts of Australia, aqueous film-forming foam (AFFF) that contained per and polyfluoroalkyl substances (PFAS) was previously used for fire fighting and training at the tracking base. PFAS refers to a very large and very complex group of synthetic chemicals that have been used in various products since the 1950s. The chain of linked carbon and fluorine atoms is extremely strong, greatly inhibiting their degradation in the environment. The first evidence for PFAS potentially having harmful effects on humans emerged in 1955 (Nordby and others 1955) and world-wide evidence of its bioaccumulation in wildlife followed. Litigation concerning PFAS contamination proceeded in the USA during the 1990s and in 1998 the US EPA consulted with at least one PFAS manufacturer about its concerns. PFAS was identified in groundwater at three USA military sites in 2003 (Nicholson 2007). By 2010 various PFAS manufacturing plants in the USA had closed down. Consuming PFAS contaminated food or water, and breathing in PFAS, results in bioaccumulation of these very persistent substances. Likely adverse impacts upon human health include increased risk of some cancers, suppression of antibody responses and hence reduction in the capacity of the immune system to resist infections, altered metabolism and body weight regulation, and increased childhood obesity risk. The presence of PFAS in groundwater at North West Cape as a result of the use of AFFF was recognised in 2016 and environmental investigations were initiated in September 2017.

The tracking base is located on a plain at 1-20 m altitude that is formed on clay, silt, sand and gravels with sand dunes up to 20 m high to its east. This surficial material overlies an irregular and deeply weathered karstified surface formed on limestone. Groundwater is locally perched within the Quaternary sediments but is nevertheless interconnected with the karst aquifer. Of the three limestone units that exist at Cape Range, the two uppermost are highly karstic while the deepest is relatively impermeable (Allen 1993). This is facilitative of lateral spreading of solution activity, which lowering of sea level during glacial climatic stages would have encouraged.

A substantial number of shallow soil boreholes drilled as part of the PFAS investigations were unable to attain even their shallow target depth, refusal occurring due in many cases to an unidentified surface and in others to confirmed bedrock that was assumed to be limestone, generally at depths of less than 5 m (Earth Tech 2005). Tidal fluctuations were found to affect some of the monitoring stations, but with no consistent pattern of decreasing tidal influence with distance from the coast. Such irregularity would perhaps be consistent with the presence of irregularly located karstic conduits rather than evenly permeable bedrock. Groundwater flow was found to be generally directed inland, but with some localised seepage to the coast. A lack of significant contamination of fish was interpreted as indicative of sufficient dilution as to signify only a low risk to Gulf ecosystems (GHD 2018). The Defence Department concluded that the overall level of risk was low. No program to treat or remove PFAS contamination was undertaken, but a PFAS Management Area plan was developed that included provisions regarding soil and groundwater management, together with increased monitoring and review (Defence 2019). Stygofauna was not considered on the basis that it is predominantly associated with fresh water and hence more likely to occur under the adjacent Cape Range rather than the more saline water beneath the plains upon which the base is located. Stygofauna beneath the Air Weapons Range further south is nevertheless potentially at risk from contaminants from live firing and UXO decay.

Water supply has long been an issue on North West Cape, Exmouth being reliant on 34 bores with the Water Corporation having projected demand for an extra 1 billion litres by 2050. This estimate did not include supplying the increased number of personnel associated with current expansion of

naval and air force facilities. The aquifer is reliant on recharge by heavy rainfall events, the future of which is in question as climate change accelerates. A desalination plant has been proposed although this may itself pose some additional environmental stresses.

## **2. Katherine, NT**

RAAF Tindal is a permanent base facility located on karst terrane just over 300 km south of Darwin. It is sited 13 km south-east of the town of Katherine which has a population ~10,000, with ~21,000 people living in the broader region. The base directly neighbours suburbs of Katherine and allotments used for residential, rural and industrial purposes. Karstic aquifers are an important water source in this region. The base lies 9 km north-west from the Cutta Cutta Caves Nature Park and its tourist caves. The comments below are based on literature review and a brief field visit in late 2024..

### *The karst connection*

The karst here is formed in carbonate units of the Cambrian Daly River Group, the basal unit of which is the karstic 204 m-thick Tindall Limestone. This is overlain by the siliclastic Jinduckin Formation, and then the karstic Oolloo Dolostone. Underground hydrogeological connectivity between the limestone and dolostone is believed to be precluded by the Jinduckin Formation (DLRM 2016). The Tindal karst plain is an exhumed pre-Cretaceous palaeokarst surface that formed under different topographical and hydrological conditions to those at present. The caves exhibit strong palaeokarst inheritance and present day drainage through the karst is dictated by palaeokarst structures that are contrary to what might be anticipated from the present day land surface contours. Convection cupolas in the Cutta Cutta caves indicate a degree of cave formation by thermally-heated waters (Lauritzen and Karp 1993). Hence subsurface drainage patterns are even less predictable from surface appearances than is already the case with conventional karst.

This karst forms part of the very extensive Cambrian Limestone Aquifer (CLA) that spans three major sedimentary basins, the Daly, Georgina and Wiso, in each of which the limestone is named differently despite their all being the same unit. The Georgina and Wiso drain northwards over basement highs into the Daly (Currell and Ndehedehe 2022). The presence of similar subterranean crustaceans



across hundreds of kilometres highlights the connectivity of aquifers beyond Katherine to the Beetaloo area, where proposals for fracking have provoked considerable controversy (Rees and others 2020). The Daly is one of few rivers in the Northern Territory that maintain significant flow throughout the dry season, the vast majority of this coming from karstic and fractured aquifers, mostly formed in Tindall Limestone and Ooloo Dolostone (Tickell and others 2002). The karst groundwater is an important resource, being used for residential, rural, industrial and other commercial purposes, including irrigation. It is obtained by means of bores and surface interception downstream of outflows. These karst waters are also an important recreational resource for swimming, boating and fishing. Bathing in warm karst spring waters is an important part of the agenda for many tourists. Because Aboriginal people construe bodies of water spiritually, socially and jurally, rather than just as physical phenomena, the karstic groundwater is deeply significant to them (Langton 2006, Jackson and others 2023).

### *Military activities*

On 2 April 1942 the then-Katherine airfield was bombed by Japanese aircraft during the most inland of the bombing raids to which Australia was subject during World War II (Coulthard-Clark 2001). The origins of the present air base date from 1942 when it was constructed by the US 43rd Engineer Regiment in preparation for use by a squadron of B24 Liberator bombers that was never actually deployed due to changes in the pattern of Japanese military activity. Originally known as Carsons Field the present base was renamed after World War II as Tindal. Between 1963 and 1970 it was restored as a “bare base” to back-up Darwin. It was redeveloped from 1984 as a permanent base to station RAAF aircraft. Subsequent development has included infrastructural improvements, enlargement and strengthening of the runway, and the establishment of additional hardstand areas for parking aircraft. It is currently being further developed. The base complex extends over 122 km<sup>2</sup>.

### *Environmental consequences*

Construction and progressive development of the base has entailed land clearing and landscape modification by both excavation and filling, including the filling of sinkholes. This has changed surface contours, and extensive areas have been rendered impermeable by sealing of the airfield

and aprons. Drainage derangements have included construction of a drain from the base fire station to a nearby wetland area. These various actions have collectively deranged the natural patterns of rainfall and floodwater infiltration into the karst. Land surface stability associated with sinkhole development is a known issue in this karst area, as is the potential for dispersal of water-borne contaminants through the subsurface karst and towards the Katherine River (Karp 2002, Tickell 2005, Kruse and Munson 2013). Water use has increased in this part of the karst due to operation of the base. Other implications of base operations include those associated with training activities and various risks in relation to the storage of substances potentially injurious to the karst. Existence of the base also implies the risk of substantial further damage to the karst should the base be targeted in the event of actual conflict. Training in fire suppression again involved the deployment of PFAS, and of combustion products used to ignite fires for training purposes.

The Defence Department used PFAS for fire-fighting and training at Tindal for a decade up to about 2004. Following recognition of PFAS contamination at some of its sites in November 2016, including at Tindal, Defence informed local residents of the hazards posed by contamination of groundwater and local streams. Because PFAS can enter the human bloodstream through drinking contaminated water, consuming food produced using contaminated water for irrigation including vegetables and meat, or inhaling contaminated dust, an advisory was issued in December 2017. It warned against drinking bore water, eating food products potentially contaminated by it, or swimming in it. Residents were advised not to eat seafood, or consume home produce such as eggs, fruit or leafy greens. After investigation of the base and surrounds, it was revealed in 2018 that PFAS, primarily from the base fire station and fire training area, had entered the groundwater and had migrated towards the Katherine River, contaminating both bore water supplies and the Katherine town water supply (Figure 13). Analyses of locally caught barramundi showed PFAS levels up to six times above safe levels, cod and catfish up to 17 times safe levels, and some other fish species up to 70 times.

Defence installed rainwater tanks on properties previously reliant on bore water, but questions arose as to whether these would be filled on an ongoing

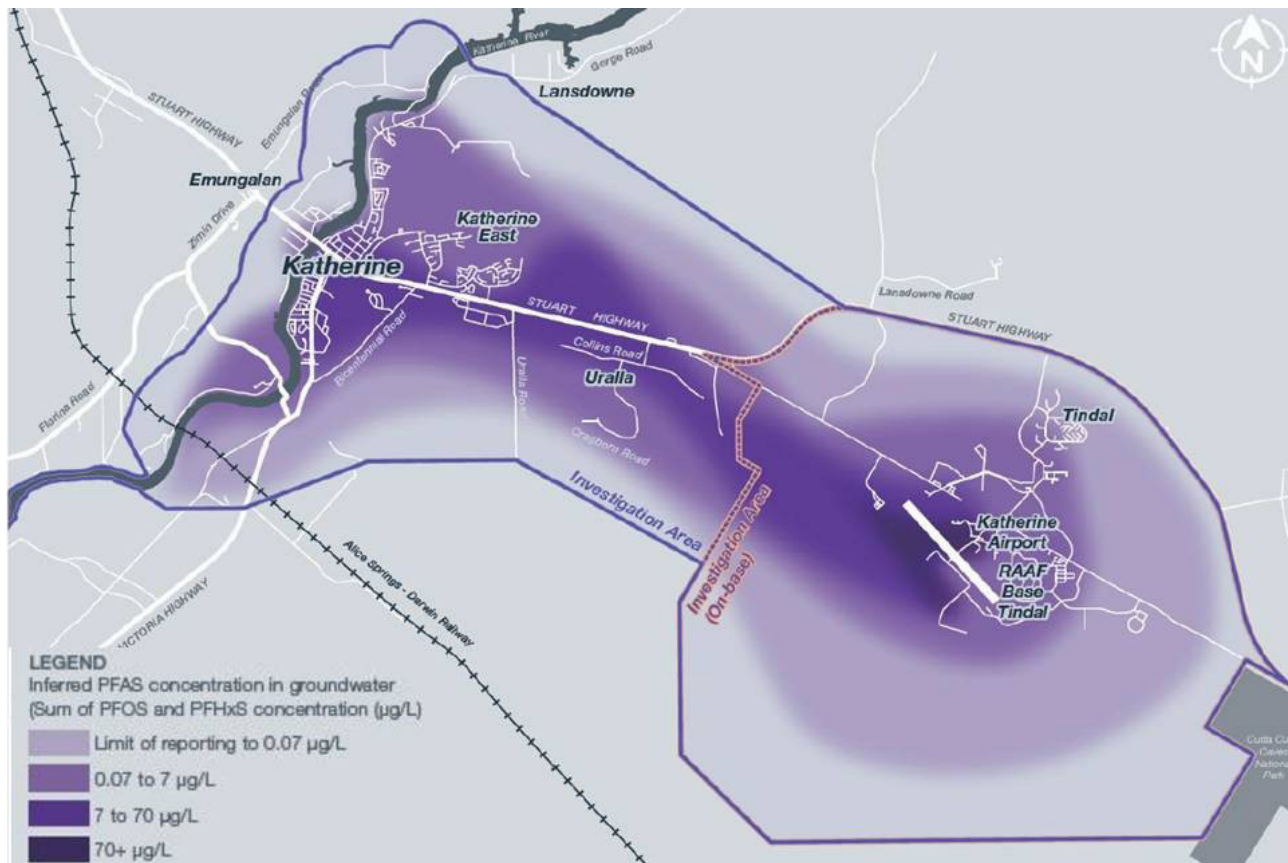


**Figure 13.** PFAS plume in karst groundwater at Katherine. From O'Brien and Edwards (2019)

basis in the event of droughts. Class action was launched by multiple parties seeking compensation on the basis of health risks, the inability to continue to use the water, and diminished property values. Despite evidence from overseas, Australian health authorities continued to assert that any hazard PFAS posed for human health remained unproven, and the Defence Department resisted performing blood tests on humans. The litigants alleged negligent behaviour and negligent failure to inform on the part of the Commonwealth, on the basis of it being reasonably foreseeable that waters, liquids and soluble materials used at the base would get into the water. It was alleged that the Commonwealth had known PFAS was harmful since 1987 but had said nothing, and that some purchasers had unknowingly acquired contaminated properties after that time. It was further argued that the Commonwealth's actions were contrary to Northern Territory water legislation with which it was obliged to comply under its own *Commonwealth Places (Application of Laws) Act 1970*, and were also in breach of section 28 of the *Environment Protection and Biodiversity Conservation Act 1999*, the latter requiring that no Commonwealth agency may take action that will have, or is likely to have, a significant detrimental impact on the environment. One class action for residents of Katherine and two other Defence sites

was settled for \$215.5 million in 2020, and another for various Defence sites was settled for \$132.7 million in 2023.

A new filtration plant developed by the Defence Department and the NT water corporation, which is capable of filtering 28 monitored PFAS compounds, commenced operations in 2023. The winning of some compensation has not entirely resolved the health concerns of some local residents who were previously exposed or are still suffering disadvantage. Nor can it remediate the persistent environmental damage inflicted upon this karst. Issues that remain concerning continued operation of the base include such things as the potential for accidents involving hazardous substances stored on site. The potential also remains for this karst to be further injured should the base be subject to attack in the event of actual conflict.

## Discussion and conclusions

Australia has not been immune from the serious environmental damage that military activities can inflict on karst areas. Legacies of past practices include damage to surface landforms, derangement of drainage causing interference with infiltration of meteoric waters and contamination of karst aquifers that cannot be remediated. These impacts have



arisen largely because the nature and sensitivity of karst environments was not recognised at the time these activities were initiated or undertaken, and/or because military objectives were prioritised to the extent that all other considerations were effectively ignored, as in the Montebello Islands and at Maralinga. However, the fact that military activities continue in some karst areas such as North West Cape and Katherine means that the issue is not just one of regrettable legacies from ignorant times past but also involves the need for careful ongoing karst environmental stewardship. The scale of investment effectively precludes relocating major facilities such as the bases at North West Cape and Katherine to less sensitive, non-karst sites, but the very highest level of environmental management is needed there. Further military facilities should not be sited on or proximal to karst.

The situation at Katherine particularly highlights management of hazardous materials as one concerning facet of environmental management on and around Australia's military bases sited on karst. The *Stockholm Convention on Persistent Organic Pollutants* (POPs) is a global treaty aimed at protecting human health and the environment from harmful chemicals that persist in the environment. In fulfilment of its obligations as a signatory, the Australian government has now banned the importation, manufacture and use of the more prominent varieties of PFAS, effective from 1 July 2025. However, we may not have heard the last of PFAS with advent of the new Australian government ban, because PFAS have a wide range of military applications beyond the fire-fighting foams that have already proven problematic. They are utilised in munitions to improve performance and durability, increase shelf life and reduce the likelihood of unwanted explosions due to shock. PFAS represents from 1 to 3% of the net explosive weight of about 20% of all common US weapons. PFAS are used as a binder in conventional and strategic weapons platforms and in aircraft and various missile systems. Hence, environmental risks are posed by firing and disposal of munitions and by the burning of some military waste (Cottrell 2025). PFAS are also found in sealants, cleaning fluids, waterproofing agents, refrigerants, electronics, batteries and protective clothing. While the Australian ban on PFAS is consistent with its obligations as a signatory to the Stockholm Convention, that convention also makes provision for exemptions for defence purposes. Moreover, arbitrary exemptions from laws can

also occur at various levels. In March 2025 it was revealed that a \$270 million fuel tank facility to support US operations at Tindal and elsewhere (Project Caymus) had been built at Darwin by a contractor without having first obtained the permit required under the *Northern Territory Building Act 1993*. The 11 large fuel tanks, to hold 300 million litres, had been due for completion in 2023 but were still not operational due to water intrusion into the leakage detection system. The Northern Territory Chief Minister, whose government enthusiastically encourages any development perceived as being financially beneficial to Darwin, indicated that no penalty would be applied (Hislop and O'Shea 2025).

Considerable further research is required to better understand the nature, extent and longevity of military impacts on karst in Australia, and indeed elsewhere. Many questions remain concerning the distribution and persistence of radioactive products from the Montebello and Maralinga nuclear tests. The extent to which transmission of radioactive contaminants via karstic groundwater, as has occurred with the PFAS at Katherine and North West Cape, is one obvious example. Such investigation of lingering radioactivity as has occurred at Maralinga to date has been confined to surface and near surface studies rather than groundwater investigations. Ascertaining whether the elevated uranium levels upwind of the Maralinga test sites at Carle Thuka (Lake Maurice) is explicable by natural erosion of uranium from granites further north, or is instead due to redistribution of fallout from the bomb testing via groundwater, warrants examination. Ascertaining whether the Carle Thuka lake basin hosts concentrations of any other non-natural radionuclides such as  $^{137}\text{Cs}$  might offer one possible avenue for resolving the question. This isotope has been produced only by nuclear weapons testing and has been distributed globally to the extent that it can be used as a marker horizon in soil erosion studies, including in Australia (Loughran and others 1992). Any particular concentration of  $^{137}\text{Cs}$  at Carle Thuka might be suggestive of its transmission by water from the Maralinga test area. Greater confidence may be achievable by more detailed studies to determine the age of non-natural isotopes present, perhaps along the lines of work by Stäger and others (2023) who were able to discriminate between “older”  $^{137}\text{Cs}$  from weapons testing fallout and “younger” fallout from the Chornobyl fallout disaster based on  $^{135}\text{Cs}/^{137}\text{Cs}$  ratios in wild boar meat samples. Similarly, the possibility of a

plume into the karstic aquifer beneath Montebello Islands and into the sea warrants investigation. The Katherine experience should mark the end of military environmental assessments that ignore what is hidden beneath our feet. A lack of baseline data typically complicates assessment of impacts on biota. One possibility worth exploring may be whether any dateable bone or other organic deposits that may allow insight into pre versus post impact populations exist in caves on the Montebellos, in crevices or blowholes at or near Tietkens Plains, or around the bases at North West Cape and Katherine.

The case studies presented in this paper represent only part of the story concerning military impacts on Australian karst. Other areas of karstic or potentially karstic terrane that have been subject to military impact occur around Lancelin in Western Australia and possibly near Murray Bridge in South Australia. The Australian Government has recently acquired land in North Queensland on which to establish its new Greenvale Training Area, consistent with the Australia-Singapore Military Training Initiative. This will cater for up to 14,000 Singaporean Armed Forces personnel involved in live firing and other operations. The site is not far from the Broken River karst from where recent remains of the Ghost Bat have been recorded, and hence operations there might conceivably impact upon this threatened species.

Less conspicuous potential military impacts on karst include the winning of construction materials such as cement, and air pollution. Climate change triggered by the massive scale and geographic spread of atmospheric emissions from military sources can have implications for karst far distant from any operational sites, through such mechanisms as changes in precipitation volume, type or seasonality, and hence infiltration and runoff, and also biotic changes that influence water chemistry (Viles 2003, Morrissey and others 2021). Most military CO<sub>2</sub> emissions result from the use of liquid fuel by aircraft. If global military CO<sub>2</sub> emissions were amalgamated as if the output of a single country, it would rank fourth behind China, the USA and India (Parkinson 2023). It seems ironic that many military organisations and governments now recognise anthropogenic climate change as having very significant national security implications, yet they seek to quarantine their own military emissions from climate change discussions and protocols (Crawford 2019). Even though its military is the world's largest institutional consumer

of hydrocarbons, the USA government insisted upon an exemption for military emissions before it would sign the 1997 Kyoto Protocol (Neimark and others 2020).

As an Annex 1 country under the Kyoto Protocol, Australia is obligated to set binding emissions reduction targets through the United Nations Framework Convention on Climate Change (UNFCCC). The guidelines produced by the Intergovernmental Panel on Climate Change (IPCC) require that military fuel use should be reported under IPCC category 1.A.5, which includes all mobile fuel (i.e. fuel used by planes, ships and ground transport) and all stationary fuel consumption (i.e. used on bases). The most disaggregated level should be provided for each source, but aggregation is permitted to protect military information, which stymies differentiation of mobile from stationary emissions, a particular concern at a time when military conflict and expansion of facilities, production and procurement of war materiel, and active field testing and training are all increasing markedly (Alexander 2025). Accounting is further stymied by the failure of some states to submit their data or their submission of incomplete data, and Australia is one of the culprits (Military Emissions Gap 2025). However, CO<sub>2</sub> is not the end of the story. Release of nitrogen oxides, vapour trails and cloud formation due to aircraft contributes nearly twice that of their CO<sub>2</sub> emissions to global warming (European Commission 2020).

A complete accounting of military impacts on Australian karst would also need to include the wider Australian defence industry which includes numerous non-governmental organisations that supply equipment, services and weapons to both the Australian Department of Defence and for export, the latter potentially also causing environmental detriment to those overseas places where they are used, stored or otherwise disposed of. Estimates of the size of this wider Australian defence industry differ because arbitrary boundaries have to be selected where companies also service a civilian market and produce both military and civilian goods. A broad impression can be gleaned from approximately 61,600 people having been employed in the Australian defence industry in 2021-22 and the Australian government having awarded over \$38 billion in contracts in 2022-23. If supply chain and supporting businesses are factored in, over 100,000 jobs are involved (Australian Government 2024). In 2018 Australia was the world's 20th largest exporter of military



products and the Gillard ALP government initiated a program aimed at increasing this ranking to 10th largest exporter. Many of the businesses involved in the Australian defence industry are of small to medium size and they occur in scattered locations across the country. The extent to which any may be located in karst areas, obtain their resources directly or indirectly from karst areas, or otherwise impact karst areas, has never been evaluated. While the Department of Defence may now undertake environmental evaluations and strive to adapt to environmental laws, the same is not necessarily the case for its suppliers or exporters.

Massive environmental harm is likely to be inflicted upon karst systems if bases or non-government defence industry sites located in karst areas should come under attack in the event of actual conflict occurring on our shores. Modern explosive ordinance is likely to result in major landscape destruction by craterisation. The surficial sediments at North West Cape and Katherine are generally thinner than the depth of some bomb craters produced by conventional weapons even back in the 1970s (Kiernan 2013). This implies that any filtering of the water being transmitted downwards into the karst is likely to be eliminated. Destruction of previously productive soil profiles and contamination with toxic materials in munitions or other weapons, or leaking from targeted facilities, also has implications for biota, including cave fauna that is commonly highly sensitive to environmental disturbance. Australia has thus far been fortunate in not having active modern conflict in any part of its karst estate, and those militarily-inflicted harms to which Australia's karstlands have been subject due to military impacts have been inadvertently inflicted in pursuance of sufficient deterrent capability to ensure this fortunate situation continues.

However, the Australian government is currently spending \$800 million to transform the Learmonth air base from a bare base to a battle-

ready facility. The US military wishes to establish its own jet fuel storage at Learmonth of 500,000 barrels, some 40 times greater than is contained in the current Australian fuel farm. The Learmonth expansion is part of an \$18 billion upgrading of bases across northern Australia, which also includes major expansion of the Tindal facility on the Katherine karst. Tindal is currently being upgraded to facilitate its stationing of six nuclear capable US bombers as part of defence agreements entered into by previous Australian governments (Figure 14), thereby increasing the likelihood of this karst being subject to attack and contamination should actual conflict arise in the future. Both North-West Cape and Tindal are likely to be prime targets, potentially nuclear targets, in the event of conflict between the USA and China. Given that international protocols aimed at reducing harm to environmental and heritage values during armed conflict are specifically nullified if military facilities are sited in the same locations, Australia's karst environments should not be put at any further risk than they already face by the establishment of any additional military or wider defence industry facilities within or proximal to them.

## Acknowledgements

I am grateful to various companions in the field; to the Maralinga Tjarutja people for allowing access onto their land; and to Darren Holden for helpful comments on a draft and provision of Figure 11.

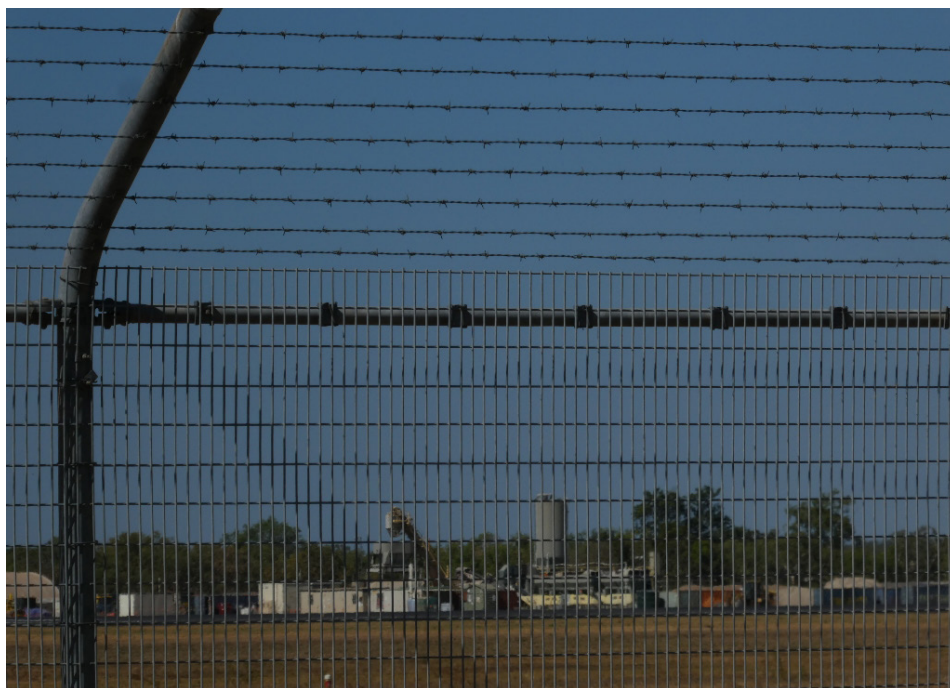


**Figure 14.** Tindal base in the Katherine karst is currently being upgraded for stationing of nuclear-capable US bombers.

## References

- ALLEN, A.D. 1993 Outline of the geology and hydrogeology of Cape Range, Carnarvon Basin, Western Australia [in] HUMPHREYS W.F. (ed.) *The Biogeography of Cape Range, Western Australia. Records of the Western Australian Museum Supplement* 45. pp. 25-38.
- ALEXANDER, G. 2026 New data reveals the military emissions gap is growing wider. ceobs.org 6 November 2026. Accessed 12 November 2026.
- ARNOLD, L. 1987 *A Very Special Relationship: British Atomic Weapon Trials in Australia*. HMSO, London, 1987.
- ARNOLD, L. & PYNE, K. 2001 *Britain and the H-bomb*. St Martins Press, NY.
- ARNOLD, L. & SMITH, M. 2006 *Britain, Australia and the Bomb. The Nuclear Tests and their Aftermath*. Palgrave MacMillan, NY.
- ARPANSA 2001 *Australian strontium 90 testing program 1957-1978*. Australian Radiation Protection & Nuclear Safety Agency.
- AUSTRALIAN GOVERNMENT 2016 *2016 Defence White Paper*. Department of Defence, Canberra.
- AUSTRALIAN GOVERNMENT 2024 *Defence Industry Development Strategy*. Department of Defence, Canberra.
- ANDERSON, I. 1993 Britain's dirty deeds at Maralinga. *New Scientist*, 12 June 1993: 12-13.
- BARKER, A.J., CLAUSEN, J.L., DOUGLAS, T.A., BEDNAR, A.J., GRIGGS, C.S. & MARTIN, W.A. 2021 Environmental impacts of metals resulting from military training activities: A review. *Chemosphere*, 265: 129110.
- BEALE, H. 1977 *This Inch of Time: memoirs of politics and diplomacy*. Melbourne University Press, Melb.
- BENBOW, M.C. 1990 Tertiary coastal dunes of the Eucla Basin, Australia. *Geomorphology*, 3: 9-29.
- BENBOW, M.C., LINDSAY, J.M., HARRIS, W.K., COOPER, B.J. 1982 Latest Eocene marine incursion, northeast of the Eucla Basin. *Geol. Surv. South Australia Qtly Geol. Notes*, 81: 2-9.
- BENJAMIN, J., O'LEARY, M., MCCARTHY, J., REYNAN, W., WISEMAN, C., LEACH, J., BOBELDYK, S., BUCHLER, J., KERMEEN, P., LANGLEY, M., BLACK, A., YOSHIDA, H., PARNUM, I., STEVENS, A., ULM, S., McDONALD, J., VETH, P. & BAILEY, G. 2023 Stone artefacts on the seabed at a submerged freshwater spring confirm a drowned cultural landscape in Murujuga, Western Australia. *Quaternary Science Reviews*, 313: 108190.
- BILLINGTON, M. 2025 Ghosts in the archives: Australian institutions still hesitate to tell the story of the atomic veteran. *Australian Policy and History Network*. <https://aph.org.au> Accessed 20 November 2025.
- BOBONIS, G.J., STABILE, M. & TOVAR, L. 2020 Military training exercises, pollution, and their consequences for health. *Journal of Health Economics*, 73: 102345.
- BURROWS, L., HOLDEN, D. & TYNAN, E. 2023 Untangling Maralinga: Spatial and temporal complexities of Australia's atomic Anthropocene. *J. Australian Studies*, 47(3): 515-530.
- CELI, M. 1991 The impacts of bombs of World War I on limestone slopes of Monte Grappa. *Proc. International Conference on Environmental Changes in Karst*. University of Padova, Italy. pp. 279-288.
- CHILD, D.P. & HOTCHKIS, M.A. 2013 Plutonium and uranium contamination in soils from former nuclear weapons test sites in Australia. *Nuclear Instruments & Methods in Physics Research B*, 294: 693.
- CHIAPPINI, R., POINTURIER, F., MILLIES-LACROIX, J.C., LEPETIT, G. & HEMET, P. 1999  $^{240}\text{Pu}/^{239}\text{Pu}$  isotopic ratios and  $^{239+240}\text{Pu}$  total measurements in surface and deep waters around Mururoa and Fangataufa atolls compared with Rangiroa atoll (French Polynesia). *Science of the Total Environment*, 237-238: 269-276.
- CLARKE, J.D., GAMMON, P.R., HOU, B. & GALLAGHER, S.J. 2003 Middle to Upper Eocene stratigraphic nomenclature and deposition in the Eucla Basin. *Aust. J. Earth Sciences*, 50(2): 231-248.
- COLLINS, B., READ, J.F., HOGARTH, J.W. & COFFEY, B.P. 2006 Facies, outcrop gamma ray and C-O isotopic signature of exposed Miocene subtropical continental shelf carbonates, North-West Cape, Western Australia. *Sedimentary Geology*, 185(1-2): 1-19.



- COMMONWEALTH OF AUSTRALIA 2000 *Official Committee Hansard, Senate Economics Legislation Committee, Consideration of Supplementary Estimates, Wednesday, 3 May 2000*: E56.
- COOK, M., ETSCHMANN, B., RAM, R., IGNATYEV, K., GERVINSKAS, G., CONRADSON, S.D., CUMBERLAND, S., WONG, V.N. & BRUGGER, J. 2021 The nature of Pu-bearing particles from the Maralinga nuclear testing site, Australia. *Scientific Reports*, 11: 10698. DOI.org/10.1038/s441598-021-89757-5.
- COOPER, M.B. & HARTLEY, B.M. 1979 Residual radioactive contamination of the Monte Bello Islands from nuclear weapons tests conducted in 1952 and 1956. *Australian Radiation Laboratory*, TR010. ARL, Yallambie, Vic.
- COTTRELL, L. 2025 PFAS contamination from the military use of firefighting foams is widespread but it's far from the whole story. CEOBS Blog, Military and the environment, February 17, 2025. <https://ceobs.org/PFAS-forever-chemicals-are-in-munitions-and-other-military-applications-too/>
- COULTHARD-CLARK, C. 2001 *The Encyclopedia of Australia's Battles*. Allen & Unwin, Sydney.
- CRAWFORD, N.C. 2019 *Pentagon fuel use, climate change, and the costs of war*. Watson Institute, Brown University.
- CROSS, R. 2001 *Hedley Marston and the British Bomb Tests in Australia*. Wakefield Press, Kent Town.
- CROWELL, J. & FRAKES, L. 2007 The Late Palaeozoic glaciation of Australia. *J. Geol. Soc. Australia*, 17(2): 2515-2540.
- CURRELL, M. & NDEHEDEHE, C. 2022. *The Cambrian Limestone Aquifer, Northern Territory: Review of the Hydrogeology and Management Rules to Ensure Protection of Groundwater Dependent Values*. Environment Centre NT, Darwin.
- DARLING, P. 2011 Maralinga sites need more repair work, files show. *The Age*, 12 November 2011.
- DAY, M. & KUENY, J. 2004 Military uses of caves. [in] GUNN, J. (ed.) *Encyclopedia of Caves and Karst Science*. pp. 509-511. Fitzroy Dearborn, NY & London.
- DEFENCE 2019 Naval Communication Station Harold E. Holt A & B – Environmental risk assessment and PMAP. [https://web.archive.org.au/awa/20230427120707mp\\_/https://defence.gov.au/Environment/PFAS/Docs/HaroldEHolt/FactSheets/201905HEHERAPMAPFactsheet.pdf](https://web.archive.org.au/awa/20230427120707mp_/https://defence.gov.au/Environment/PFAS/Docs/HaroldEHolt/FactSheets/201905HEHERAPMAPFactsheet.pdf) Accessed 19 May 2025.
- DEPARTMENT OF DEFENCE 2020 Submission to EPA's Public Consultation in Relation to Strategic Advice on Cumulative Impacts in Exmouth Gulf [https://www.epa.wa.gov.au/sites/default/files/Department%20of%20Defence\\_Redacted.pdf](https://www.epa.wa.gov.au/sites/default/files/Department%20of%20Defence_Redacted.pdf)
- DIAZ, E., SAVARD, S. & POULIN, I. 2012 Air residues from live firings during military training. *Air Pollution*, XX(157): 399-408.
- DLRM 2016 *Background Brief – Ooloo Dolostone Aquifer Water Allocation Plan*. Department of Land Resource Management, Darwin.
- EARTH TECH ENGINEERING PTY LTD 2005 *Naval Communication Station Harold E. Holt Stage 2 Environmental Investigation*. August 2006.
- EDEN, A. 1961 *Full Circle. The Memoirs of Sir Anthony Eden*. Casell, London
- EUROPEAN COMMISSION 2020 *Updated analysis of the non-CO<sub>2</sub> climate impacts of aviation and potential policy measures pursuant to EU Emissions Trading System Directive Article 30(4)*. Commission Staff Working Document, EU, Brussels.
- EUROPEAN UNION 2006 Regulation (EC) No. 1907/2006 of the European Parliament and of the Council-concerning the Registration, Evaluation, Authorisation and Restriction of Chemicals (REACH). *Official Journal of the European Union* L396 49. <https://eur-lex.europa.eu/legal-content/EN/TXT/?uri=OJ:L:2006:396:TOC>. Accessed 12 May 2025.
- FAIRCLOUGH, M.C., BENBOW, M.C., ROGERS, P.A. 2007 *Explanatory Notes for the OOLDEA 1:250 000 Geological Map*. South Australia Dept. Primary Industries & Resources Report Book 2007/11.
- FIELDING, C.R., FRANK, T.D. & BIRGENHEIER, L.P. 2023 A revised, late Palaeozoic glacial time-space framework for eastern Australia, and comparisons with other regions and events. *Earth-Science Reviews*, 236: 104263.

## Military Impacts on Australian Karsts

- FINLAYSON, B. & HAMILTON-SMITH, E. (eds.) 2003 *Beneath the Surface: A natural history of Australian caves*. UNSW Press, Sydney. 216 pp.
- GHD 2018 *Department of Defence. Naval Communications Station Harold E Holt – Area A PFAS Investigations* DSI Report. <https://defence.gov.au/Environment/PFAS/docs/HaroldEHolt/Reports/201812.HEHA.DSI.pdf>. Accessed 13 February 2023
- GRACE, P. 2023 *Operation Hurricane: The story of Britain's first atomic test in Australia and the legacy that remains*. Hachette, Australia.
- HALLIDAY, W.R. 1976 *Depths of the Earth*. Harper & Row, NY.
- HAMILTON-SMITH, E., KIERNAN, K. & SPATE, A. 1996 *Karst Management Considerations for the Cape Range Karst Province Western Australia*. Report to WA Dept. Environmental Protection.
- HIBBURT, J. 1990 *Petroleum Exploration Opportunity Officer Basin*. Department of Minerals & Energy Data Package Brochure Rpt. BK 90/64. South Australia.
- HISLOP, J. & O'SHEA, D. 2025. Project Caymus fuel tanks for US military built unlawfully on Darwin Harbour. *ABC News*, 10 March 2024. <https://www.abc.net.au/news/2025-03-10/project-caymus-darwin-fuel-tanks-us-military-built-unlawfully/105021774>. Accessed 23 May 2025.
- HOCKING, R.M., MOORS, H.T. & VAN DE GRAAFF, W.J. 1987 Geology of the Carnarvon Basin Western Australia. *Geological Survey of Western Australia Bulletin*, 133. GSWA, Perth.
- HOLDEN, D. 2021. *Maralinga by the Sea: Heterotopographia and the transition into the Anthropocene*. Presentation to Geological Society of Australia (Western Australian Division), Perth, 6 October 2021 (supplied by author).
- HOU, B., FRAKES, L.A., ALLEY, N.F. & HEITHERSAY, P. 2003 Evolution of Beach Placer Shorelines and Heavy-Mineral Deposition in the Eastern Eucla Basin, South Australia. *Australian Journal of Earth Sciences*, 50: 955-965.
- HOU, B., FRAKES, L.A., SANDIFORD, M., WORRALL, L., KEELING, J., & ALEY, N.F. 2008 Cenozoic Eucla Basin and associated palaeovalleys, southern Australia – Climatic and tectonic influences on landscape evolution, sedimentation and heavy mineral accumulation. *Sedimentary Geology*, 203: 112-130.
- HOU, B., PETTS, A., KRAPP, C., IRVINE, J., STOLAN, L., HEATH, P., REED, G. & FOSS, C. 2023 *Remapping the palaeovalley systems of the central-western Gawlewe Craton, South Australia*. Geological Survey of South Australia Report Book 2023/00043. S.A. Dept. for Energy and Mining.
- HUMPHREYS, W.F. (ed.) 1993 The Biogeography of Cape Range, Western Australia. *Records of the Western Australian Museum, Supplement* 45. 248 pp.
- HUMPHREYS, W.F. 2004 Cape Range, Australia: Biospeleology [in] Gunn, J. (ed.) *Encyclopedia of Cave and Karst Science*. Fitzroy Dearborn, NY & London. pp. 181-183.
- HUMPHREYS, W.F. 2008 The hypogean fauna of the Cape Range Peninsula and Barrow Island, Northwestern Australia [in] WILKENS, H., CULVER, D.C. & HUMPHREYS, W.F. (eds.) *Ecosystems of the world. Subterranean ecosystems*. Elsevier, Amsterdam. pp. 581-601.
- IKEDA-OHNO, A., SHAHIN, L.M., HOWARD, D.L., COLLINS, R.N., PAYNE, T.E. & JOHANSEN, M.P. 2016 Fate of plutonium at a former nuclear testing site in Australia. *Environ. Sci. Technol.* 50, 9098-9104. <https://doi.org/10.1021/acs.est.6b01864> (2016).
- JACKSON, S., O'DONNELL, E., GODDEN, L., LANGTON, M. 2023 Ontological collisions in the Northern Territory's Aboriginal water rights policy. *Oceania*, 93(3): 259-281 DOI:10.1002/ocea.5388
- JAMES, J.M. & WILLIAMS, G.A. 1988 *Tietkins Plain Karst – Maralinga*. ARL/TR081, Australian Radiation Laboratory. Yallambie, Victoria.
- JEBREEN, H., WOHNICH, S., BANNING, A., WISOTZKY, F., NIEDERMAYR, A. & GHANEM, M. 2018 Recharge, geochemical processes and water quality in karst aquifers: Central West Bank, Palestine. *Environmental Earth Sciences*, 77(261).
- JENNINGS, J.N. 1987 *Karst Geomorphology*. 2nd Edn. Blackwell, Oxford.
- JOHANSEN, M.P., CHILD, D.P., CRESSWELL, T., HARRISON, J.J., HOTCHKIS, M.A., HOWELL, N.R.,



- JOHANSEN, A., SDRAULIG, S., THIRUVOTH, S., YOUNG, E., WHITING, S.D. 2019 Plutonium and other radionuclides persist across marine-to-terrestrial ecotopes in the Montebello Islands sixty years after nuclear tests. *Science of the Total Environment*, 691: 572-583.
- JOHANSEN, M.P., CHILD, D.R., HOTCHKIS, M.A., JOHANSEN, A., THIRUVOTH, S. & WHITING, S.D. 2020 Radionuclides in sea turtles at the Montebello Islands former nuclear test sites: Current and historical dose rates for adults and embryos. *Marine Pollution Bulletin*, 158: 111390.
- KAGI, J. 2018 Montebello nuclear testing veterans exposed to radiation vent anger over gold card refusal. *ABC News*, 15 March 2018. <https://www.abc.net.au/news/2018-03-15/nuclear-testing-veterans-hold-protest-at-wa-parliament/9551658>. Accessed 10 August 2025.
- KARP, D. 2002 Land degradation associated with sinkhole development in the Katherine region. *Technical Report*, 11/2002, Resource Assessment Branch, Department of Infrastructure, Planning & Environment.
- KEARNEY, A., O'LEARY, M. & PLATTEN, S. 2023. Sea Country: Plurality and knowledge of saltwater territories in Indigenous Australian contexts. *The Geographical Journal*, 87, Article 1891104116.
- KIERNAN, K. 2012 Impacts of war on geodiversity and geoheritage: case studies of karst caves from northern Laos. *Geoheritage*, 26(4): 225-247.
- KIERNAN, K. 2013 Nature, severity and persistence of geomorphological damage caused by armed conflict. *Land Degradation and Development*, 26(4):380-396.
- KIERNAN, K. 2021a Some impacts of war on karst environments and caves. *Helictite*, 46: 15-45.
- KIERNAN, K. 2021b Geodiversity also needs protection during armed conflicts. CEOBS, UK <https://ceobs.org/geodiversity-also-needs-protection-during-armed-conflicts/> Accessed 9 May 2025.
- KRUSE, P.D. & MUNSON, T.J. 2013 Daly Basin [in] KRUSE, P.D. & MUNSON, T.J. (compilers) Geology and Mineral Resources of the Northern Territory. *Northern Territory Geological Survey Special Publication 5*.
- LANGTON, M. 2006 Earth, wind, fire and water: The social and spiritual construction of water in Aboriginal societies [in] BRUNO, D., BARKER, B. & MCNIVEN, I. (eds.) *The Social Archaeology of Australian Indigenous Landscapes*. pp. 139-160. Aboriginal Studies Press, Canberra.
- LAURITZEN, S.E. & KARP, D. 1993 *Speleological Assessment of Karst Aquifers developed within the Tindal Limestone Katherine, NT. Report 63/1993*. Interim Report to the Director, Water Resources Division of the Power and Water Authority, Darwin.
- LEBREC, U., RIERA, R., O'LEARY, M., WEBSTER, J.M., YOKOYAMA, Y., GLIGANIC, L.A., LANA S.C. & PAUMARD, V. 2023 Drilling 1100-km-long seafloor ridges reveals how palaeoshorelines control carbonate shelf morphologies (North West Shelf, Australia). *Quaternary Science Reviews*, 312.
- LOUGHRAN, R.J., CURTIS, S.J., ELLIOTT, G.L., CAMPBELL, B.L., KIERNAN, K. & TEMPLE-SMITH, M.G. 1992 A reconnaissance survey of soil erosion in Australia. *Proc. 7th International Soil Conservation Conference – People Protecting Their Land*. pp. 52-63.
- LOWRY, D.C. 1967 The origin of blowholes and the development of domes by exsudation in caves of the Nullarbor Plain. *Geol. Surv. WA Annual Report 1967*: 40-44.
- LUDBROOK, N.H. 1958 The subsurface stratigraphy of the Maralinga area, South Australia. *South Australia. Department of Primary Industries and Resources. Report Book*. Aesis.200101811. <https://search.informit.org/doi/10.3316/aesis.200101811>
- MANSOUR, M.M., PEACH, D.W., HUGHES, A.G. & ROBINS, N.S. 2012 Tension over equitable allocation of water: Estimating renewable groundwater resources beneath the West Bank and Israel. *Geol. Soc. Lond. Spec. Publ.* 362, 355-361.
- MATTHEWS, P.G. 1985 *Australian Karst Index*. Australian Speleological Federation, Broadway, NSW. 481 pp.
- MCCLELLAND, J., FITCH, J. & JONES, W.J. 1985 *Royal Commission into British Nuclear Tests in Australia Report*. AGPS, Canberra.

## Military Impacts on Australian Karsts

- MILITARY EMISSIONS GAP 2025 The military emissions gap – data. <https://militaryemissions.org>. Accessed 13 November 2025.
- MIMI, Z.A. & ASSI, A. 2009 Intrinsic vulnerability, hazard and risk mapping for karst aquifers: A case study. *Journal of Hydrology*, 364(3-4): 298-310.
- MORRIS, L.J. & BENBOW, M.C. 1986 Geology and hydrology of the Maralinga area, South Australia. *South Australian Department of Mines & Energy Book* 843.
- MORRISSEY, P., NOLAN, P., MCCORMACK, T., JOHNSTON, P., NAUGHTON, O., BHATNAGAR, S. & GILL, L. 2021 Impacts of climate change on groundwater flooding and ecohydrology in lowland karst. *Hydrol. Earth Syst. Sci.*, 25: 1923-1941
- MORSE, K. 1993 Shell beads from Mandu Mandu Creek rock-shelter, Cape Range, Western Australia, dated before 30,000 bp. *Antiquity*, 67: 877-883.
- MORY, A., REDFERN, J. & MARTIN, J. 2008 A review of Permian–Carboniferous glacial deposits in Western Australia. *Special Paper of the Geological Society of America*, 441: 29-40.
- NICHOLSON, T. 2007 The safety & benefits of AFFF agents – Let the facts speak? *Industrial Fire Journal*, 68: 70–75.
- NINEZ JIMINEZ, A. 1987 *Geografia y Espeleología en Revolución*. Imprenta Central de las Fuerzas Armadas Revolucionarias, Habana.
- NORDBY, G.L. & LUCK, J.M. 1955 Perfluorooctanoic acid interactions with human serum albumin. *J. Biological Chemistry*, 219(1): 399-404.
- O'BRIEN, T.E. & EDWARDS, W.A. 2019 Amended statement of claim to the Federal Court of Australia No. 1388 of 2018 [draft]. Shine Lawyers, Brisbane.
- PARKINSON, A. 2007 *Maralinga, Australia's Nuclear Waste Cover-up*. ABC Books, Sydney.
- PARKINSON, S. 2023 How big are global military carbon emissions? *Responsible Science Journal*, 5. [sgr.org.uk/sites/default/files/2023-07/SGR\\_RS5\\_2023-Parkinson2.pdf](https://sgr.org.uk/sites/default/files/2023-07/SGR_RS5_2023-Parkinson2.pdf). Accessed 15 October 2025.
- PLAYFORD, P.E. 2014 Recent mega-tsunamis in the Shark Bay, Pilbara and Kimberley areas of Western Australia. *J. Roy. Soc. WA*, 97(1): 173-188.
- RABBITT ROFF, S. 2022 *Making the British H Bomb in Australia*, Vol. 2. <https://www.rabbittreview.com/wp-content/uploads/Making-the-British-H-Bomb-in-Australia-Vol-2-Sue-Roff.pdf>
- REES, G.N., OBERPRIELER, S., NIELSEN, D., WATSON, G., SHACKLETON, M. & DAVIS, J.A. 2020 *Characterisation of the stygofauna and microbial assemblages of the Beetaloo Sub-basin, Northern Territory*. CSIRO, Australia.
- ROFE & RAFETY 1965 *West Bank Hydrology 1963-65: Analysis*. Report for Hashemite Kingdom of Jordan Central Water Authority, Rofe & Rafferty Consulting Engineers Ltd., Amman, Jordan.
- SCHEFFERS, S.R., SCHEFFERS, A., KELLETAT, D. & BRYANT, E.A. 2008 The Holocene paleo-tsunami history of West Australia. *Earth and Planetary Science Letters*, 270(1-2): 137-146
- SMITH, K. 2019 Environmental protection, exemptions and the military. *PA Times*, 15 October 2019. American Society for Public Administration. <https://patimes.org/environmental-protection-exemptions-and-the-military/>. Accessed 11 May 2025.
- SOUTH AUSTRALIAN RESOURCES INFORMATION GATEWAY 2024 Gawler Craton airborne survey merged data packages, <https://pid.sarig.sa.gov.au/dataset/mesac151>
- SPATE, A., KIERNAN, K. & HAMILTON-SMITH, E. 1998 Geoconservation in land-use planning: Some lessons from North West Cape, Western Australia. [in] BLISS, E (ed.) *Islands: Economy, Society and Environment. Proc. Second Joint Conf., Institute of Australian Geographers & New Zealand Geographical Society*. pp. 451-453
- STÄGER, F., ZOK, D., SCHILLER, A-K., FENG, B. & STEINHAUSER, G. 2023 Disproportionately High Contributions of 60 Year Old Weapons-137Cs Explain the Persistence of Radioactive Contamination in Bavarian Wild Boars. *Environmental Science & Technology*, 57(36): 13601-13611.
- TICKELL, S.J. 2005 Groundwater resources of the Tyndall limestone. *Report 34/2005* Natural Resources Division, Department of Natural Resources, the Environment and the Arts.



- TICKELL, S.J., CRUIKSHANK, S., KERLE, E. & WILLIS, G. 2002 *Stream baseflows in the Daly Basin*. Natural Resources Division, Dept of Infrastructure, Planning & Environment, Darwin.
- TYNAN, E. 2016 *Atomic Thunder. The Maralinga Story*. Newsouth, Sydney.
- TYNAN, E. 2022 *The Secret of Emu Field*. Newsouth, Sydney.
- TOOHEY, B. 1978 Killen warns on plutonium pile. *Australian Financial Review*, 5 October 1978.
- UNEP 2004 *From conflict to sustainable development: Assessment and clean-up in Serbia and Montenegro*. United Nations Environment Programme, Nairobi.
- UNEP 2007 *Lebanon post-conflict environment assessment*. United Nations Environment Programme, Nairobi.
- UNEP/UNCHS 1999 *The Kosovo conflict: consequences for the environment and human settlements*. United Nations Environment Programme and United Nations Centre for Human Settlements (Habitat). Nairobi.
- VETH, P. 1993 The Aboriginal occupation of the Montebello Islands, northwest Australia. *Australian Aboriginal Studies*, 2: 39-50.
- VETH, P., APLIN, K., WALLIS, L., MANNE, T., PULSFORD, T., WHITE, E. & CHAPPELL, A. 2007. *The Archaeology of Montebello Islands, North-West Australia: Late Quaternary Foragers on an Arid Coastline*. Archaeopress, Oxford.
- VILES, H.A. 2003 Conceptual modelling of the impacts of climate change on karst geomorphology in the UK and Ireland. *Journal for Nature Conservation*, 11(1): 59-66.
- WALKER, F. 2014 *Maralinga*. Hachette, Sydney. p. 146.
- WALSH, J., WATSON, R., DARBYSHIRE, E. & WEIR, D. 2024 *The environmental costs of the escalating Middle East crisis*. CEOBS, UK. <https://ceobs.org/the-environmental-costs-of-the-escalating-middle-east-crisis/> Accessed 9 May 2025.
- WATSON, R. & SHEKHUNOVA, S. 2025 *Wartime geomorphological damage and geodiversity loss in Ukraine*. CEOBS, UK. <https://ceobs.org/wartime-geomorphological-damage-and-geodiversity-loss-in-ukraine/> Accessed 9 May 2025
- WEBB, J.A., WHITE, S. & SMITH, G.K. (eds.) 2023 *Australian Caves and Karst Systems*. Springer Nature, Switzerland. 398 pp.
- WEBB, J.A. & JAMES, J.M. 2023 Nullarbor [in] Webb, J., White, S. & Smith, G.K. (eds.) *Australian Caves and Karst Systems*. Springer Nature, Switzerland. pp. 171-187.
- WEBER, D. & PIESSE, E. 2017. Budget 2017: Veterans exposed to nuclear bomb tests welcome Government decision to grant Gold Card access. *ABC News*, 7 May 2017. <https://www.abc.net.au/news/story-streams/federal-budget-2017/2017-05-07/federal-budget-2017-veterans-welcome-gold-card-decision/8504884>. Accessed 10 August 2025.
- WHITE, S., BROOKS, D. & WEBB, J.A. 2023 Cape Range [in] WEBB, J.A., WHITE, S. & SMITH, G.K. (eds.) *Australian Caves and Karst Systems*. Springer Nature, Switzerland. pp. 201-208.
- WILLIAMS-HOFFMAN, M., JOHANSEN, M., LAVERY, P., THIRUVOTH, S., SERRANO, O. & MASQUÉ, P. 2022 Anthropogenic radionuclides persist in marine sediment at the Montebello Islands nuclear legacy site in Western Australia. *SPERA Conference 2022 - Connecting People, developing solutions for a Changing Environment*. 28-30 November 2022, *E-Handbook*: 27. South Pacific Environmental Radioactivity Association.
- YAMAGUCHI, M. 2021 Japan grants medical benefits to 'black rain' survivors. *Breaking News*, 26 July 2021. <https://www.breakingnews.ie/world/japan-grants-medical-benefits-to-hiroshima-black-rain-survivors-1163052.html>. Accessed 21 February 2023.
- ZEITOUN, M., MESSERSCHMID, C. & ATTILI, S. 2009 Asymmetric abstraction and allocation: The Israeli-Palestinian water pumping record. *Groundwater*, 47: 146-160.



This page is intentionally blank



# Observations on the geology and geomorphology of a large doline in dolostone at Forest Hills, Tasmanian Wilderness World Heritage Area

**Rolan Eberhard**

Conservation Science Section, Environment Strategic Business Unit, Department of Natural Resources and Environment Tasmania      Rolan.Eberhard@nre.tas.gov.au

**Chris Sharples**

School of Spatial Sciences, Planning and Geography, University of Tasmania      Chris.Sharples@utas.edu.au



---

## Abstract

The Forest Hills is a remote karst area in the Tasmanian Wilderness World Heritage Area. The principal evidence for karst at this location is the Forest Hills Depression – a large (80 ha) doline and associated stream sink cave. The depression is formed in dolomitic strata, probably a correlate of the Weld River Dolomite (Calver 1989). This paper provides an updated geological map of the Forest Hills and upper New River Gorge plus the first descriptions of the associated karst features, including the large Forest Hills Cave. The Forest Hills Depression is a significant example of an enclosed depression that is noteworthy for its undisturbed condition and remote wilderness setting. Compared to other large karst depressions in Tasmania, several of which are derived from glacio-karstic interactions, the Forest Hills Depression stands out as a genetically less complex example formed chiefly by conventional solution-driven karstification.

Keywords: karst, caves, dolostone, Tasmanian Wilderness World Heritage Area, Forest Hills

---

## Introduction

The Proterozoic rocks of western Tasmania include fractured, folded and variably silicified dolomitic strata, within the Togari, Weld River and Clarke Groups (Calver 1989, Calver and others 2014). The surface expressions of these strata exhibit diverse styles of karstification (Kiernan 1995), including rugged alpine karst at Mt Anne, Mt Weld and Mt Ronald Cross, steep-sided cavernous residual hills in valley floor settings at Maxwell River and Lightning Plains, highly decorated caves in hill flank karst at Hastings, spectacular riverine gorges and natural arches at Jane River and Weld River, polje-like depressions and spring mounds at Smithton and Dismal Swamp, probable hydrothermal karst at Mt Weld, and karren-rich coastal karst at Birthday Bay and Point Hibbs. The extent and variety of karstification of dolomitic strata in western Tasmania challenges the conventional view that dolostone (often referred to simply as ‘dolomite’, the dominant mineral in dolostone rock) is less susceptible to karstification than typical limestones, due to the lesser solubility of the mineral dolomite compared to calcite (Rauch & White 1970).

The Forest Hills are located within the catchment of the New River, which rises on the Eastern Arthur Range at Lake Geeves and then flows in a broadly south-easterly direction to New River Lagoon on Tasmania’s south coast. The closest vehicular access is 25 and 28 km east of the Forest Hills at Hartz Mountains and Hastings Caves respectively, and the closest walking track is 23 km away at the mouth of the New River Lagoon on the South Coast (Figure 1). The difficulty of access is compounded by gorges and deeply dissected fluvial terrain mantled by a dense and almost unbroken forest cover (Figures 2 and 5). Consequently, Forest Hills remains one of the least explored and minimally documented karst areas in Tasmania.

The possible presence of karst at the Forest Hills came to attention in the early 1970s following publication of the 1:100,000 scale Tasmap Huon sheet. Depression contours on the map (based on aerial photogrammetry) suggested the existence of a large, fully enclosed perched basin overlooking the New River Gorge between the Forest Hills to the south and the Crest Range to the north. We refer to

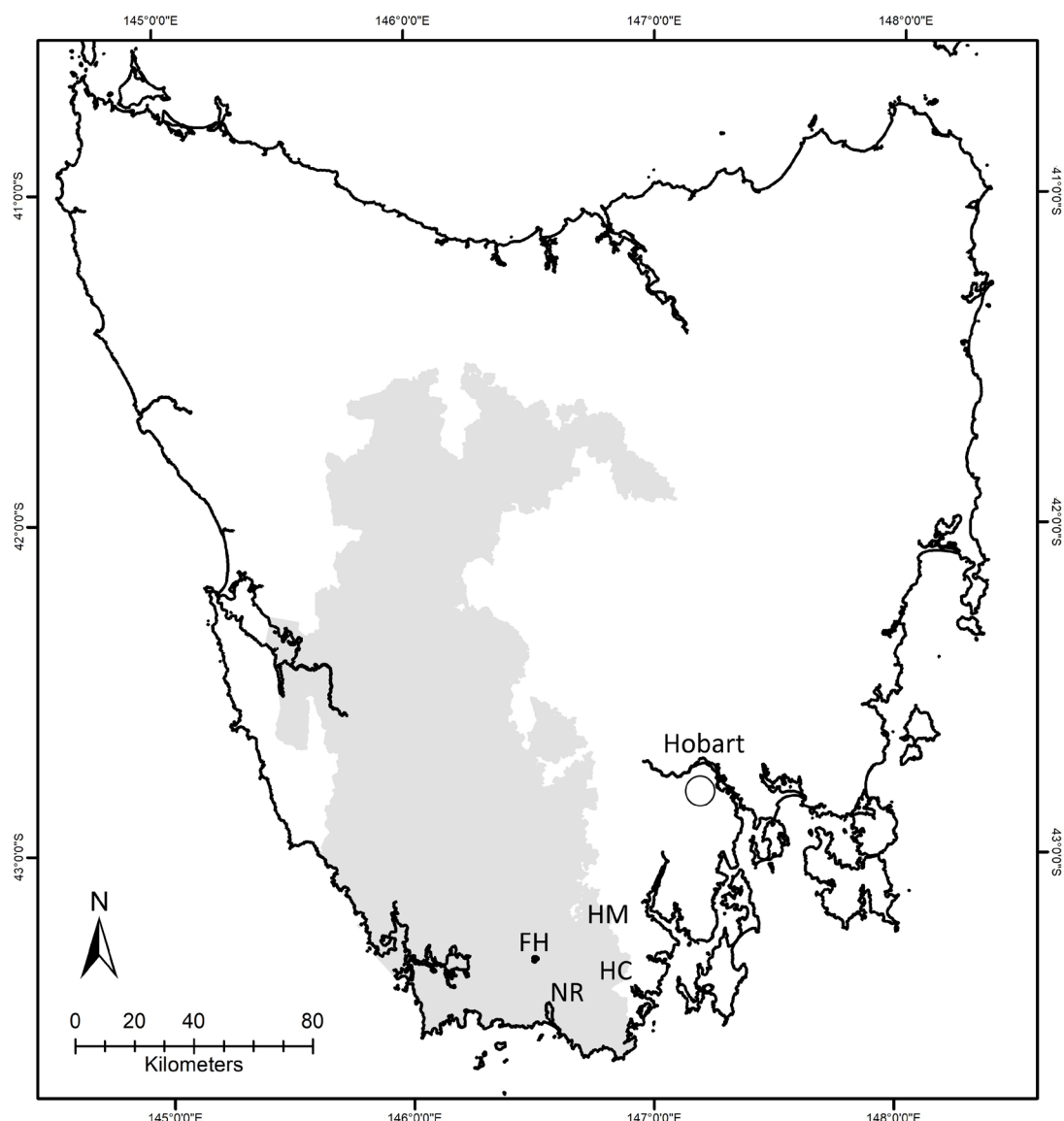


**Figure 1.** Tasmania showing the locations of the Forest Hills (FH), Hartz Mountains (HM), Hastings Caves (HC), New River Lagoon (NR) and the Tasmanian Wilderness World Heritage Area (shaded). The map co-ordinates are geographical (degrees latitude and longitude) based on the WGS84 datum.

this feature as the Forest Hills Depression<sup>1</sup> (Figures 2 and 3). Members of the Tasmanian Caverneering Club (TCC) initiated an aerial reconnaissance of the Forest Hills in 1972 (Shaw 1973), sighting a large cave entrance within the depression (see Figure 4). Two members of the club – Attila Vrana and Jeanette Collin – subsequently mounted a ground-based expedition to explore the cave. They left no published account of this but in conversation with one of us (RE) in 2013, Collin confirmed that she and Vrana had successfully navigated to the

depression and explored the cave seen previously from the air. Her recollection of the cave was vague but suggested that it terminated at a sump or log blockage not far underground.

There appears to have been no further interest in the Forest Hills karst until 1985 when one of us (CS) and Grant Dixon made geological observations during a rafting trip through the New River Gorge. The depression itself was not explored but dolomitic rock was noted cropping out close by on the New River, leading the authors to infer the presence of similar strata within the Forest Hills Depression (Dixon & Sharples 1986). This prediction was confirmed by us during fieldwork at Forest Hills by the (then) Department of Primary Industries, Parks, Water and Environment in February 2012, part of a broader survey of the karst systems of the

1. We adopt the term ‘depression’ for the purpose of naming the Forest Hills feature, because this avoids the regionally derived morpho-genetic connotations of more specific words often applied to large, enclosed karst basins (e.g. uvala, polje). In doing so, we note that the Forest Hills Depression conforms to the accepted definition for a doline or sinkhole (Field 2002).



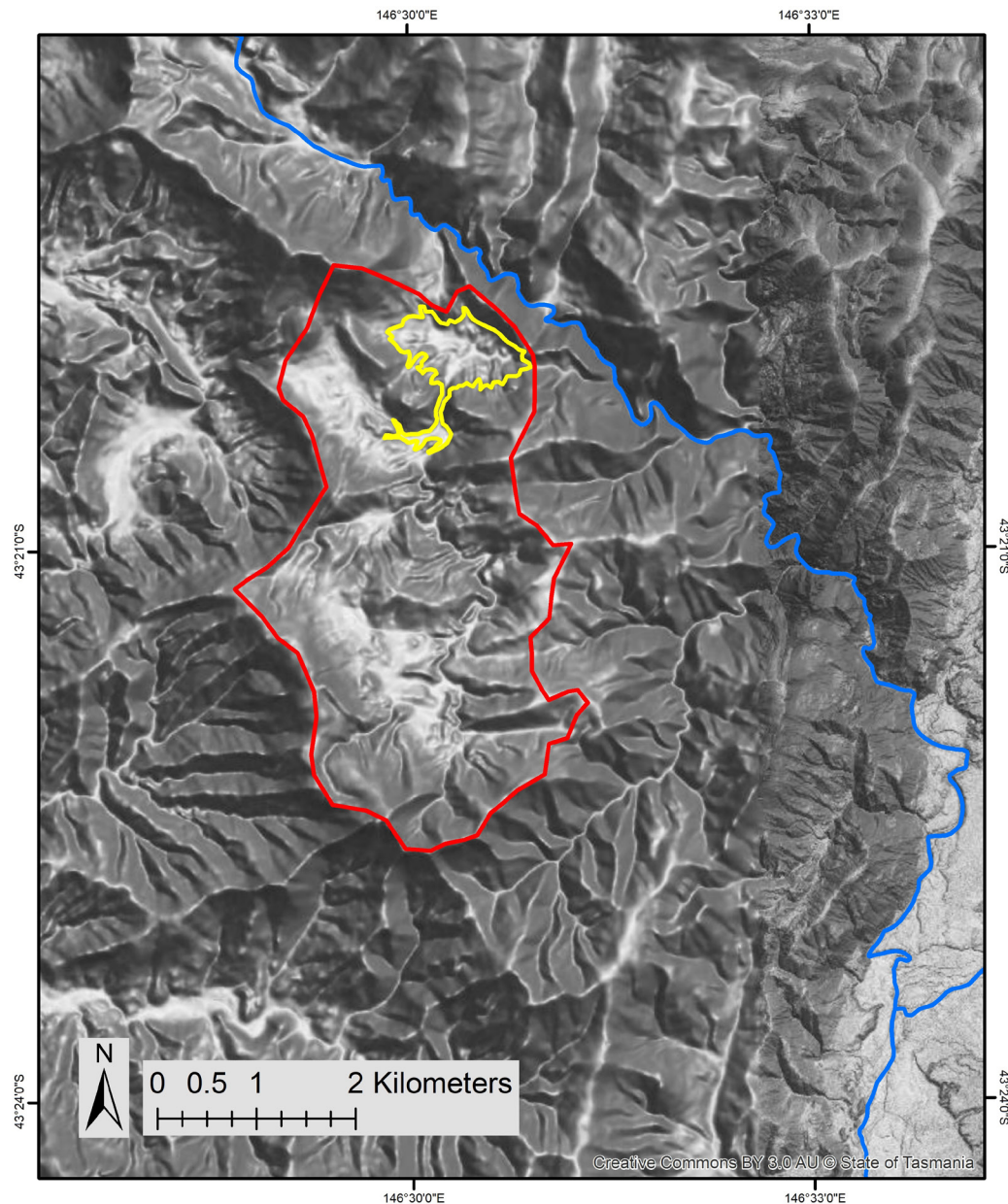


**Figure 2.** Digital elevation model of the Forest Hills identifying the Forest Hills Depression (yellow polygon), its catchment area (red polygon) and the New River (blue line). Basemap: hill shade (source: Land Information System Tasmania LISTmap). The map co-ordinates are geographical (degrees latitude and longitude) based on the WGS84 datum.

Tasmanian Wilderness World Heritage Area. In this paper we present the results of the Forest Hills component of that survey.

## Methods

### Access

We gained access to the Forest Hills from the Crest Range by descending from a point near Satellite Lake to the New River at the upstream end of the New River Gorge (Figures 5 & 6). After bivouacking on a mid-stream shingle bar in the river, we traversed a narrow ridge extending between the upstream end of the New River Gorge

and the Forest Hills Depression, entering it from the north (Figure 6).

### Map co-ordinate system and grid references

Location data in this paper is based on hand-held GPS waypoints collected in the field. The results are shown on the map figures as geographical (latitude-longitude) co-ordinates based on the WGS84 datum, but waypoint locations are recorded in Appendix 1 as both geographical co-ordinates and as Map Grid of Australia (MGA) Zone 55 eastings and northings based on the Geodetic Datum of Australia (GDA94) and the Universal Transverse Mercator (UTM) projection.

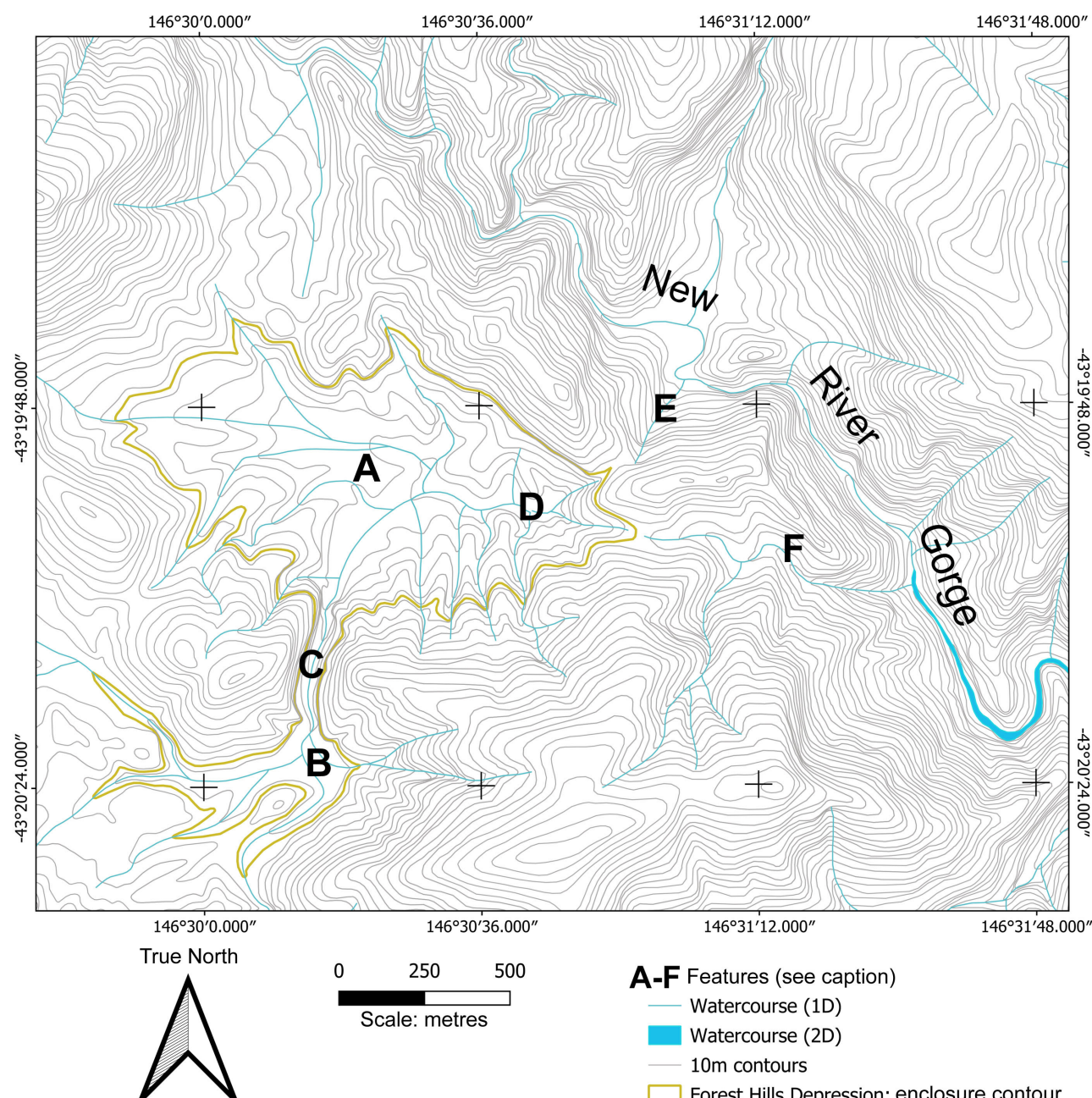


**Figure 3.** Contour map of the Forest Hills Depression showing: the northern (A) and southern (B) lobes of the depression, connected by a breach (C) in the intervening ridge (item 4 on Figure 5). Water sinking underground at Forest Hills Cave (D) probably discharges from one of two candidate tributaries (E, F) feeding the New River (see geomorphology text for discussion). Map Source: 10 m contours and watercourses from Land Information System Tasmania (LISTmap). The map co-ordinates are geographical (degrees latitude and longitude) based on the WGS84 datum.

### Geological bedding dip and strike measurements

Bedding dip and strike measurements were measured in the field as inclinations in conventional degrees and as magnetic compass directions. Compass readings are reported ‘as read’, noting that the 2012 magnetic north (MN) was 15.05° east of true north for this location.

### Cave maps

Cave maps presented here (Figures 16 and 18) are based on conventional point to point survey traverses using Suunto compass and clinometer ( $\pm 0.5^\circ$ ) and handheld laser rangefinder ( $\pm 0.05$  m). The standard conforms to ASF Mapping Grade 54 or better.





**Figure 4.** Aerial view of the deepest point of the Forest Hills Depression. The apparent cavity at the centre of the image is a 20 m high overhanging cliff directly above Forest Hills Cave (see Figure 15). In this image the point of entry to the cave is concealed by vegetation (Photo by Rolan Eberhard).

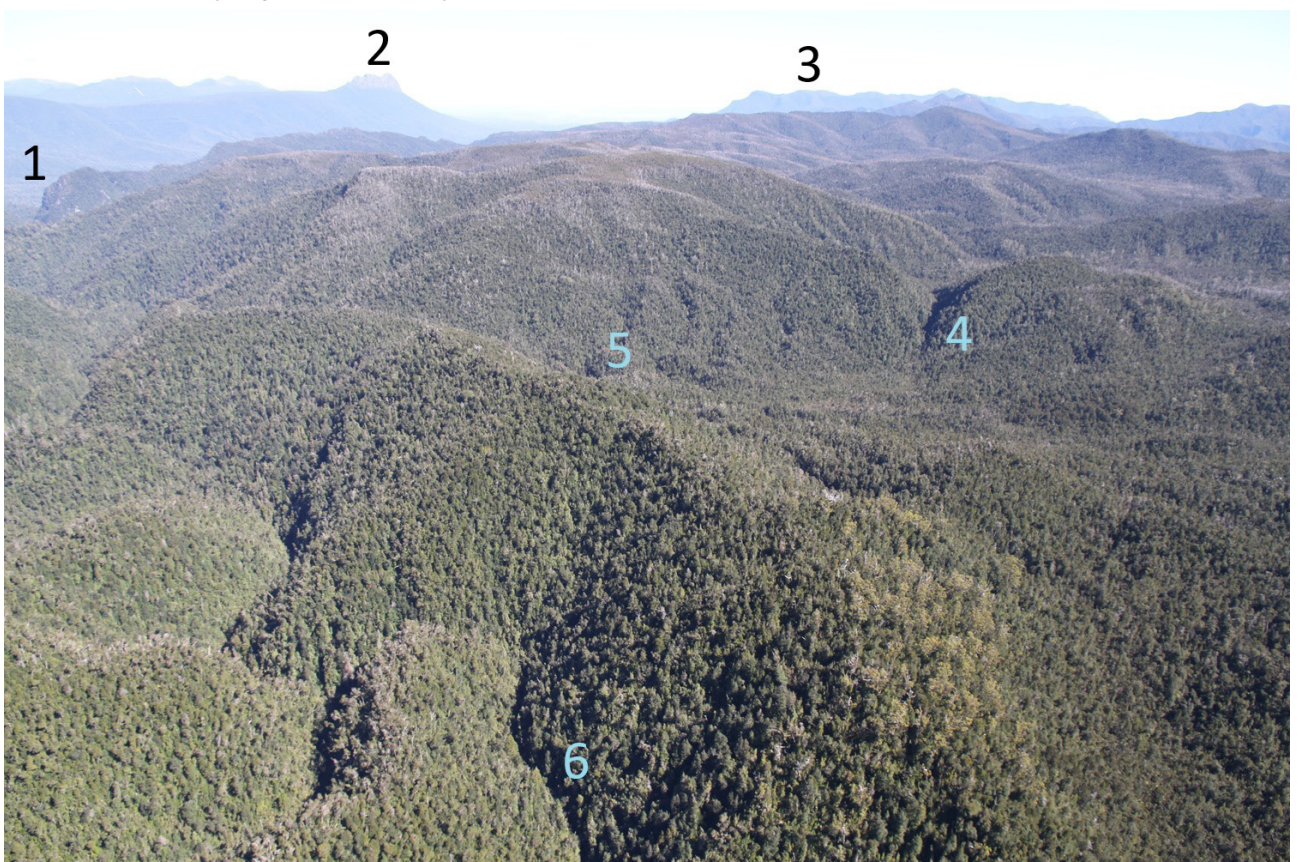


**Figure 5.** Oblique aerial view of the Forest Hills looking south from the Crest Range. 1: Gibraltar (bluff on the New River, see Figure 13); 2: Precipitous Bluff; 3: Ironbound Range; 4: gorge connecting northern and southern lobes of the Forest Hills Depression (breaching a presumed strike ridge in siliclastic rock); 5: Forest Hills Cave (deepest point in the Forest Hills Depression); 6: upstream end of New River Gorge (Photo by Rolan Eberhard).



## Results

### 1. Geology

This section provides a summary of the bedrock geology observed in the upper sections of the New River Gorge and in the Forest Hills Depression. An updated interpretation of the local geological structure is also provided. Geological observations at some individual waypoints are tabulated at Appendix 1.

### New River Gorge Section

The following observations refer to bedrock exposures in the upper New River Gorge, 1 km north of the Forest Hills Depression. Rock units are described from upstream to downstream, referencing GPS waypoints shown at Figure 6. The most downstream observation aligns with, and corroborates, the most upstream observation on the New River by Dixon and Sharples (1986).

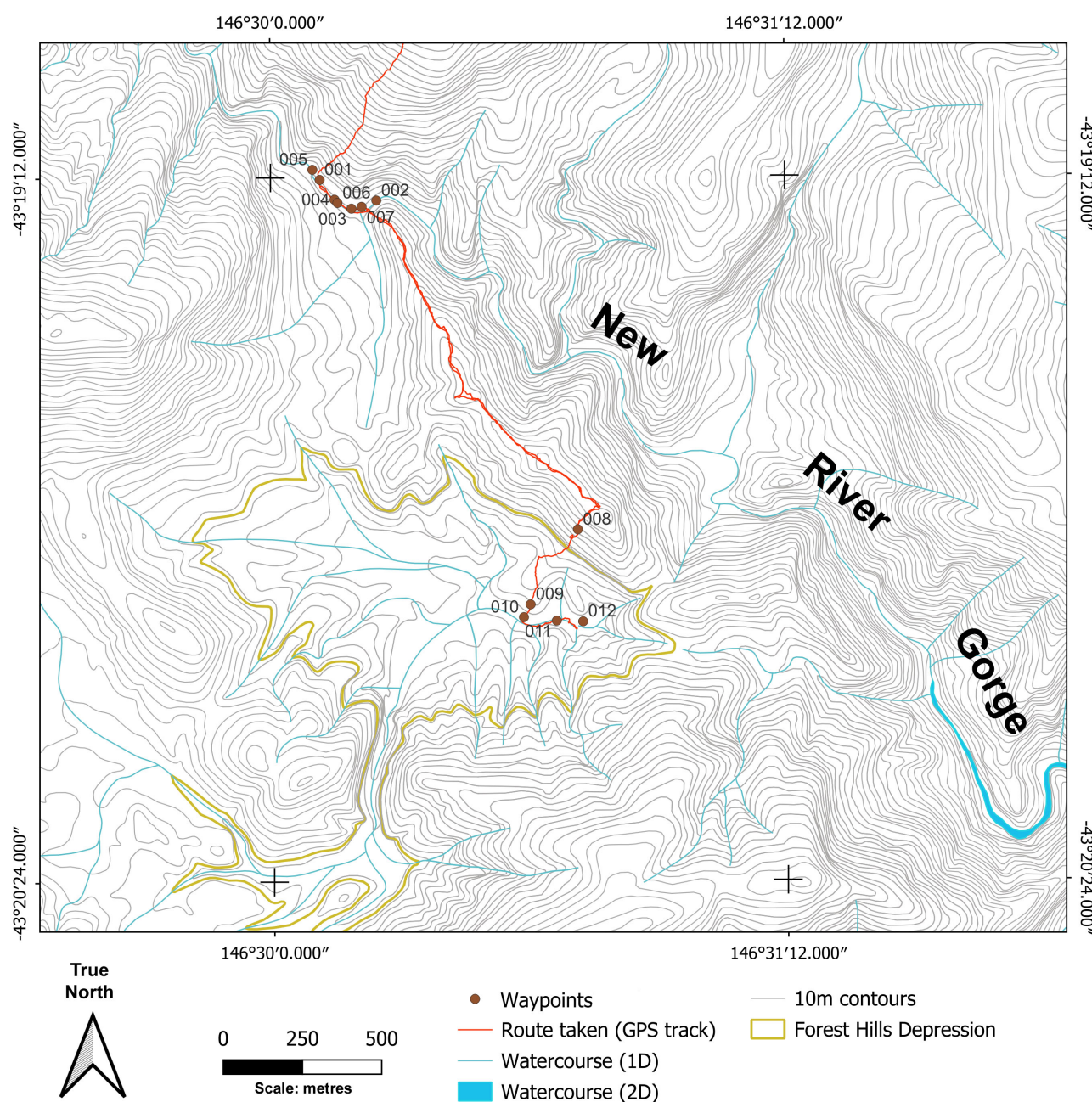


**Figure 6.** Map of the part of the upper New River Gorge and Forest Hills Depression visited during 2012, showing numbered waypoints and tracks as recorded by GPS. Map Source: 10 m contours and watercourses from Land Information System Tasmania (LISTmap) The map co-ordinates are geographical (degrees latitude and longitude) based on the WGS84 datum.

***Quartzite (upstream exposures)***

Well-bedded hard grey fine-grained quartzite with planar beds and finer planar laminations crops out at Waypoint 005 and at least 100 m upstream of this point. The bedding dips at 50° towards 340° MN (striking ~70° MN). Bed facing is unknown. No outcrop was detected for about 100 m downstream of Waypoint 005.

***Reddish-brown slates***

Fine-grained reddish-brown slate crops out along this stretch of the river from Waypoint 004 to 003, including Waypoint 006. At Waypoint 006 the bedding dips 70° towards 25° MN (striking ~295° MN). A strong cleavage dipping 35° towards 265° MN was noted. Bed facing is unknown. Planar vertical joint fractures spaced 30-40 cm apart were observed in an outcrop at Waypoint 004. A dominant joint set strikes ~300° MN, and a secondary vertical set strikes roughly normal to this.

***Quartzite (downstream exposures)***

Well-bedded hard fine-grained grey quartzite with generally planar to finely laminated bedding crops out between Waypoints 003 and 002, including Waypoint 007. At Waypoint 007 the beds dip 80° towards 30° MN (strike ~300° MN). Bed facing is unknown. Tight isoclinal folds with roughly 0.5 metre wavelengths were observed in several places.

***Dolomitic siltstones and interbedded quartzite***

Fine-grained grey-to-pale-brownish well-bedded laminated dolomitic siltstone crops out at Waypoint 002. A specimen from this site was previously confirmed in stained thin section to be dolomitic siltstone (Dixon & Sharples 1986). A fine-grained planar-bedded quartzite bed which crops out immediately downstream of the dolomitic siltstone is interpreted as an interbed within the broader dolostone sequence of the New River Gorge. This sequence extends for several kilometres downstream of Waypoint 002 and includes siliceous conglomerate interbeds, as mapped by Dixon & Sharples (1986).

The dolomitic siltstone at Waypoint 002 dips steeply at 80° towards 30° MN (strike ~300° MN), suggesting it is conformable with the quartzites and slates upstream.

The outcrops show fine slightly undulous laminations (possibly algal laminations) and some

breaks in the laminations are suggestive of mud cracks, consistent with deposition in a low-energy intertidal to supratidal environment. Considerable variation in dolomite content is apparent, with sporadic small lenses of relatively pure pale brown dolostone 10-20 mm thick and 100-150 mm long being present, and some more dolomitic brown siltstone interbeds showing recessive weathering surfaces compared to less dolomitic grey beds standing proud adjacent.

A tight isoclinal fold axis striking approximately 350° MN is visible in the quartzite beds immediately downstream of the dolomitic siltstones at Waypoint 002; folding along this axis may explain the strong cleavage observed in the reddish-brown slates upstream (see above). A weak cleavage is also visible in the dolomitic siltstones at Waypoint 002, dipping about 45° towards the north and striking roughly east-west, although this cleavage is not explained by the aforementioned folding.

***Siliceous conglomerate boulders***

Sporadic allochthonous boulders of hard siliceous conglomerate with coarse well-rounded siliceous clasts were observed in the New River Gorge between Waypoints 001 and 002. These may be derived from upslope outcrops of the conglomerate beds reported downstream of Waypoint 006 by Dixon & Sharples (1986).

**Forest Hills Depression**

The following observations are presented in the order they were made when entering the depression from the north, via a high-relief and south-east trending ridge rising from the south side of the New River Gorge (Figure 6). This ridge is roughly aligned with quartzite bedding strikes observed in the New River bed directly below its northwest end between Waypoints 003 and 002 (Figure 6) and is therefore inferred to be a mainly clastic bedrock strike ridge. No outcrop was observed on the densely vegetated ridge-top; however, clastic rocks were noted at waypoints 008 and 009 on the south-western flanks of the ridge as described below. The route taken joins the main watercourse draining across the base of the depression to sink at the Forest Hills Cave (Waypoint 012). Approaching the sinking point of the stream at Forest Hills Cave, the channel narrows to a small ravine with plunge pools and a high-level cave (Canyon Cave). These features provide clear exposures of bedrock within the eastern portion of the depression.



### *Siliceous cleaved pink siltstone (slate)*

Angular lag fragments of moderately hard, very fine-grained, well-sorted, siliceous, orange-pink (Munsell 10 R 7/4) to brownish-pink laminated siltstones were observed high on the strike ridge forming the north-eastern slope of the Forest Hills Depression at Waypoint 008. No in situ bedding orientation was apparent. The rock shows a distinct cleavage indicative of low-grade regional metamorphism and is inferred to be an extension of the reddish-brown slate unit observed in the New River Gorge.

### *Siltstones with secondary carbonate*

Laminated siltstone bedrock crops out low on the strike ridge forming the north-eastern slope of the Forest Hills Depression at Waypoint 009. The beds dip at 80° towards 20° MN (strike ~290° MN). Patches of chalky surficial deposits suggestive of tufa were observed at the base of the siltstone outcrop, implying a local carbonate source. This outcrop is almost certainly a siltstone interbed within dolostone strata that crop out a short distance downslope (see below). Angular lag fragments of similar siltstone were also noted upslope at Waypoint 008.

### *Dolostone with minor phyllitic siltstone interbeds*

No outcrop was observed between Waypoints 009 and 011. However, numerous outcrops of dolostone bedrock were observed on the watercourse between Waypoints 011 and 012 and inside Canyon Cave and Forest Hills Cave, as described below.

### *Canyon Cave*

Waypoint 011 marks the location of Canyon Cave, an upper-level conduit in the side of the ravine draining to Forest Hills Cave. Canyon Cave is formed in a hard, relatively pure, creamy-white to creamy-pale brown coloured fine-grained rock with generally thin to laminated planar bedding. In places, purer dolostone is interbedded with fine-grained, dark brown, laminated silty layers 0.5-20 mm thick. The latter may be clastic and/or carbonaceous layers, and a silty algal mat origin is possible. The bedding is mostly planar but distinctly 'wavy' bedforms (with wavelengths of ~100 mm) are evident in some sections. These may be fine tectonic or soft-sediment deformation folds



**Figure 7.** Apparent small-scale folding of interbedded dolostone and dark silty (carbonaceous?) beds or laminae exposed at Canyon Cave (Waypoint 011). These may be tectonic folds, soft-sediment deformation features, or stromatolitic algal mat fossils (Photo by Chris Sharples).



**Figure 8.** Thin silica boxwork veins standing proud of the dolostone matrix in Canyon Cave (Waypoint 011) (Photo by Chris Sharples).

or stromatolitic algal mat growth forms (Figure 7). Thin silica veins are also present, commonly in several cross-cutting parallel sets. Differential weathering of these features has produced minor silica boxworks within the cave (Figure 8). Some of the dolomite beds are offset by small faults.

Planar-laminated dolostone bedding orientation was measured at two points in the cave. At the back end of the cave the dolostone bedding dips at 70° towards 30° MN (strike ~300° MN), and at the cave entrance the dolostone bedding dips very steeply (close to vertical) towards 25° MN and strikes about 295° MN. Bed facing is unknown.



### Forest Hills Cave

Similar dolostone occurs within Forest Hills Cave near Waypoint 012. Here, the rock is a hard, crystalline and fine-grained, varying in colour from white (Munsell N9) on fresh surfaces to creamy-yellow (Munsell very pale orange 10 YR 8/2) on weathered surfaces. Multiple cross-cutting sets of parallel thin linear silica veins 0.5-10 mm thick have weathered to form boxworks within the cave. Bedding generally appears massive but fine planar laminae are visible in some exposures and thin planar beds in others. Bedding dip at two points was measured at 50° towards 35° MN (strike ~305° MN) and 55° towards 30° MN (strike ~300° MN). Bed facing is unknown.

Large displaced dolostone boulders at the cave entrance exhibit sub-ordinate foliated fine-grained clastic sedimentary interbeds generally 50-100 mm thick but up to 1.0 metre thick at one point. In hand specimen this is a fine-grained siliceous siltstone. The colour is pale greenish (Munsell light olive grey 5 Y 6/1) on fresh surfaces but weathered to brown on weathered surfaces. The rock is distinctly foliated with a micaceous sheen on slightly undulose broken cleavage planes and may be best described as a phyllite or phyllitic siltstone indicative of low-grade regional metamorphism.

A clast of the dolostone collected outside Forest Hills Cave was submitted for analysis at the Mineral Resources Tasmania laboratory, Rosny (MRT collection No. G403296). Images of the hand specimen and thin sections are provided at Figures 9 to 11. The report (Bottrill & Woolley 2015) describes the rock as a banded, veined and brecciated carbonate rock, with a mostly white colour and brown/fawn coloured carbonate veins and discontinuous bands to a few millimetres in width. Based on acid tests, the presence of dolomite as the main carbonate is inferred. In thin section the rock is described as a brecciated, veined dolostone, with micritic to finely sparry dolomite (neomorphic pseudospar?) cut by discontinuous bands and veins of chert and macroquartz. The specimen shows good indications of early banding resembling cryptalgal or stromatolitic laminations, partly altered by layer-parallel diagenetic formation of sparry dolomite. Also, coarser carbonates and quartz clots appear to have formed in tectonic veins and fractures, along with moderate primary foliation (sedimentary banding), some conjugate veining due to brittle deformation, and strong indications of the introduction of silica as chert



**Figure 9.** Hand sample of dolostone from the Forest Hills Depression, collected just outside Canyon Cave at Waypoint 011 (Mineral Resources Tasmania collection No. G403296). Banded and stock worked quartz-dolostone rock with probable sedimentary layers (sub-vertical, brown), variably silicified and cut by a network of brown quartz-carbonate veinlets in a white dolostone matrix (Bottrill and Woolley 2015). Field of view: 100 mm.

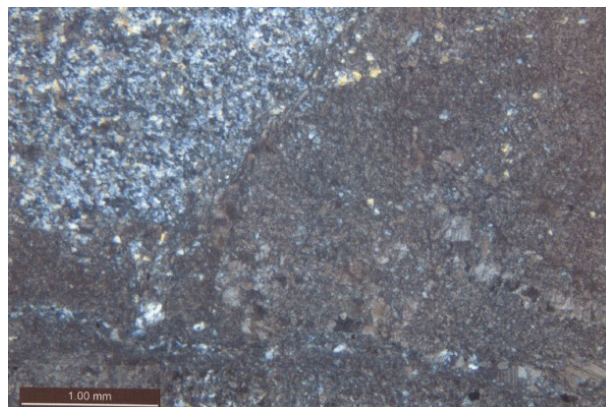


**Figure 10.** Thin section of sample G403296, collected just outside Canyon Cave at Waypoint 011. Brecciated quartz-dolostone rock, showing a block of quartz dolomite (white-pale grey-yellow) in the top left, in a micritic to finely sparry dolomite (brownish grey) matrix, with some dolomite (Bottrill and Woolley 2015)

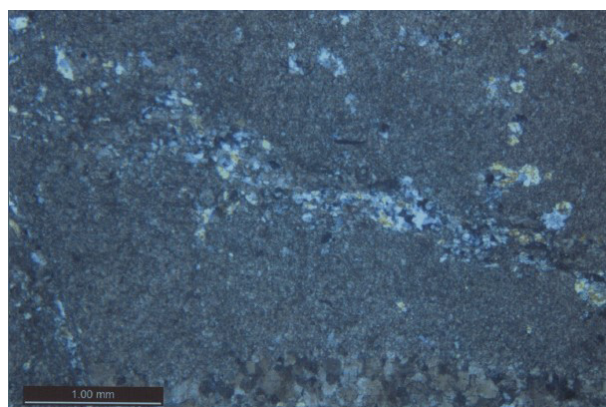


**Figure 11.** Thin section of sample G403296, collected just outside Canyon Cave at Waypoint 011. Brecciated quartz-dolostone rock, showing disseminated (detrital or authigenic) quartz dolomite (white-pale grey-yellow) grains in a micritic to finely sparry dolomite (brownish grey) matrix, with some dolomite veins and cherty quartz veins (Bottrill and Woolley 2015).



replacing sedimentary bands during the brecciation and veining. The textures are interpreted as the products of diagenesis and deformation, with no indications of hydrothermal alteration, sulphides or other mineralisation.

## Geological Interpretation and Synthesis

Figure 12 presents an interpretive geological map of the Forest Hills Depression. Figure 13 is a larger scale map integrating our observations with those of Dixon & Sharples (1986) on the New River between the Forest Hills Depression and the prominent quartzite strike ridge, “Gibraltar”, to the east. We infer that dolostone within the Forest Hills Depression is part of a conformable sequence of dolostones, low-grade metamorphic cleaved reddish slates, quartzites and interbedded dolomitic siltstones and siliceous conglomerates dipping steeply towards the northeast, between the Forest Hills Depression and the upper part of the New River Gorge. This sequence is truncated by *en echelon* faults trending broadly north-south. The most westerly of these faults accounts for significant differences in observed bedding directions at Waypoints 004 and 005 on the New River. The east-facing slope of the large hill immediately southwest of the waypoints is interpreted as a fault-line escarpment associated with this fault. The cleaved reddish-brown or pinkish slates (siliceous siltstones) observed at Waypoints 003 to 004 on the New River, and as lag fragments within the Forest Hills Depression at Waypoint 008, are interpreted as along-strike expressions of the same stratigraphic unit.

The alignment of a prominent north-south gorge draining into the Forest Hills Depression from the south (C on Figure 3) can be interpreted as a structural effect associated with a second fault to the east of the first fault. The upstanding form of the ridge cut by the gorge suggests a strike ridge in siliclastic rock. A third fault further east again is consistent with the abrupt termination of the large passage in Forest Hills Cave, interpreted as evidence of a major structural deflection of underground drainage at a fault contact. It is inferred that a band of dolostone extends east of the cave through the topographic saddle between it and the New River Gorge. Within this block, the strike of the dolostone bedding potentially swings from north-west to west, in accordance with the orientation of the probable strike ridge immediately north of the saddle. This interpretation allows for the transmission of water from the Forest Hills Depression to the

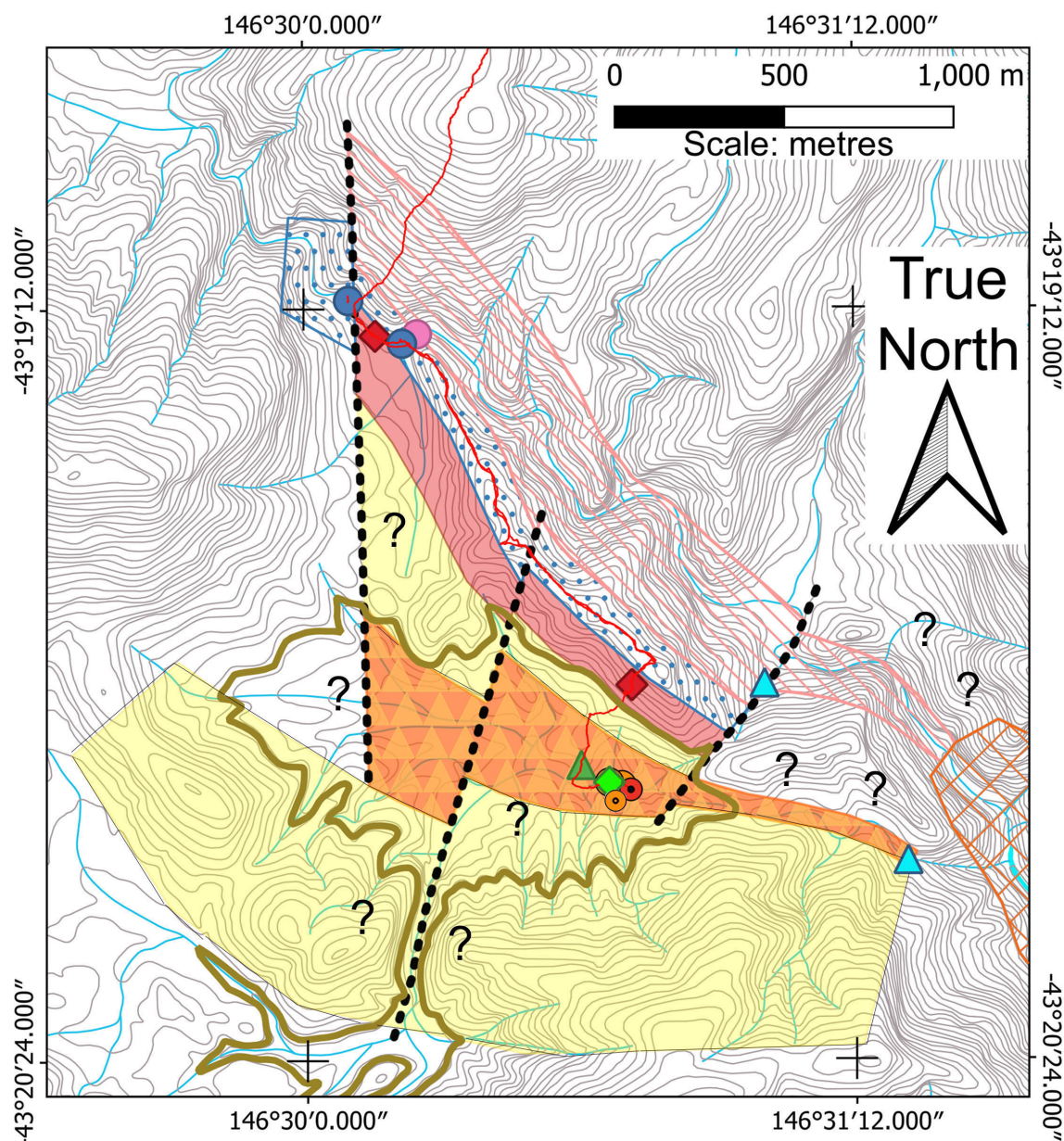
New River via sub-surface conduits in dolostone, to an inferred spring resurging in the New River Gorge (E or F on Figure 3), outside the Forest Hills Depression. Without such a connection the Forest Hills Depression would be a permanent lake.

Aspects of the broader structural setting of the Forest Hills Depression remain uncertain. Whereas the dolostone is probably truncated to the west against northwards-dipping quartzites along an inferred north-south fault, to the south-east and east the dolostone abuts a thick north-south striking metamorphosed phyllite sequence. The latter rocks crop out for several kilometres downstream of the depression and include at least two thick north-south striking quartzite units near its eastern end, including the prominent ridge of “Gibraltar” (see Figure 13). The dolostone sequence and the phyllite sequence are probably in faulted contact. The suggestion by Dixon & Sharples (1986, Figure 1) that the dolostone outcrop extends for some distance south of the Forest Hills Depression is unconfirmed. The broad upstanding strike ridge which bounds the southern side of the depression is suggestive of siliclastic or meta-siliclastic rocks. The geology of a flat-floored basin immediately south of this ridge and connected to the Forest Hills Depression via a gorge has not been verified and is not interpreted on Figures 12 and 13. However, on present evidence, we cannot exclude the possibility that the basin is underlain by dolostone. This question is considered later in the paper.

Based on lithological similarity, we consider it likely that the Forest Hills Dolostone is a correlate of dolomitic rocks within the Weld River Group, potentially the massive dolostones and intercalated mixtite, mudstones and sandstones of the Cotcase Creek Formation (Calver 1989). The Forest Hills Dolostone is dissimilar to the Precambrian dolostones of the Clark Group, which comprise thinner, less pure dolomite beds (Clive Calver pers. comm. 2012).

## 2. Geomorphology

The Forest Hills is the central portion of a larger region of hills and ridges bounded by the valleys of the New, Old and Solly Rivers. The terrain is strongly dissected with several hundred metres of relief and a high density of low order dendritic surface channels. The Forest Hills Depression is a closed basin at the termination of an un-named watercourse draining northwards from the Forest Hills towards the New River (Figures 2, 3 & 5).



## Legend:

- Depression enclosure contour
- Route taken 2012 (GPS track)
- 10m contours
- Watercourse (1D)
- Watercourse (2D)

### Notable karst features

- Main streamsink cave entrance (Forest Hills Cave)
- ◆ High-level horizontal cave entrance (Canyon Cave)
- ▲ Possible spring location

### Observed bedrock

- Dolostone with sub-ordinate phyllitic siltstone (Weld R. Gp. inferred)
- ▲ Siltstone with secondary carbonate
- ◆ Reddish-brown slate
- Quartzite
- Dolomitic siltstone with interbedded quartzite

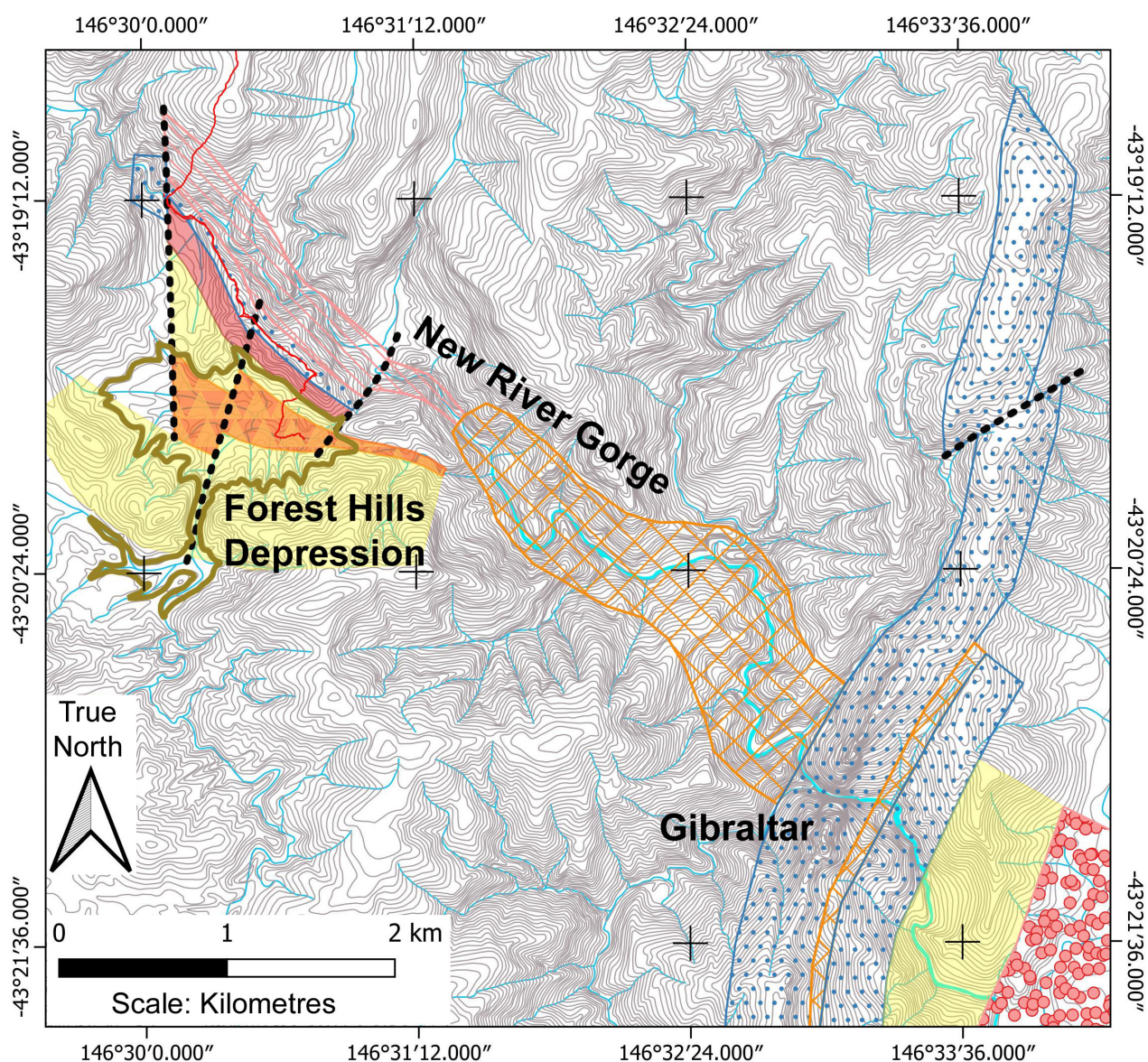
### Inferred bedrock

- Dolomitic siltstones with interbedded quartzites and siliceous conglomerate
- Phyllite
- Quartzite
- Reddish-brown slate
- Weld River Gp. dolostone with sub-ordinate phyllitic siltstone
- Unknown bedrock (inferred likely metaclastics)

- - - Inferred faults

**Figure 12.** Geological map of the upper New River Gorge and Forest Hills Depression area showing observed features and interpreted Precambrian geology based on integrating geological observations from the 2012 field trip with those of Dixon & Sharples (1986). Areas of uncertainty that require more field data to resolve are indicated thus: '?'. Base map source: 10 m contours and watercourses from Land Information System Tasmania (LISTmap). The map co-ordinates are geographical (degrees latitude and longitude) based on the WGS84 datum.





## Legend:

- Depression enclosure contour
- Route taken 2012 (GPS track)
- 10m contours
- Watercourse

## Bedrock:

- - - Inferred faults
- Cambro-Ordovician**
  - Denison Group Siliceous conglomerates
- Late Precambrian**
  - Dolomitic siltstones with interbedded quartzites and siliceous conglomerates
  - Phyllite
  - Quartzite
  - Reddish-brown slate
  - Weld River Gp. dolostone with sub-ordinate phyllitic siltstone
  - Unknown bedrock (inferred likely metaclastics)

**Figure 13.** Interpretive geological map of the broader New River Gorge area integrating geological observations from the 2012 field trip with those of Dixon & Sharples (1986). Base map source: 10 m contours and watercourses from Land Information System Tasmania (LISTmap). The map co-ordinates are geographical (degrees latitude and longitude) based on the WGS84 datum.



The principal tributary to the depression has cut a deep, narrow breach in an inferred strike ridge which separates the main northern portion of the depression from a secondary lobe that extends south for several hundred metres. At other points the internal flanks of the basin are incised by multiple, mostly shallow surface channels. The difference between the highest (390 m ASL) and lowest (340 m ASL) depression contours, as mapped by Land Information System Tasmania (LIST), indicates that the depression is at least 50 m deep. The feature is thickly vegetated with locally dense thickets of horizontal scrub (*Anodopetalum biglandulosum*) and occasional large King Billy Pines (*Athrotaxis selaginoides*).

Tributary surface streams draining into the depression coalesce within a 10 m deep V-shaped canyon in dolostone bedrock (Figure 14), commencing near Waypoint 011 about 100 m above the sink point. A short distance above the sink the gradient of the channel steepens, with minor cascades and plunge pools, and swings from a dominantly easterly alignment to a northerly one. The surface channel terminates in a jumble of massive dolostone boulders at the deepest point of the depression (Forest Hills Cave, near Waypoint

12; see Appendix 1), which is enclosed by steep slopes and cliffs more than 20 m high. A smaller tributary joins from the south at this point, while another small stream from the east joins the cave stream amongst boulders a few metres inside the cave entrance. The cliff above the cave is steeply overhanging with a dripline up to 15 m from its base, creating a sheltered south-east facing bench on silty sediment vegetated by ferns (Figure 15).

Forest Hills Cave (Figure 16) is accessed via holes between boulders that partially fill what appears to be a formerly spacious canyon or conduit in bedrock. About 50 m into the cave the zone of collapse gives way to a tunnel up to 15 m wide and 5 m high. This feature cuts obliquely across the strike of steeply dipping dolostone beds, suggesting that its alignment is controlled by fractures or faults. The base of the passage is formed in pebbly gravels locally cemented by a dark amorphous matrix encountered in many Tasmanian caves which entrain tannin-stained water. Banks of pale, silty sediments have been deposited above the gravel base in places. The open passage extends for about 60 m and then abruptly terminates at a froth-covered pond (sump) (Figure 17). Coarse woody debris and traces of frothy scum were noted high on the walls



**Figure 14.** V-shaped canyon in dolostone at the point where the stream enters rockfall at the entrance to Forest Hills Cave, which is directly in front of the figure in the image (Photo by Rolan Eberhard).





**Figure 15.** Bivvy site below overhanging cliff at Forest Hills Cave (approximately Waypoint 012). The point of entry to the cave is a few tens of metres to the rear and left of the tent at the lower left in the image. Whitish frothy scum from earlier flooding partly coats the vegetation and overhanging rock wall here (Photo by Rolan Eberhard)

and ceiling at various points in the cave. Similar evidence was also observed outside the cave (Figure 15), indicating that water backs up in the base of the depression during flood events, fully submerging the cave under a temporary lake.

A second cave, Canyon Cave (Figure 18; Waypoint 011), is located on the south side of the stream canyon and about 10 m above the base of the active watercourse. The cave comprises a simple horizontal tunnel about 50 metres long, which for most of its length is developed along the strike of the dolostone beds, which dip steeply in a northerly direction. The passage is generally 4–5 m wide and 2–3 m high (Figure 19) but becomes lower approaching the back end of the cave. At this point the passage trends upwards for a short distance before terminating at an apparently slumped blockage of silt. Canyon Cave lacks a perennial stream and appears to be a fossil feature related to a phase of cave development pre-dating downcutting by the stream and the initiation of Forest Hills Cave. However, fragments of leaf litter deposited on the cave walls indicate that Canyon Cave remains subject to at least occasional inundation by back-flooding within the Forest Hills Depression.

Neither of the two recorded caves show significant speleothem development, which is limited to minor stalactites and botryoidal deposits in Canyon Cave. In keeping with many other caves in silicified dolostone in Tasmania, both Canyon Cave and Forest Hills Cave contain well-developed silica boxwork standing proud of the dolostone matrix (Figure 8).

## Discussion

Confirmation that the Forest Hills Depression is formed in dolostone rock, likely a correlate of the Weld River Group, corroborates earlier inferences (Dixon & Sharples 1986) regarding the geology of the upper New River and the Forest Hills. Our updated geological map (Figures 12 and 13) interprets the Forest Hills Dolostone outcrop as relatively small (37 ha) and formed by three contiguous fault-bounded blocks that do not extend far beyond their surface expression as a karst landform, i.e. the Forest Hills Depression. The ridges that enclose the depression, and portions of the depression itself, are underlain by non-karstic siliclastic rocks, within a conformable but fault-disrupted sequence of low-grade metamorphic

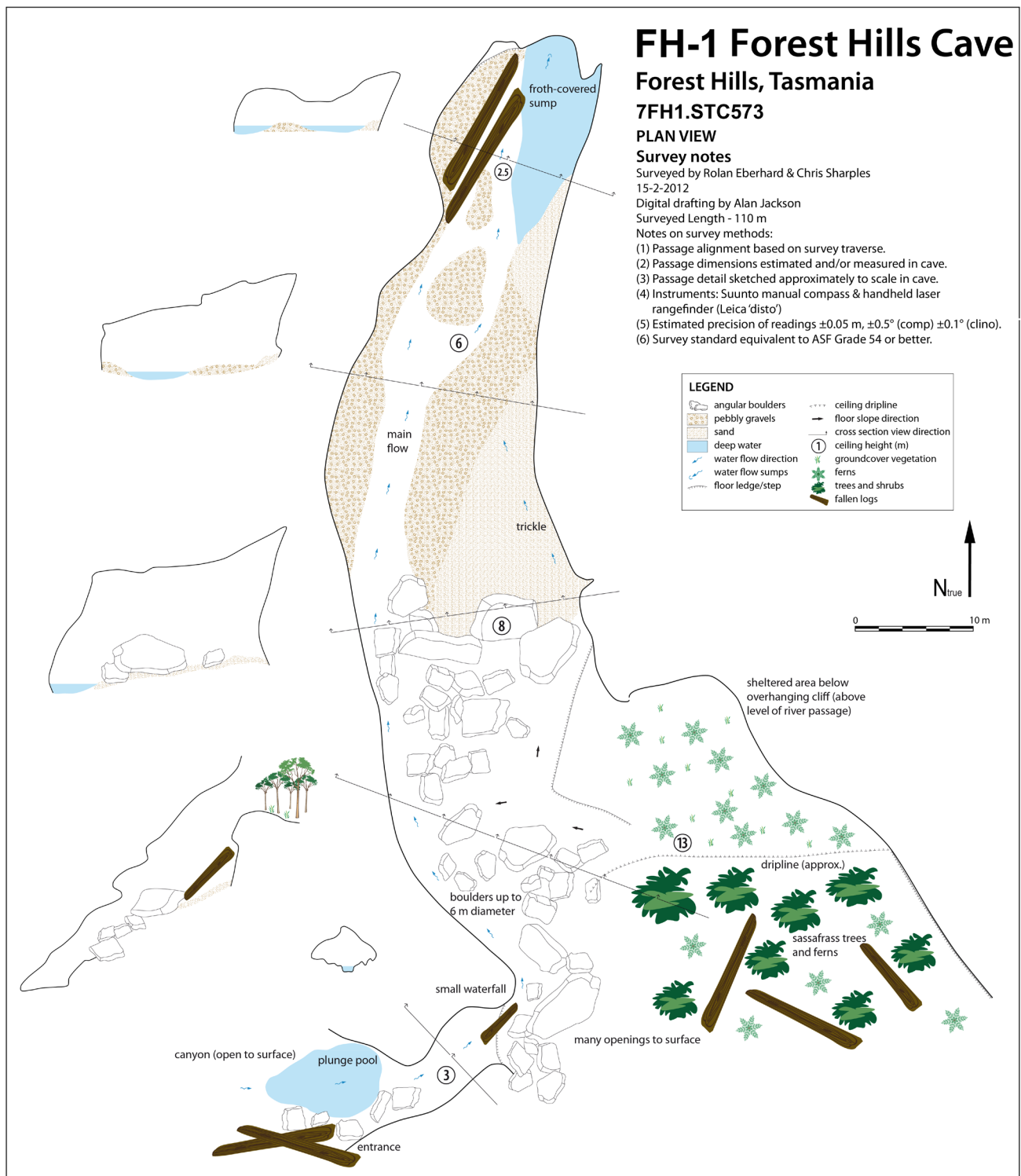


**Figure 16.** Map of Forest Hills Cave, FH-1.

strata. Beyond these two main findings, other elements of the geology remain speculative. For example, we infer the southern lobe of the Forest Hills Depression (upstream of a straight narrow gorge through an inferred siliclastic strike ridge) to be underlain by siliclastic rocks, based on the conclusion that the upstanding ridge that separates the depression into northern and southern lobes is not a karst landform and that it delineates the

southern limit of the dolostone (Figure 12). On the other hand, the structural complexity of the geology raises the possibility of additional, presently un-mapped fault-bounded blocks of dolostone. The presence of such a block to the south of the upstanding ridge could account for the lack of relief within the southern lobe of the depression. However, we have taken a conservative approach and not mapped the southern lobe as dolostone.





**Figure 17.** Termination of large passage in Forest Hills Cave. The figure in the image stands at the edge of a thick bank of stream froth. Traces of froth can also be seen attached to the ceiling above the figure; also, a log of wood can be seen to the left of the figure (Photo by Rolan Eberhard).

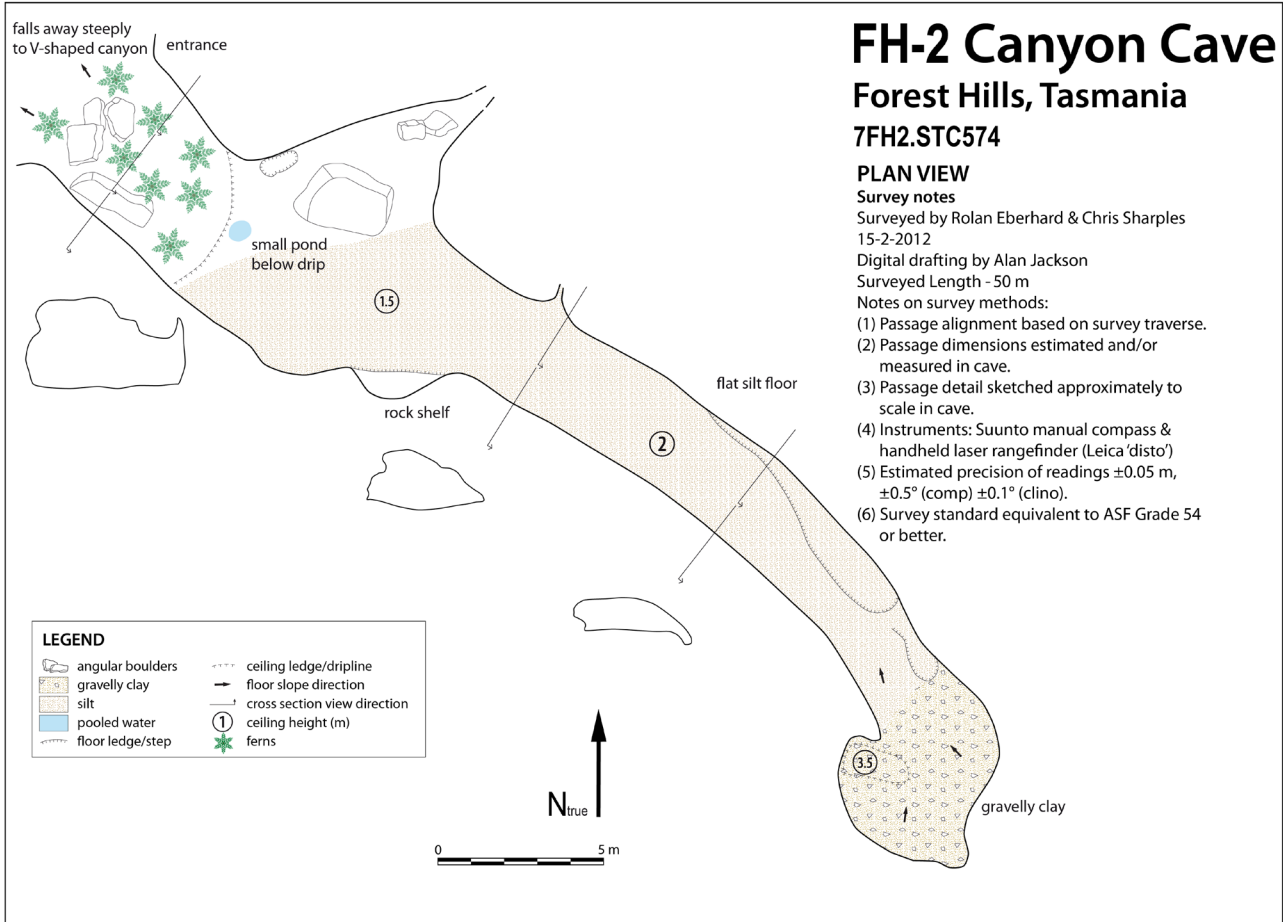


**Figure 18.** Map of Canyon Cave, FH-2.





**Figure 19.** View towards the entrance from inside Canyon Cave, showing small drip-water pool. The spacious horizontal form of the passage and its silty base are typical of most of the cave (Photo by Rolan Eberhard).

Our geological model incorporates a putative narrow eastern extension of the dolostone that likewise has not been directly verified but, in this case, is supported by the abrupt termination of Forest Hills Cave at an inferred fault. The immediate cause of the termination appears to be a blockage of fluvial sediment; however, we suspect that the ultimate cause is a structural effect related to the juxtaposition of dolostone and siliclastic strata by faulting. This would have the effect of deflecting the alignment of the passage, trapping woody debris and sediment at that point. The deflection implies the existence of a pathway for underground drainage, which we infer is eastwards via a third fault-bounded block of dolostone.

This geological interpretation constrains the location of potential resurgence points for water sinking underground within the Forest Hills Depression. Based on proximity and hydraulic gradient, candidate discharge points include two minor tributary valleys which join the New River north and east of the Forest Hills Depression respectively (Figures 3 and 12). An outlet at E implies a fall of ~60 m over ~0.6 km; an outlet at F implies a fall of ~90 m over ~1.1 km. Whilst the

steeper hydraulic gradient favours the former as the resurgence point, the inferred fault at the termination of Forest Hills Cave suggests that underground drainage towards E is impeded by a block of siliclastic strata. This would cause underground drainage from the Forest Hills Depression to be directed eastwards towards a discharge point near F, beyond a broad W-E elongated saddle that we have inferred on topographic and structural grounds to be underlain by an eastern extension of the faulted dolostone (Figures 12 and 13).

As observed under baseflow conditions in February 2012 and when visited by TCC in 1972 (Shaw 1973), the Forest Hills Depression was free draining. However, it is apparent that this condition does not apply during high stage flows, based on our observation of fresh deposits of silt, vegetable debris and frothy scum coating surfaces several metres above the level of the entrance to Forest Hills Cave (Figure 15) and within Canyon Cave. Both caves had evidently been fully submerged by water backing up at the sink not long prior to our visit. An event of this type would also submerge portions of the forested low point of the depression, creating an ephemeral body of ponded water, possibly some



hundreds of metres in diameter during major floods. The frequency of such events is unknown, but the large catchment and heavy seasonal precipitation experienced by Tasmania's south-west suggest that flooding of the depression may be a semi-regular occurrence. In any case, the frequency and duration of flooding is not sufficient to inhibit the rainforest which colonises the base of the depression.

A further consideration in characterising the hydrology of the depression is the possibility that some surface runoff is lost to underground flow above the cave. We suspect this because the discharge of the stream at the entrance to Forest Hills Cave (see Figure 14) is subjectively less than would be expected given its sizeable catchment (1280 ha). As a point of comparison, the observed discharge of this stream is no greater and probably less than the baseflow discharge of the well-known Growling Swallet streamsink (Mt Field Range). Growling Swallet has a catchment area half the size of that of the Forest Hills Depression and on average likely receives less annual precipitation. If the baseflow discharge of the Forest Hills stream is attenuated by partial capture of its flow to subsurface pathways above Forest Hills Cave, this would condition the scale and frequency of flood events capable of inundating the base of the depression. A spectacular example of this is available 12 km from the Forest Hills at Vanishing Falls, which engulfs the baseflow of the Salisbury River but episodically overtops, redirecting the flood peak to the limestone gorge below the falls (Eberhard and others 1992). We suspect something similar at Forest Hills Cave, whereby stream stage fluctuates in response to the finite capacity of diffuse or point source sink points above the cave to take water.

Canyon Cave differs from Forest Hills Cave in that it follows the strike of the steeply dipping beds of the host rock rather than obliquely cutting across the beds. In this case the passage is aligned with the inferred direction of underground drainage from the Forest Hills Depression to the New River, i.e. east. We interpret Canyon Cave as a former inflow point of the stream that now flows to Forest Hills Cave. The height difference between the cave entrances is modest (<10 m) compared to the height difference (40-50 m) between the caves and topographic low points on the surface drainage divides which separate the Forest Hills Depression from the New River. The scale of downcutting required to account for the abandonment of Canyon Cave in favour of

Forest Hills Cave is therefore much less than that required to account for the overall depth of the depression.

It can be assumed that speleogenesis within the depression has been intimately connected with downcutting by the New River to form the present-day gorge. This has progressively lowered the hydrological baselevel and increased the hydraulic gradients within tributary catchments. This would have the effect of enhancing the susceptibility of runoff from Forest Hills to capture by an incipient karstic aquifer propagating headwards from the gorge. Enlargement of the depression to its modern size (80 ha) required it to propagate outwards in the surrounding siliclastic strata. The resultant landform occupies more than twice the area of the dolostone outcrop (37 ha) that initiated its development.

The status of the Forest Hills Depression as a distinctive landform of high conservation value is formally recognised by its inclusion as a listed geosite in the Tasmanian Government's Natural Values Atlas ([www.naturalvaluesatlas.tas.gov.au](http://www.naturalvaluesatlas.tas.gov.au)). The geosite statement of significance reads:

*This is Tasmania's largest fully-enclosed karst depression (sinkhole) in terms of depth, with the only larger karst depressions (the Mayberry and Dismal Swamp poljes) being much shallower (<10 m) flat-floored polje-type depressions. The Forest Hills Depression is also the least disturbed large karst depression in Tasmania, with an unbroken forest cover having no visible signs of burning, and no artificial ground disturbances except for two small tent-sized platforms of flattened soil adjacent the streamsink cave.*

This statement raises two points of difference in claiming exceptional significance for the Forest Hills Depression. Firstly, it proposes that this is the deepest karst depression in Tasmania and third largest in areal extent. This claim is open to question (Table 1). However, unlike Dismal Swamp and Mayberry, the Forest Hills Depression does not present as an alluviated basin resembling a European polje. This difference highlights the role of site-specific factors in conditioning the development of karst depressions in different environmental settings. In the case of the Forest Hills Depression, significant local factors include its modest elevation, which has protected the feature from heavy clastic sedimentation typical of

glacial or periglacial settings. This difference draws attention to the fact that several of Tasmania's largest karst depressions (Table 1) are composite features derived from glacio-karstic interactions. That is, they are the products of both solution by meteoric water and mechanical erosion by moving bodies of ice. In contrast, the Forest Hills Depression stands out as a genetically less complex example, the initiation of which has been chiefly due to conventional solution-driven karstification. The existence of a significant hydraulic gradient between the depression and the New River, lowering the base level and promoting cavernous downcutting, is a further critical site-specific point of difference. Secondly, the statement proposes that

the Forest Hills Depression is 'the least disturbed large karst depression in Tasmania', highlighting the absence of fire-tolerant vegetation indicative of anthropogenic burning or other visible disturbance by humans (excluding minor equivocal old tent platforms at the entrance to Forest Hills Cave). Given the increasingly pervasive effect of humans on the environment, we concur that the essentially natural condition of the Forest Hills Depression adds significantly to its geoconservation value. This underlines the appropriateness of its inclusion in the Tasmanian Wilderness World Heritage Area (TWWHA) and management to protect these remote areas from anthropogenic disturbance.

**Table 1.** Indicative metrics for large karst depressions in Tasmania. Area was calculated conservatively using the highest enclosing depression contour. Depth was calculated conservatively using the highest and lowest depression contours (or mapped spot height), as published by Land Information System Tasmania ([www.thelist.tas.gov.au](http://www.thelist.tas.gov.au)). Catchment area includes karstic and non-karstic portions. Dismal Swamp is a polje-like feature, portions of which are fully enclosed. The currently available mapping only delineates the broader feature.

Location	GDA Easting & Northing (m)	Area (ha)	Depth (m)	Highest enclosing depression contour (m)	Catchment area (ha)
Dismal Swamp	318300 5462500	600	<10	<50	1030
Liena	439000 5399300	240	38	400	1460
Lake Timk	457100 5246400	98	69	520	1090
Forest Hills	460400 5202100	80	50	390	1280
Lake Sydney	468300 5207100	15	4	680	290
Weld River	455940 5253730	15	50	380	33
Mt Gell	417300 5335580	14	30	810	83
Cook Creek	468200 5216500	9	30	480	380
Lake Ovoid	466150 5218000	8	30	770	40
Styx River	465255 5258650	7	<10	420	47



## Conclusions

The status of the Forest Hills Depression as a substantial karst landform in dolostone, probably a correlate of the Weld River Dolomite (Calver 1989), is confirmed. Cavernous development within the depression includes at least two spacious caves, the larger of which is the sinking point of a stream that likely drains to a presently unknown resurgence on the New River. Considerable scope exists to further improve the very limited geological mapping in this remote area and to extend the exploration of karst features, beyond the present reconnaissance-level study. However, the standard of documentation is now adequate to confirm the evaluation of the Forest Hills Depression as a significant element of the karst geodiversity protected within the Tasmanian Wilderness World Heritage Area.

## References

- BOTTRILL, R.S. & WOOLLEY, R.N. 2015 Petrology and Mineragraphy: SW Tasmania. *Mineral Resources Tasmania Mineralogy/Petrology Report* LJN2015/038.
- CALVER, C. 1989 The Weld River Group: A major upper Precambrian dolomite sequence in southern Tasmania. *Papers and Proceedings of the Royal Society of Tasmania*, 123: 43-53.
- CALVER, C.R., EVERARD, J.L., BERRY, R.F., BOTTRILL, R.S. & SEYMOUR, D.B. 2014 Proterozoic Tasmania [in] CORBETT, K.D., QUILTY, P.G. & CALVER, C.R. (Eds) Geological Evolution of Tasmania. *Geological Society of Australia Special Publication*, 24. pp. 33-94
- DIXON, G. & SHARPLES, C. 1986 Reconnaissance geological observations on Precambrian and Palaeozoic Rocks of the New and Salisbury Rivers, Southern Tasmania. *Papers and Proceedings of the Royal Society of Tasmania*, 120: 87-94.
- EBERHARD, R., EBERHARD, S. & WONG, V. 1992 Karst geomorphology and biospeleology at Vanishing Falls, south-west Tasmania. *Helictite*, 30(2): 25-32.
- FIELD, M.S. 2002 *A Lexicon of Cave and Karst Terminology with Special Reference to Environmental Karst Hydrology*. EPA/600/R-01/003. United States Environment Protection Agency, Washington.
- KIERNAN, K. 1995 An Atlas of Tasmanian Karst. *Tasmanian Forest Research Council, Research Report*, 10.
- RAUCH, H.W. & WHITE, W.B. 1970 Lithologic controls on the development of solution porosity in carbonate aquifers. *Water Resources Research*, 6: 1175-1192.
- SHAW, P. 1973 Aerial exploration of S.W. caving areas – 22.12.72. *Speleo Spiel*, 77: 3.



## Appendix 1

**Table 2.** Waypoints relevant to observations presented in this paper (see also map Figure 6). Waypoint co-ordinates were obtained with a hand-held Garmin Etrex Summit HC GPS (estimated horizontal accuracy +/- 4 metres), except note Waypoint 12 had poor GPS reception, and this position was estimated manually.

Waypoint (shown on Figure 6)	Feature (including bedrock outcrop type)	Geographical co-ordinates (decimal degrees, WGS84 datum)		Projected co-ordinates (metric MGA Zone 55 UTM, GDA94 datum)	
		Longitude	Latitude	Easting	Northing
001	New River: entry point / bivvy site.	146.501906	-43.320077	459 612	5203 519
002	New River: dolomitic siltstones.	146.504108	-43.320671	459 791	5203 455
003	New River: red-brown slate.	146.503137	-43.320900	459 713	5203 429
004	New River: red-brown slate.	146.502483	-43.320642	459 659	5203 457
005	New River just upstream of bivvy site: well-bedded quartzite.	146.501625	-43.319790	459 589	5203 551
006	New River: red-brown slate outcrop.	146.502595	-43.320735	459 669	5203 447
007	New River: well-bedded quartzite.	146.503534	-43.320847	459 745	5203 435
008	Forest Hills Depression: point on route high on north slope: red-brown slate lag fragments.	146.511876	-43.330043	460 427	5202 417
009	Forest Hills Depression: point on route low on north slope. Siltstone with secondary carbonate.	146.510022	-43.332168	460 278	5202 181
010	Forest Hills Depression: surface watercourse with no exposed bedrock at this point.	146.509758	-43.332529	460 257	5202 141
011	Forest Hills Depression: dolostone outcrop at cave entrance (Canyon Cave).	146.511038	-43.332632	460 361	5202 130
012	Forest Hills Depression: dolostone cliff at cave entrance bivvy site (Forest Hills Cave); poor GPS reception at this location, waypoint position estimated from existing 1:25,000 mapping (error margin approximately $\pm 20$ metres).	146.512066	-43.332644	460 444	5202 127